LEAD BIO-REDUCTION AND POLYHYDROXYALKANOATE PRODUCTION

FUNDAMENTAL STUDIES ON MICROBIAL LEAD REDUCTION AND POLYHYDROXYALKANOATE PRODUCTION

By

ABDELRAHMAN FATHY IBRAHIM AMER, B.Sc., M.Sc.

A Thesis Submitted to the School of Graduate Studies in Partial Fulfillment of the Requirements for the Degree of Doctor of Philosophy

McMaster University DOCTOR OF PHILOSOPHY (2022)

Hamilton, Ontario (Civil Engineering)

TITLE: Fundamental Studies on Microbial Lead Reduction and Polyhydroxyalkanoate Production

AUTHOR: Abdelrahman Fathy Ibrahim Amer, B.Sc., M.Sc.

SUPERVISOR: Dr. Younggy Kim

NUMBER OF PAGES: xxii, 143.

Lay abstract

This thesis aimed to provide sustainable biotechnological solutions to three environmental challenges: lead contamination, petroleum-based plastics, and elevated CO_2 levels in the atmosphere. Certain metal-reducing bacteria can grow by consuming toxic Pb(II) ions from aqueous environments and thus reduce their toxicity. Furthermore, various microorganisms can store biodegradable polymers, known as polyhydroxyalkanoates (PHAs), in their cells. The stored PHA polymers can be extracted and processed to produce biodegradable plastics. PHA accumulators can produce significant amounts of PHA by utilizing organic substrates or CO_2. Therefore, PHA-based plastics can reduce environmental deterioration due to non-degradable plastics and elevated CO_2 levels. Lab-scale experiments and mathematical modeling can provide a better understanding of the growth and enrichment of PHA accumulators in engineered PHA-production systems. Research findings in this thesis will allow cost-effective and sustainable production of biodegradable plastics from organic wastes and flue gas.

Abstract

Lead contamination threatens human life and the environment. The biological reduction of Pb(II) to metallic Pb is an attractive solution for Pb(II) pollution. *Delftia acidovorans*, *Azonexus caeni*, and *Comamonas testosteroni* were isolated and studied for their capabilities to utilize Pb(II) as a terminal electron acceptor. *D. acidovorans* strain Pb11 and *A. caeni* strain Pb2 cultures showed a 5.2- and 8.1-fold growth at 10.0 mg-Pb(II)/L in 3 d, respectively. Petroleum-based plastics are another emergent environmental concern. Polyhydroxyalkanoates (PHAs), a sustainable alternative to conventional plastics, are biodegradable polymers produced by PHA accumulators under autotrophic or heterotrophic conditions. In this thesis, the growth and enrichment of PHA accumulators, such as *Plasticicumulans acidivorans* and *Cupriavidus necator*, were investigated as they can accumulate 90% of their cell weight as PHA. An energetic model was developed to calculate theoretical PHA yields. The true autotrophic and heterotrophic PHB yields were estimated as 2.97 ($g_{PHB}/\,mol_{H_2}$) and 0.66 ($g_{PHB}/\,g_{acetate}$), respectively. Moreover, the growth of *C. necator* was investigated in lab-scale experiments under various autotrophic, heterotrophic, and mixotrophic conditions. When *C. necator* was cultivated in two-stage systems, high optical densities were attained in less than 24 h. In addition, a mathematical model for the competition between PHA and non-PHA accumulators in the feast-famine enrichments was developed. The calibrated and validated model for *P. acidivorans* suggested that microbial diversity in mixed cultures impacted the enrichment process. Another aspect of this thesis was to propose an innovative method for enriching PHA accumulators in mixed cultures. By applying autotrophic and autotrophic-heterotrophic enrichment strategies, *C. necator* dominated the mixed cultures (> 90%) in less than five days. Based on this thesis findings, it can be concluded that biotechnology applications in Pb(II) remediation and PHA production could reduce the severe impacts of Pb contamination, petrochemical plastics, and climate change due to elevated CO_2 levels.

Preface

This thesis has been prepared in accordance with the guidelines of the sandwich thesis format from the School of Graduate Studies at McMaster University. Five papers are included in this thesis as listed below.

- Amer, A., and Kim, Y. (2022). Isolation of Pb (II)-reducing bacteria and demonstration of biological Pb (II) reduction to metallic Pb. Journal of Hazardous Materials, 423, 126975.
- Amer, A., and Kim, Y. Theoretical estimation for the yield coefficients for microbial polyhydroxyalkanoate production (under preparation).
- Amer, A., and Kim, Y. Minimizing the lag phase of *Cupriavidus necator* growth under autotrophic, heterotrophic, and mixotrophic conditions (under review).
- Amer, A., and Kim, Y. Modeling the growth of diverse microorganisms during feast-famine enrichment (under review).
- Amer, A., and Kim, Y. Highly selective enrichment of *Cupriavidus necator* using its autotrophic and heterotrophic characteristics (under review).

The first manuscript is presented in Chapter 2. The work was started in January 2019. The manuscript was submitted in April 2021 and accepted in August 2021. The work was conducted under the supervision of Dr. Younggy Kim. The manuscript is included in this thesis as it provided a novel approach to remove Pb(II) from water streams by isolating bacteria that can reduce Pb(II) to metallic Pb^0. The suggested remediation method could be applied to efficiently treat water streams and soils contaminated with Pb(II). My contributions include:

- Literature review
- Design and conducting the experiments
- Writing the manuscript

The second manuscript is presented in Chapter 3. The work was started in May 2021. The work was conducted under the supervision of Dr. Younggy Kim. The manuscript is included in this thesis as it provided a novel modeling study on the estimation of theoretical yield coefficients of polyhydroxyalkanoate and cell in PHA accumulators under distinct cultivation conditions. My contributions include:

- Literature review
- Model development
- Data collection
- Writing the manuscript

The third manuscript is presented in Chapter 4. The work was started in October 2021. The work was conducted under the supervision of Dr. Younggy Kim. The manuscript is included in this thesis as it demonstrated a novel study on the impact of growth conditions on the metabolic responses of *Cupriavidus necator*, commonly employed in commercial PHA production. My contributions include:

- Literature review
- Design and perform the experiments
- Writing the manuscript

The fourth manuscript is presented in Chapter 5. The work was started in May 2020. The work was conducted under the supervision of Dr. Younggy Kim. The manuscript is included in this thesis as it provided a novel study on modeling the enrichment of PHA accumulators in mixed microbial cultures using the feast-famine strategy. The mathematical model can be applied to optimize the cultivation conditions to ensure successful enrichment of PHA accumulators in mixed cultures. My contributions include:

- Literature review

- Conceptualization and model development
- Data collection
- Model calibration and validation
- Writing the manuscript

The fifth manuscript is presented in Chapter 6. The work was started in May 2022. The work was conducted under the supervision of Dr. Younggy Kim. The manuscript is included in this thesis as it introduced innovative methods to enrich *Cupriavidus necator* in mixed microbial cultures. The suggested enrichment methods can be employed to obtain mixed cultures dominated by *C. necator* within a few days. The enriched cultures can utilize organic wastes directly without sterilization requirements, which can significantly reduce the PHA production costs. These findings can substantially reduce the high prices of biodegradable plastics. My contributions include:

- Literature review
- Conceptualization
- Design and conducting the experiments
- Collecting and analyzing experimental data
- Writing the manuscript

Copyright Permission

I have secured permission to include copyright material in this Ph.D. thesis from the copyright holder. The permission includes a grant of an irrevocable, non-exclusive license to McMaster University and to Library and Archives Canada to reproduce the material as part of the thesis.

Acknowledgment

All praise to Allah, Lord of all realms.

Firstly, I would like to dedicate this work to my father in his 19th memorial; he has always been our beacon and pioneer in the life.

Secondly, I would like to thank Dr. Younggy Kim (my Ph.D. supervisor) for his continuous support and encouragement during the four-year journey. I admired Dr. Kim's eagerness to transfer scientific and leadership skills to his students. I am so grateful to him for giving me the opportunity to pursue my degree in his lab. I wish all the best for him and his family.

I also would like to thank Dr. Sarah Dickson-Anderson and Dr. Herbert Schellhorn for their participation in the supervisory committees and their insightful comments and suggestions. Also, I am thankful for Dr. Tyagi Rajeshwar (the external examiner) for his intuitive comments and discussions in the Ph.D. defence.

I would like to present my sincere thankfulness to my dear mother "Karima"; my wife "Ghada"; and my siblings "Dr. Naglaa and Dr. Ahmed" for their great roles in my life. I also dedicate this work to my beloved children: Tasnim and Hamza. I hope this will make them so proud of their dad in the future. I also thank my extended family and all my childhood friends for their endless support.

I also thank my previous and recent lab colleagues for their support and assistance during my study in the Kim's water lab, especially Monica Han, our lab technician. I enjoyed the fruitful discussions and cooperation with: Ahmed Tark, Hui Guo, Andrew Alex, Sama Al-Ani, Ijaj Mahmud, Sarah Hemmati, Sandali Panagoda, Natalia Shiu, and all other students. I wish you all the best in your current and future endeavors.

Finally, I would like to thank all my mentors, professors, and colleagues at McMaster University and Menoufia University (Egypt), who always encouraged and supported me to achieve this milestone in my academic career.

Contents

List of Figures

List of Tables

List of Symbols and Nomenclature

ASMs	Activated sludge models
atm	Atmospheric pressure
b_{NA}	Decay rate coefficient for X_{NA} (h^{-1})
b_{PA}	Decay rate coefficient for X_{PA} (h^{-1})
C/N	Carbon to nitrogen ratio
Cmol	Carbon mole
DTE	Dilution to extinction
f_I	Fraction of X_I in biomass lysis (g-COD. g-COD^{-1})
$f_{(PHA)}^{max}$	Maximum ratio of PHA to active biomass $\left(\frac{X_{PHA}}{X_{PA}} = \left(\frac{100}{PHA\ storage\ (\%)} - 1\right)^{-1}\right)$
ICP-OES	Inductively coupled plasma - optical emission spectrometry
i_{NBM}	Nitrogen content of biomass (g-N. g-COD^{-1})
i_{NXI}	Nitrogen content in X_I (g-N. g-COD^{-1})
i_{PBM}	Phosphorus content in biomass (g-P. g-COD^{-1})
i_{PXI}	Phosphorus content in X_I (g-P. g-COD^{-1})
K_H	Maximum hydrolysis rate (h^{-1})
$K_{N,\,NA}$	N affinity constant for X_{NA} (g-N.m^{-3})
$K_{N,\,PA}$	N affinity constant for X_{PA} (g-N.m^{-3})
$K_{O,\,NA}$	Oxygen affinity constant for X_{NA} (g-O_2.m^{-3})
$K_{O,\,PA}$	Oxygen affinity constant for X_{PA} (g-O_2.m^{-3})
$K_{PHA,\,PA}$	PHA half-saturation constant for X_{PA} (g-COD_{PHA}. g-COD_X^{-1})
$K_{P,\,NA}$	P affinity constant for X_{NA} (g-P.m^{-3})
$K_{P,\,PA}$	P affinity constant for X_{PA} (g-P.m^{-3})
$K_{S,\,NA}$	Half-saturation constant for X_{NA} on S_S (g-COD_S. m^{-3})
$K_{S,\,PA}$	Half-saturation constant for X_{PA} on S_S (g-COD_S. m^{-3})
ksto	PHA storage rate (g-COD_{PHA}.g-COD_X^{-1}.h^{-1})
K_X	Hydrolysis affinity constant (g-COD. g-$COD^{-1)}$
MEC	Microbial electrolysis cells
MMC	Mixed microbial cultures
$m_{PA,\,PHA}$	Maintenance coefficient for X_{PA} on X_{PHA} (h^{-1})
$m_{PA,S}$	Maintenance coefficient for X_{PA} on S_S (h^{-1})
$m_{S,\,NA}$	Maintenance coefficient for X_{NA} on S_S (h^{-1})

Pb	Lead
P_{CO_2}	Partial pressure of CO_2
PCR	Polymerase chain reaction
P_{H_2}	Partial pressure of H_2
PHA	Polyhydroxyalkanoate
PHA storage	Maximum accumulated PHA ratio in cells ($\frac{X_{PHA}}{X_{PHA}+X_{PA}}$) (%)
PHB	Ploy hydroxybutyrate
PHV	Polyhydroxyvalerate
P_{N_2}	Partial pressure of N_2
P_{O_2}	Partial pressure of O_2
Q	Reaction quotient
qPCR	Quantitative polymerase chain reaction
SEM-EDS	scanning electron microscopy and energy dispersive X-ray spectroscopy
SRT	Solids retention time
R	Universal gas constant (8.31 J/mole.K)
R_a	Electron acceptor reduction half-reaction
R_c	PHA or biomass synthesis reduction half-reaction
R_d	Electron donor reduction half-reaction
TEA	Terminal electron acceptor
TEEM1	thermodynamic electron equivalents model
$\mu_{NA,S}$	Maximum growth rate for X_{NA} on S_S (h^{-1})
$\mu_{PA,PHA}$	Specific growth rate for X_{PA} on X_{PHA} (h^{-1})
$\mu_{PA,S}$	Specific growth rate for X_{PA} on S_S (h^{-1})
$Y_{NA,S}$	Yield coefficient for X_{NA} on S_S (g-COD_X.g-COD_S^{-1})
$Y_{PA,PHA}$	Yield coefficient for X_{PA} growth on X_{PHA} (g-COD_X. g-COD_{PHA}^{-1})
$Y_{PA,S}$	Yield coefficient for X_{PA} on S_S (g-COD_X.g-COD_S^{-1})
$Y_{PHA,S}$	Yield coefficient for PHA storage on S_S (g-COD_{PHA}.g-COD_S^{-1})
XPS	X-ray photoelectron spectroscopy
ΔG_p	The energy required to convert the carbon source activated acetate.
$\Delta G_{f,298}^{0\prime}$	Gibs free energy of formation at standard conditions
$\Delta G^{0\prime}$	Difference in free energy of formation for reduction half-reaction

Declaration of Academic Achievement

Abdelrahman Amer was the main contributor to the five manuscripts presented in this thesis. The contributions from the co-authors are detailed at the beginning of each Chapter.

1. Introduction

1.1. Overview

Lead (Pb) contamination is a major concern that causes serious environmental pollution in the last decades. Lead is classified as the second most hazardous heavy metal after arsenic. Pb is released to groundwater and soils from mining and ore processing, Pb-acid batteries recycling plants, and industrial wastewater effluents (Rahman & Singh, 2019). Pb has severe health effects on natural aquatic life and human bodies (Bao et al., 2017; Levinson et al., 1996; Tiquia-Arashiro, 2018). Pb has several chemical forms such as Pb^0, Pb(IV) and P(II). Among them, Pb(II) is highly mobile and bio-available, and thus Pb(II) is considered the most toxic inorganic form in aquatic environments (Matta & Gjyli, 2016). Thus, this thesis focused on providing biotechnological solutions to Pb(II) contamination by employing microorganisms that can utilize and reduce Pb(II) as a promising alternative to the current chemical treatment methods that produce large amounts of wastes (Modestra et al., 2017; Peens et al., 2018).

Another serious environmental concern is the petroleum-based plastics. Conventional chemical plastics have been extensively utilized since 1950s in all aspects of modern life. The current chemical plastics are produced from fossil fuels which increase the greenhouse gas (GHG) emissions. The massive production of petroleum-based plastics exceeded 368 million metric tons in 2019 (Almeida et al., 2021; Matos et al., 2021). Chemical plastics are widely used because of their chemical resistance and thermostability (Fang et al., 2019). However, petroleum-based plastics cause severe pollution issues when they are released into the environment. Around 90% of consumed plastics end in landfills or oceans and thus contaminate nearby soil and groundwater by leaking toxic contaminations (J. Lee et al., 2021). Thus, bioplastics are promising alternatives to conventional petroleum plastics because of their similar physical and chemical properties (Mascarenhas & Aruna, 2017). Polyhydroxyalkanoate (PHA) is a bioplastic polymer accumulated inside microbial cells as stored granules. The PHA

polymers can be extracted and processed to produce biodegradable plastics (J. Lee et al., 2021). Therefore, applying biotechnological approaches to produce PHA from organic substrates, waste feedstocks, and/or inorganic carbon sources (e.g., CO_2) can provide ecofriendly alternatives to the petroleum-based plastics (Estévez-Alonso, Pei, et al., 2021; Sohn et al., 2021).

1.2. Literature review on biological Pb(II) remediation

Chemical precipitation, membrane filtration, adsorption, electrodialysis, and photocatalysis are currently applied to remove Pb(II) from contaminated water streams and soils. Nevertheless, these methods cause several environmental, operation, and maintenance problems such as hazard wastes and production of huge amounts of sludge (Modestra et al., 2017; Peens et al., 2018). Biological removal methods of Pb from wastewater are more attractive alternatives as they suit wastewater characteristics and can lower the capital and operation costs. Potential Pb(II) bioremediation includes mechanisms such as adsorption (biosorption), intracellular bioaccumulation, extracellular sequestration, and bio precipitation (Naik et al., 2013a; Naik & Dubey, 2011a, 2013; Tiquia-Arashiro, 2018).

The biological reduction of metals is a promising biotechnological approach for the remediation of contaminated water streams. The dissimilatory metal reduction was previously reported for various metals such as Fe(III), Mn(IV), U(VI), Se(VI), Se(IV), and Cr(VI) (Lloyd, 2003; Lovley, 1993; Lovley et al., 1991; Schmieman et al., 1998). Under anaerobic conditions, microorganisms can obtain the energy required for microbial growth by coupling the oxidation of an organic substrate (i.e., electron donor) with the reduction of an oxidized metal cation (i.e., terminal electron acceptor), which is not related to metal assimilation inside microbial cells (Lovley, 1993). For instance, *Geobacter metallireducens* (formerly strain GS-15) was reported to couple the oxidation of acetate with the reduction of Fe(III) to Fe(II) under anaerobic conditions (Lovley et al., 1987).

Similarly, Pb(II) can be reduced to Pb^0 when microorganisms are provided with an organic substrate as the electron donor and Pb(II) as the only terminal electron acceptor under anaerobic conditions. When Pb(II) is reduced to Pb^0, the latter will not be available for metabolic uptake and biodegradation (Modestra et al., 2017). The microbial Pb(II) reduction to Pb^0 was previously demonstrated in the literature (Brink et al., 2017, 2019, 2020a; Colantonio & Kim, 2016b; Jannati, 2019; Peens et al., 2018). For instance, Colantonio and Kim (2016) reported microbial Pb(II) reduction to Pb^0 in microbial electrolysis cells (MECs) at the anode chamber under open-circuit conditions (Colantonio & Kim, 2016b). A subsequent study utilized an enriched MEC anode to reduce and remove lead from synthetic wastewater (Jannati, 2019). Also, a microbial consortium was employed to reduce and remove up to 90% of 80 ppm of Pb(II) under anaerobic conditions (Brink et al., 2017). The same consortium was subsequently studied to remove up to 1000 ppm of Pb(II) with 99% efficiency (Peens et al., 2018). However, the isolation of bacteria that can reduce Pb(II) to Pb^0 was not previously demonstrated. Therefore, one of the main objectives of this thesis was to isolate, identify, and study Pb(II)-reducing bacteria that can be applied in Pb remediation applications.

1.3. Polyhydroxyalkanoate (PHA): a biodegradable plastic

Bioplastics are sustainable substitutes to synthetic petroleum plastics because of their similar physical and chemical properties (Mascarenhas & Aruna, 2017). Bioplastics include biodegradable biological-based plastics in addition to petrochemical plastics (Bishop et al., 2021). Biodegradable bioplastics include several polyesters such as polylactic acid (PLA), polyhydroxyalkanoates (PHA), starch blends, polysaccharides (carbohydrates polymers), and aliphatic polyesters (Kumar et al., 2020). The production of biological-based biodegradable plastics currently accounts for 55.5% of the global bioplastic production (Carpine et al., 2020).

PHAs are microbiologically produced polymers with tunable physical, mechanical, and thermal properties (J. Lee et al., 2021). PHAs are highly biocompatible, biodegradable, and sustainable (Khatami et al., 2021). Under standard conditions, PHAs can be biodegraded into biomass, water, and CO_2 in approximately two months, which significantly reduces the environmental impact of wasted plastics (Hassan et al., 2013). PHAs have been applied in many applications and commercial products such as biomedical applications, agriculture, packaging, and biochemicals (Khatami et al., 2021).

PHAs are classified into short chain length (scl), medium chain length (mcl), and long chain length (lcl) according to the number of carbon atoms in the side chain. The scl-PHAs (e.g., 3-hydroxyvalerate and 3-hydroxybutyrate) have less than five carbon atoms while the mcl-PHAs (e.g., 3-hydroxydecanoate, 3-octanoate and 3-hydroxyhexanoate) have 5 – 14 carbon atoms. The lcl-PHAs have more than 14 carbon atoms but they are uncommon and less studied (Raza et al., 2018). PHAs are composed of homo (e.g., ploy-3-hydroxybutyrate (PHB), poly-3-hydroxyvalerate (PHV)) or copolymers (e.g., poly-3-hydroxybutyrate-co-3-hydroxyvalerate (P(3HB-co-3HV)). Thus, PHAs differ in their properties and chemical composition depending on the structural variations of the building monomers (Raza et al., 2018). For instance, PHB has properties comparable to polypropylene with strong resistance to moisture and low gas permeability. However, the low thermal stability and high brittleness hinder the wide PHB application in the industry. The copolymer P(3HB-co-3HV) is more flexible than PHB and can be used to in a variety of products including compost bags, disposable food containers, and bottles (S. Y. Lee, 1996).

1.4. Literature review on microbial PHA production

The first PHA polymer, identified as PHB, was identified by Maurice Lemoige in 1926 as intercellular granulates accumulated by *Bacillus megaterium* (Lemoigne, 1926). Since this first discovery, over 300 microbial species were studied for their abilities to accumulate PHA

(Grothe & Chisti, 2000; Hänggi, 1990; S. Y. Lee, 1996b). PHA accumulators store intercellular PHA granules as carbon and energy reserves to be used as an alternate source of fatty acids under harsh conditions with low organic substrates (Kourmentza et al., 2017). Both prokaryotic and eukaryotic microorganisms have been reported to accumulate different PHA compositions depending on the provided organic substrate (Raza et al., 2018). For instance, acetate was found to induce PHB production while PHV was produced when propionate was used as the carbon source. When a mixture of acetate and propionate was used, the polymer composed of a mixture of PHB/PHV with ratios similar to the fractions between acetate and propionate in the supplied substrates (Jiang et al., 2011; Woraittinun & Suwannasilp, 2017).

Based on the cultivation conditions required to trigger PHA accumulation, PHA accumulators are classified into two main distinct groups: growth-associated and nutrient-limited PHA accumulators (Kourmentza et al., 2017). In the growth-associated PHA accumulation, PHA accumulators can accumulate high PHA fractions during the growth phase. For instance, *Azohydromonas australica* can produce up to 80% of the cell dry weight as PHB while growing on inexpensive carbon sources such as sucrose (Gahlawat & Srivastava, 2013). The second group of PHA accumulators cannot simultaneously grow and synthesize significant amounts of PHA in the growth phase. Various types of bacteria, such as *Cupriavidus necator*, *Pseudomonas oleovorans*, and *Pseudomonas putida*, require a nutrient-limitation condition such as nitrogen (N), phosphorus (P), or oxygen (O) to accumulate significant PHA amounts. *Cupriavidus necator* (previously *Alcaligenes eutrophus* (Kärst & Friedrich, 1984; Repaske & Repaske, 1976) and *Ralstonia eutropha* (Cramm, 2009; Müller et al., 2013; Tiemeyer et al., 2007; Volova et al., 2002)) can accumulate PHA up to 90% of their cell dry weight under nutrient limited conditions (Grothe & Chisti, 2000; Hänggi, 1990; S. Y. Lee, 1996b).

Based on the carbon source, PHA can be produced under heterotrophic or autotrophic conditions. Heterotrophic microorganisms utilize organic substrates as the carbon and energy

sources for growth and/or PHA accumulation. Several pure organic carbon substrates have been investigated such as glucose (Biglari et al., 2020; Ryu et al., 2008); glycerol (Mohamad Fauzi et al., 2019; Moita et al., 2014; Moralejo-Gárate et al., 2014; Mothes et al., 2007; Pérez Rivero et al., 2016; Tanadchangsaeng & Yu, 2012); lactate (Jiang, Marang, et al., 2011b); and acetate (Chua et al., 2003; Marang et al., 2014). In addition, organic wastes were also investigated for heterotrophic PHA production (Agustín Martinez et al., 2015; Mannina et al., 2020; Verlinden et al., 2011). Heterotrophic PHA production was reported under aerobic, anaerobic, and anoxic conditions (Tiemeyer et al., 2007). In chemolithotrophic PHA production, autotrophic bacteria can utilize an inorganic carbon source (e.g., CO_2, CO) in the presence of H_2 as the electron donor and O_2 as the terminal electron acceptor to grow and accumulate PHA (DeCicco & Stukus, 1968; E. & T., 1970; Ishizaki et al., 2001; Miyahara et al., 2020; Takeshita & Ishizaki, 1996; Volova et al., 2002). The recommended gas mixture composition to attain sufficient cell growth has a volume-based ratio of H_2: O_2: CO_2 = 7: 2: 1 (Ishizaki et al., 2001).

PHA formation under heterotrophic or autotrophic conditions is similar to the cell synthesis pathway. To synthesize PHA granules or new cells, bacteria first convert the carbon source (i.e., organic substrate or CO_2) to an intermediate organic compound (e.g., acetyl-CoA), and then the latter is used to synthesize PHA monomers (Jiang et al., 2011; van Aalst-van Leeuwen et al., 1997). Several models have been described in the literature to estimate theoretical PHB yields. For instance, Beun et al. (2002) modified a metabolic model to perform detailed energetic and stochiometric analysis, which enabled to estimate the theoretical yields and maintenance coefficients (Beun et al., 2002; van Aalst-van Leeuwen et al., 1997). However, since PHA and cell are synthesized similarly, theoretical cell and PHA yields can be estimated by following the same procedure. Several approaches have been suggested to estimate theoretical cell yields in the literature (Dias et al., 2005; van Aalst-van Leeuwen et al.,

1997). For example, the Thermodynamic Electron Equivalents Model (TEEM1) was introduced to predict bacterial cell yields based on electron equivalents (Rittmann & McCarty, 2001). The TEEM1 utilizes the reduction half-reactions of electron donors, terminal electron acceptors, and cell synthesis to obtain balanced stoichiometric equations, which can be used to predict biomass yields (McCarty, 2007; Rittmann & McCarty, 2001). Therefore, we applied the TEEM1 to predict theoretical PHA and cell yields in PHA accumulators under autotrophic and heterotrophic conditions.

Cupriavidus necator has unique metabolic capabilities as it can grow under autotrophic or heterotrophic conditions. As a heterotrophic bacterium, *C. necator* can grow and accumulate PHB by utilizing organic substrates such as acetate (Marudkla et al., 2018; Sugimoto et al., 1999), glucose (Biglari et al., 2020), commercial glycerol (Mothes et al., 2007; Tanadchangsaeng & Yu, 2012). *C. necator* can also grow autotrophically by utilizing a mixture of H_2, O_2, and CO_2 (DeCicco & Stukus, 1968; Takeshita & Ishizaki, 1996). *C. necator* can also consume organic substrates along with inorganic carbon, which is known as mixotrophic growth (Rittenberg et al., 1969; Jawed et al., 2022; Kärst & Friedrich, 1984). In addition, *C. necator* can accumulate up to 90% (w/w) of the cell dry weight as PHB using different metabolic pathways (Jawed et al., 2022; López-Cuellar et al., 2011; Passanha et al., 2013). Therefore, we conducted lab-scale experiments to assess the impact of cultivation conditions on the metabolic responses of *C. necator*, and to study the impact of supplied organic and inorganic substrates on the lag phase length of *C. necator*.

1.5. Literature review on the enrichment of PHA accumulators

The current commercial large-scale facilities utilize pure cultures for PHA production (Argiz et al., 2020; Korkakaki et al., 2016). Among over 300 identified PHA accumulators, only a few microorganisms such as *Cupriavidus necator*, *Alcaligenes latus*, *Protomonas extorquens*, *Pseudomonas oleovorans*, *Azotobacter vinelandii*, *Paracoccus denitrificans*, and

recombinant *E. coli* are employed in industrial PHA production because of their high PHA-production capacities (Grothe & Chisti, 2000; Hänggi, 1990; S. Y. Lee, 1996b).

The current production costs of PHA-based plastics are higher than that of the petroleum-based plastics by 5 to 10 times. Around 50% of the overall production cost is due to the organic substrates (Kim, 2000). As a result, PHA production using mixed microbial cultures (MMCs) is gaining an increased attention over pure culture-based production. The application of MMCs to produce PHA has many advantages including the availability of inexpensive organic substrates (e.g., organic wastes) and elimination of the requirements for sterilized conditions (Fang et al., 2019; Kumar et al., 2020; Oliveira et al., 2017).

To allow PHA production using MMCs, the enrichment of PHA accumulators in mixed cultures is an essential step before PHA accumulation using specific waste feedstocks. Several approaches were applied to select and enrich microbial populations with high-PHA storing capacities. The aerobic dynamic feeding strategy, known also as feast-famine process, is the most accepted strategy for enriching PHA accumulators in mixed cultures (Chen et al., 2016). In the feast stage, the external carbon substrates are supplied in excess so that PHA accumulators can simultaneously grow and store PHA inside their cells. In the famine cycle, only PHA accumulators can continue to grow using the internally stored PHA after the consumption of external organic substrates, while non-PHA accumulators start to starve because of the absence of carbon sources. This ecological advantage enables PHA accumulators to strongly outcompete with other heterotrophs and eventually dominate the cultures after several enrichment cycles (Chen et al., 2016; Fang et al., 2019). The feast-famine enrichment method was successfully applied to obtain enriched cultures that can accumulate PHA up to 89% of the cell dry weight (Johnson et al., 2009).

The competition between PHA-accumulating and non-PHA-accumulating bacteria in mixed cultures was not comprehensively modeled in previous studies (Fang et al., 2019; Marang et al., 2015; Mozumder et al., 2020). For instance, Activated Sludge Model No. 3 (ASM3) does not describe the simultaneous microbial growth and PHA storage. Instead, the model assumed that all heterotrophs convert organic substrates into internal storage products inside bacterial cells before utilizing the stored products for growth purposes (Gujer et al., 1999; Henze et al., 2000; Ni et al., 2009, 2010; Ni & Yu, 2007, 2008). As a result, ASM3 cannot be applied to simulate feast-famine enrichments (Sin et al., 2005). Therefore, in this thesis, we aimed to develop and calibrate a comprehensive mathematical model (based on ASM3) to describe the distinct PHA-storage capabilities of heterotrophs, and to simulate the competition between PHA accumulators and non-PHA accumulators in conventional feast-famine enrichments.

The major drawback of the feast-famine enrichment strategy is the long time required to obtain a culture with high PHA-accumulating capacities (Jiang, Marang, et al., 2011b; Johnson, Kleerebezem, et al., 2010a, 2010b; Marang et al., 2014). For instance, it took 23 months to obtain a mixed culture able to accumulate PHA up to 70% (w/w) by using the conventional feast-famine strategy (Marang et al., 2016). In addition, some stability issues such as sludge bulking were reported to impact the process operation (Martins et al., 2011; Wen et al., 2012). Therefore, alternative enrichment methods have been suggested to overcome the drawbacks of the feast-famine strategy. For example, the addition of settling and withdrawal steps to the feast-famine cycles exerted additional physical pressure on the selectivity of PHA accumulators, resulting in an enriched culture with PHA-accumulating capacity up to 74% after 30 days of operation (Chen et al., 2015). The focus of previous studies was mainly on improving PHA accumulation without trying to minimize the enrichment time which substantially affects the PHA production costs using MMCs. Thus, this thesis aimed to develop

a rapid enrichment strategy for mixed microbial cultures by including the autotrophic growth conditions.

1.6. Research objectives

The research work conducted in this thesis aims to provide sustainable biotechnological solutions to three major environmental challenges: Pb(II) contamination, petroleum-based plastics, and climate change due to greenhouse gas emissions. In this thesis, we investigated microorganisms to reduce Pb(II) to metallic Pb to decrease Pb(II) toxicity. Also, we studied and modeled the enrichment and growth of representative PHA accumulators such as *Cupriavidus necator* and *Plasticicumulans acidivorans* in pure and mixed microbial cultures. The specific research objectives were:

- To isolate and identify Pb(II)-reducing bacteria; investigate the microbial growth of the isolated microbes using Pb(II) as a terminal electron acceptor; and demonstrate metallic Pb formation separately from lead phosphate precipitation (Chapter 2).
- To estimate theoretical PHA yields by using the thermodynamic energetics for organic and organic substrates, electron donors, electron acceptors, and products; estimate the free energy of formation of several PHA monomers; calculate theoretical PHB and cell yields for PHA accumulators under autotrophic and heterotrophic conditions; and study the impact of ambient conditions on theoretical PHA yields (Chapter 3).
- To investigate the impact of cultivation conditions on the microbial responses of *Cupriavidus necator*; study the impact of the compositions and pressures of the gaseous substrates (O_2, CO_2, and H_2) on autotrophic growth; investigate several strategies to increase autotrophic biomass yields; examine the heterotrophic and mixotrophic growth on acetate, glucose, and glycerol; and study *C. necator* ability to switch between heterotrophic and autotrophic conditions in two-stage cultivation systems (Chapter 4).

- To develop and calibrate a mathematical model to comprehensively describe heterotrophs with distinct PHA-storage capabilities; simulate the competition between PHA accumulators and non-PHA accumulators in feast-famine enrichments; investigate the influence of the uncertainty in model kinetics on the enrichment of PHA accumulators; study the impact of operational parameters such as solids retention time, carbon-to-nitrogen ratio, and cycle length on the enrichment of PHA accumulators in mixed cultures (Chapter 5).
- To develop a rapid enrichment method for PHA accumulators as a potential alternative to the feast-famine enrichment strategy; cultivate *Cupriavidus necator* in mixed cultures without the need to sterilize growth solutions; compare between the autotrophic, alternating autotrophic-heterotrophic, and heterotrophic enrichment cycles; and study PHA accumulation by the enriched cultures (Chapter 6).

References

Agustín Martinez, G., Bertin, L., Scoma, A., Rebecchi, S., Braunegg, G., & Fava, F. (2015). Production of polyhydroxyalkanoates from dephenolised and fermented olive mill wastewaters by employing a pure culture of *Cupriavidus necator*. *Biochemical Engineering Journal*, *97*, 92–100. https://doi.org/10.1016/j.bej.2015.02.015

Almeida, J. R., Serrano, E., Fernandez, M., Fradinho, J. C., Oehmen, A., & Reis, M. A. M. (2021). Polyhydroxyalkanoates production from fermented domestic wastewater using phototrophic mixed cultures. *Water Research*, *197*, 117101. https://doi.org/https://doi.org/10.1016/j.watres.2021.117101

Argiz, L., Fra-Vázquez, A., del Río, Á. V., & Mosquera-Corral, A. (2020). Optimization of an enriched mixed culture to increase PHA accumulation using industrial saline complex wastewater as a substrate. *Chemosphere*, *247*, 125873. https://doi.org/10.1016/j.chemosphere.2020.125873

Bao, S., Li, K., Ning, P., Peng, J., Jin, X., & Tang, L. (2017). Highly effective removal of mercury and lead ions from wastewater by mercaptoamine-functionalised silica-coated magnetic nano-adsorbents: Behaviours and mechanisms. *Applied Surface Science*, *393*, 457–466. https://doi.org/10.1016/j.apsusc.2016.09.098

Beun, J. J., Dircks, K., Van Loosdrecht, M. C. M., & Heijnen, J. J. (2002). Poly-β-hydroxybutyrate metabolism in dynamically fed mixed microbial cultures. *Water Research*, *36*(5), 1167–1180. https://doi.org/10.1016/S0043-1354(01)00317-7

Biglari, N., Orita, I., Fukui, T., & Sudesh, K. (2020). A study on the effects of increment and decrement repeated fed-batch feeding of glucose on the production of poly(3-hydroxybutyrate) [P(3HB)] by a newly engineered *Cupriavidus necator* NSDG-GG mutant in batch fill-and-draw fermentation. *Journal of Biotechnology*, *307*, 77–86. https://doi.org/https://doi.org/10.1016/j.jbiotec.2019.10.013

Bishop, G., Styles, D., & Lens, P. N. L. (2021). Environmental performance comparison of bioplastics and petrochemical plastics: A review of life cycle assessment (LCA) methodological decisions. *Resources, Conservation and Recycling*, *168*, 105451. https://doi.org/https://doi.org/10.1016/j.resconrec.2021.105451

Brink, H. G., Hörstmann, C., & Feucht, C. B. (2019). Microbial Pb(II) precipitation: Minimum inhibitory concentration and precipitate identity. *Chemical Engineering Transactions*, *74*, 1453–1458. https://doi.org/10.3303/CET1974243

Brink, H. G., Hörstmann, C., & Peens, J. (2020). Microbial Pb(II)-precipitation: the influence of oxygen on Pb(II)-removal from aqueous environment and the resulting precipitate identity. *International Journal of Environmental Science and Technology*, *17*(1), 409–420. https://doi.org/10.1007/s13762-019-02502-4

Brink, H. G., Lategan, M., Naude, K., & Chirwa, E. M. N. (2017). Microbial precipitation of lead (II) by industrially obtained consortia. *International Conference on Energy, Environment and Climate Change (ICEECC 2017), Mauritius*.

Rittenberg, S. C., & Goodman, N. S. (1969). Mixotrophic Growth of *Hydrogenomonas eutropha*. *Journal of Bacteriology*, *98*(2), 617–622. https://doi.org/10.1128/jb.98.2.617-622.1969.

Carpine, R., Olivieri, G., Hellingwerf, K. J., Pollio, A., & Marzocchella, A. (2020). Industrial production of poly-β-hydroxybutyrate from CO_2: Can cyanobacteria meet this challenge? *Processes*, *8*(3), 323. https://doi.org/10.3390/pr8030323

Chen, Z., Guo, Z., Wen, Q., Huang, L., Bakke, R., & Du, M. (2015). A new method for polyhydroxyalkanoate (PHA) accumulating bacteria selection under physical selective pressure. *International Journal of Biological Macromolecules*, *72*, 1329–1334. https://doi.org/10.1016/j.ijbiomac.2014.10.027

Chen, Z., Guo, Z., Wen, Q., Huang, L., Bakke, R., & Du, M. (2016). Modeling polyhydroxyalkanoate (PHA) production in a newly developed aerobic dynamic discharge (ADD) culture enrichment process. *Chemical Engineering Journal*, *298*, 36–43. https://doi.org/10.1016/j.cej.2016.03.133

Chua, A. S. M., Takabatake, H., Satoh, H., & Mino, T. (2003). Production of polyhydroxyalkanoates (PHA) by activated sludge treating municipal wastewater: Effect of pH, sludge retention time (SRT), and acetate concentration in influent. *Water Research*, *37*(15), 3602–3611. https://doi.org/10.1016/S0043-1354(03)00252-5

Colantonio, N., & Kim, Y. (2016). Lead(II) Removal at the Bioanode of Microbial Electrolysis Cells. *ChemistrySelect*, *1*(18), 5743–5748. https://doi.org/10.1002/slct.201601539

Cramm, R. (2009). Genomic View of Energy Metabolism in *Ralstonia eutropha* H16. *Microbial Physiology*, *16*(1–2), 38–52. https://doi.org/10.1159/000142893

DeCicco, B. T., & Stukus, P. E. (1968). Autotrophic and heterotrophic metabolism of *hydrogenomonas*. growth yields and patterns under dual substrate conditions. *Journal of Bacteriology*, *95*(4), 1469–1475.

Dias, J. M. L., Serafim, L. S., Lemos, P. C., Reis, M. A. M., & Oliveira, R. (2005). Mathematical modelling of a mixed culture cultivation process for the production of polyhydroxybutyrate. *Biotechnology and Bioengineering*, *92*(2), 209–222. https://doi.org/10.1002/bit.20598

E., S. P., & T., D. B. (1970). Autotrophic and Heterotrophic Metabolism of *Hydrogenomonas*: Regulation of Autotrophic Growth by Organic Substrates. *Journal of Bacteriology*, *101*(2), 339–345. https://doi.org/10.1128/jb.101.2.339-345.1970

Estévez-Alonso, Á., Pei, R., Van Loosdrecht, M. C. M., Kleerebezem, R., & Werker, A. (2021). Scaling-up microbial community-based polyhydroxyalkanoate production: status and challenges. *Bioresource Technology*, *327*, 124790. https://doi.org/https://doi.org/10.1016/j.biortech.2021.124790

Fang, F., Xu, R. Z., Huang, Y. Q., Wang, S. N., Zhang, L. L., Dong, J. Y., Xie, W. M., Chen, X., & Cao, J. S. (2019). Production of polyhydroxyalkanoates and enrichment of associated microbes in bioreactors fed with rice winery wastewater at various organic loading rates. *Bioresource Technology*, *292*, 121978. https://doi.org/10.1016/j.biortech.2019.121978

Gahlawat, G., & Srivastava, A. K. (2013). Development of a mathematical model for the growth associated Polyhydroxybutyrate fermentation by *Azohydromonas australica* and its use for the design of fed-batch cultivation strategies. *Bioresource Technology*, *137*, 98–105. https://doi.org/10.1016/j.biortech.2013.03.023

Grothe, E., & Chisti, Y. (2000). Poly(β-hydroxybutyric acid) thermoplastic production by *Alcaligenes latus*: Behavior of fed-batch cultures. *Bioprocess Engineering*, *22*(5), 441–449. https://doi.org/10.1007/s004490050757

Gujer, W., Henze, M., Mino, T., & Van Loosdrecht, M. (1999). Activated sludge model no. 3. *Water Science and Technology*, *39*(1), 183–193.

Hänggi, U. J. (1990). Pilot scale production of PHB with *Alcaligenes latus*. In *Novel Biodegradable Microbial Polymers* (pp. 65–70). Springer. https://doi.org/10.1007/978-94-009-2129-0_6

Hassan, M. A., Yee, L.-N., Yee, P. L., Ariffin, H., Raha, A. R., Shirai, Y., & Sudesh, K. (2013). Sustainable production of polyhydroxyalkanoates from renewable oil-palm biomass. *Biomass and Bioenergy*, *50*, 1–9. https://doi.org/https://doi.org/10.1016/j.biombioe.2012.10.014

Henze, M., Gujer, W., Mino, T., & Van Loosedrecht, M. (2000). Activated Sludge Models ASM1, ASM2, ASM2d and ASM3. In *Water Intelligence Online* (Vol. 5, Issue 0). IWA publishing. https://doi.org/10.2166/9781780402369

Ishizaki, A., Tanaka, K., & Taga, N. (2001). Microbial production of poly-D-3-hydroxybutyrate from CO_2. *Applied Microbiology and Biotechnology*, *57*(1–2), 6–12.

Jannati, M. (2019). Bio-electrochemical removal of Lead by exoelectrogens and phosphate removal using zeolite for potential industrial wastewater treatment (Master dissertation).

Jawed, K., Irorere, V. U., Bommareddy, R. R., Minton, N. P., & Kovács, K. (2022). Establishing mixotrophic growth of *Cupriavidus necator* H16 on CO_2 and volatile fatty acids. In *Fermentation* (Vol. 8, Issue 3). https://doi.org/10.3390/fermentation8030125

Jiang, Y., Hebly, M., Kleerebezem, R., Muyzer, G., & Van Loosdrecht, M. C. M. (2011). Metabolic modeling of mixed substrate uptake for polyhydroxyalkanoate (PHA) production. *Water Research*, *45*(3), 1309–1321. https://doi.org/10.1016/j.watres.2010.10.009

Jiang, Y., Marang, L., Kleerebezem, R., Muyzer, G., & Van Loosdrecht, M. C. M. (2011). Polyhydroxybutyrate production from lactate using a mixed microbial culture. *Biotechnology and Bioengineering*, *108*(9), 2022–2035. https://doi.org/10.1002/bit.23148

Johnson, K., Jiang, Y., Kleerebezem, R., Muyzer, G., & Van Loosdrecht, M. C. M. (2009). Enrichment of a mixed bacterial culture with a high polyhydroxyalkanoate storage capacity. *Biomacromolecules*, *10*(4), 670–676. https://doi.org/10.1021/bm8013796

Johnson, K., Kleerebezem, R., & Van Loosdrecht, M. C. M. (2010a). Influence of ammonium on the accumulation of polyhydroxybutyrate (PHB) in aerobic open mixed cultures. *Journal of Biotechnology*, *147*(2), 73–79. https://doi.org/10.1016/j.jbiotec.2010.02.003

Johnson, K., Kleerebezem, R., & Van Loosdrecht, M. C. M. (2010b). Influence of the C/N ratio on the performance of polyhydroxybutyrate (PHB) producing sequencing batch reactors at short SRTs. *Water Research*, *44*(7), 2141–2152. https://doi.org/10.1016/j.watres.2009.12.031

Kärst, U. W. E., & Friedrich, C. G. (1984). Mixotrophic capabilities of *Alcaligenes eutrophus*. *Microbiology*, *130*(8), 1987–1994. https://doi.org/10.1099/00221287-130-8-1987

Khatami, K., Perez-Zabaleta, M., Owusu-Agyeman, I., & Cetecioglu, Z. (2021). Waste to bioplastics: How close are we to sustainable polyhydroxyalkanoates production? *Waste Management*, *119*, 374–388. https://doi.org/https://doi.org/10.1016/j.wasman.2020.10.008

Korkakaki, E., Van Loosdrecht, M. C. M., & Kleerebezem, R. (2016). Survival of the fastest: Selective removal of the side population for enhanced PHA production in a mixed substrate enrichment. *Bioresource Technology*, *216*, 1022–1029. https://doi.org/10.1016/j.biortech.2016.05.125

Kourmentza, C., Plácido, J., Venetsaneas, N., Burniol-Figols, A., Varrone, C., Gavala, H. N., & Reis, M. A. M. (2017). Recent advances and challenges towards sustainable polyhydroxyalkanoate (PHA) production. *Bioengineering*, *4*(2), 55. https://doi.org/10.3390/bioengineering4020055

Kumar, M., Rathour, R., Singh, R., Sun, Y., Pandey, A., Gnansounou, E., Lin, K.-Y. A., Tsang, D. C. W., & Thakur, I. S. (2020). Bacterial polyhydroxyalkanoates: Opportunities, challenges, and prospects. *Journal of Cleaner Production*, 121500.

Lee, J., Park, H. J., Moon, M., Lee, J.-S., & Min, K. (2021). Recent progress and challenges in microbial polyhydroxybutyrate (PHB) production from CO_2 as a sustainable feedstock: A state-of-the-art review. *Bioresource Technology*, 125616.

Lee, S. Y. (1996). Plastic bacteria? Progress and prospects for polyhydroxyalkanoate production in bacteria. *Trends in Biotechnology*, *14*(11), 431–438.

Lemoigne, M. (1926). Produits de deshydration et de polymerisation de l'acide β= oxybutyrique. *Bull. Soc. Chim. Biol.*, *8*, 770–782.

Levinson, H. S., Mahler, I., Blackwelder, P., & Hood, T. (1996). Lead resistance and sensitivity in *Staphylococcus aureus*. *FEMS Microbiology Letters*, *145*(3), 421–425. https://doi.org/10.1016/S0378-1097(96)00443-0

Lloyd, J. R. (2003). Microbial reduction of metals and radionuclides. *FEMS Microbiology Reviews*, *27*(2–3), 411–425. https://doi.org/10.1016/S0168-6445(03)00044-5

Lovley, D. R. (1993). Dissimilatory metal reduction. *Annual Review of Microbiology*, *47*(1), 263–290. https://doi.org/10.1146/annurev.mi.47.100193.001403

Lovley, D. R., Phillips, E. J. P., Gorby, Y. A., & Landa, E. R. (1991). Microbial reduction of uranium. *Nature*, *350*(6317), 413–416. https://doi.org/10.1038/350413a0

Lovley, D. R., Stolz, J. F., Nord, G. L., & Phillips, E. J. P. (1987). Anaerobic production of magnetite by a dissimilatory iron-reducing microorganism. *Nature*, *330*(6145), 252–254.

Mannina, G., Presti, D., Montiel-Jarillo, G., Carrera, J., & Suárez-Ojeda, M. E. (2020). Recovery of polyhydroxyalkanoates (PHAs) from wastewater: A review. *Bioresource Technology*, *297*, 122478. https://doi.org/https://doi.org/10.1016/j.biortech.2019.122478

Marang, L., Jiang, Y., Van Loosdrecht, M. C. M., & Kleerebezem, R. (2014). Impact of non-storing biomass on PHA production: An enrichment culture on acetate and methanol. *International Journal of Biological Macromolecules*, *71*, 74–80. https://doi.org/10.1016/j.ijbiomac.2014.04.051

Marang, L., Van Loosdrecht, M. C. M., & Kleerebezem, R. (2015). Modeling the competition between PHA-producing and non-PHA-producing bacteria in feast-famine SBR and staged CSTR systems. *Biotechnology and Bioengineering*, *112*(12), 2475–2484. https://doi.org/10.1002/bit.25674

Marang, L., Van Loosdrecht, M. C. M., & Kleerebezem, R. (2016). Combining the enrichment and accumulation step in non-axenic PHA production: Cultivation of Plasticicumulans acidivorans at high volume exchange ratios. *Journal of Biotechnology*, *231*, 260–267. https://doi.org/10.1016/j.jbiotec.2016.06.016

Martins, A. M. P., Karahan, Ö., & Van Loosdrecht, M. C. M. (2011). Effect of polymeric substrate on sludge settleability. *Water Research*, *45*(1), 263–273. https://doi.org/https://doi.org/10.1016/j.watres.2010.07.055

Marudkla, J., Lee, W.-C., Wannawilai, S., Chisti, Y., & Sirisansaneeyakul, S. (2018). Model of acetic acid-affected growth and poly(3-hydroxybutyrate) production by *Cupriavidus*

necator DSM 545. *Journal of Biotechnology*, *268*, 12–20. https://doi.org/https://doi.org/10.1016/j.jbiotec.2018.01.004

Mascarenhas, J., & Aruna, K. (2017). Screening of Polyhydroxyalkanoates (PHA) accumulating bacteria from diverse habitats. *Journal of Global Biosciences*, *6*(3), 4835–4848. http://www.mutagens.co.in/jgb/vol.06/3/060304.pdf

Matos, M., Cruz, R. A. P., Cardoso, P., Silva, F., Freitas, E. B., Carvalho, G., & Reis, M. A. M. (2021). Sludge retention time impacts on polyhydroxyalkanoate productivity in uncoupled storage/growth processes. *Science of The Total Environment*, *799*, 149363. https://doi.org/https://doi.org/10.1016/j.scitotenv.2021.149363

Matta, G., & Gjyli, L. (2016). Mercury, lead and arsenic: Impact on environment and human health. *Journal of Chemical and Pharmaceutical Sciences*, *9*(2), 718–725.

McCarty, P. L. (2007). Thermodynamic electron equivalents model for bacterial yield prediction: modifications and comparative evaluations. *Biotechnology and Bioengineering*, *97*(2), 377–388.

Miyahara, Y., Yamamoto, M., Thorbecke, R., Mizuno, S., & Tsuge, T. (2020). Autotrophic biosynthesis of polyhydroxyalkanoate by Ralstonia eutropha from non-combustible gas mixture with low hydrogen content. *Biotechnology Letters*, *42*(9), 1655–1662. https://doi.org/10.1007/s10529-020-02876-3

Modestra, J. A., Velvizhi, G., Krishna, K. V., Arunasri, K., Lens, P. N. L., Nancharaiah, Y., & Venkata Mohan, S. (2017). Bioelectrochemical Systems for Heavy Metal Removal and Recovery. In *Sustainable Heavy Metal Remediation* (pp. 165–198). Springer. https://doi.org/10.1007/978-3-319-58622-9_6

Mohamad Fauzi, A. H., Chua, A. S. M., Yoon, L. W., Nittami, T., & Yeoh, H. K. (2019). Enrichment of PHA-accumulators for sustainable PHA production from crude glycerol. *Process Safety and Environmental Protection*, *122*, 200–208. https://doi.org/https://doi.org/10.1016/j.psep.2018.12.002

Moita, R., Freches, A., & Lemos, P. C. (2014). Crude glycerol as feedstock for polyhydroxyalkanoates production by mixed microbial cultures. *Water Research*, *58*, 9–20. https://doi.org/10.1016/j.watres.2014.03.066

Moralejo-Gárate, H., Kleerebezem, R., Mosquera-Corral, A., Campos, J. L., Palmeiro-Sánchez, T., & Van Loosdrecht, M. C. M. (2014). Substrate versatility of polyhydroxyalkanoate producing glycerol grown bacterial enrichment culture. *Water Research*, *66*, 190–198. https://doi.org/10.1016/j.watres.2014.07.044

Mothes, G., Schnorpfeil, C., & Ackermann, J. (2007). Production of PHB from crude glycerol. *Engineering in Life Sciences*, *7*(5), 475–479.

Mozumder, M. S. I., Amin, M. S. A., & Shishir, M. F. R. (2020). Unified model to predict and enhance the mixed culture polyhydroxyalkanoates (PHA) production. *Bioresource Technology Reports*, *11*, 100537. https://doi.org/10.1016/j.biteb.2020.100537

Müller, J., MacEachran, D., Burd, H., Sathitsuksanoh, N., Bi, C., Yeh, Y. C., Lee, T. S., Hillson, N. J., Chhabra, S. R., Singer, S. W., & Beller, H. R. (2013). Engineering of Ralstonia

eutropha H16 for autotrophic and heterotrophic production of methyl ketones. *Applied and Environmental Microbiology*, *79*(14), 4433–4439. https://doi.org/10.1128/AEM.00973-13

Naik, M. M., & Dubey, S. K. (2011). Lead-enhanced siderophore production and alteration in cell morphology in a Pb-resistant *Pseudomonas aeruginosa* strain 4EA. *Current Microbiology*, *62*(2), 409–414.

Naik, M. M., & Dubey, S. K. (2013). Lead resistant bacteria: Lead resistance mechanisms, their applications in lead bioremediation and biomonitoring. *Ecotoxicology and Environmental Safety*, *98*, 1–7. https://doi.org/10.1016/j.ecoenv.2013.09.039

Naik, M. M., Khanolkar, D., & Dubey, S. K. (2013). Lead-resistant *Providencia alcalifaciens* strain 2 EA bioprecipitates Pb^{+2} as lead phosphate. *Letters in Applied Microbiology*, *56*(2), 99–104.

Ni, B. J., Fang, F., Rittmann, B. E., & Yu, H. Q. (2009). Modeling microbial products in activated sludge under feast-famine conditions. *Environmental Science and Technology*, *43*(7), 2489–2497. https://doi.org/10.1021/es8026693

Ni, B. J., Rittmann, B. E., Fang, F., Xu, J., & Yu, H. Q. (2010). Long-term formation of microbial products in a sequencing batch reactor. *Water Research*, *44*(13), 3787–3796. https://doi.org/10.1016/j.watres.2010.04.035

Ni, B. J., & Yu, H. Q. (2007). A new kinetic approach to microbial storage process. *Applied Microbiology and Biotechnology*, *76*(6), 1431–1438. https://doi.org/10.1007/s00253-007-1104-8

Ni, B. J., & Yu, H. Q. (2008). Simulation of heterotrophic storage and growth processes in activated sludge under aerobic conditions. *Chemical Engineering Journal*, *140*(1–3), 101–109. https://doi.org/10.1016/j.cej.2007.09.017

Oliveira, C. S. S., Silva, C. E., Carvalho, G., & Reis, M. A. (2017). Strategies for efficiently selecting PHA producing mixed microbial cultures using complex feedstocks: Feast and famine regime and uncoupled carbon and nitrogen availabilities. *New Biotechnology*, *37*, 69–79. https://doi.org/10.1016/j.nbt.2016.10.008

Peens, J., Wu, Y. W., & Brink, H. G. (2018). Microbial Pb(II) precipitation: The influence of elevated Pb(II) concentrations. *Chemical Engineering Transactions*, *64*, 583–588. https://doi.org/10.3303/CET1864098

Pérez Rivero, C., Sun, C., Theodoropoulos, C., & Webb, C. (2016). Building a predictive model for PHB production from glycerol. *Biochemical Engineering Journal*, *116*, 113–121. https://doi.org/https://doi.org/10.1016/j.bej.2016.04.016

Rahman, Z., & Singh, V. P. (2019). The relative impact of toxic heavy metals (THMs) (arsenic (As), cadmium (Cd), chromium (Cr)(VI), mercury (Hg), and lead (Pb)) on the total environment: an overview. *Environmental Monitoring and Assessment*, *191*(7), 1–21.

Raza, Z. A., Abid, S., & Banat, I. M. (2018). Polyhydroxyalkanoates: Characteristics, production, recent developments and applications. *International Biodeterioration & Biodegradation*, *126*, 45–56.

Repaske, R., & Repaske, A. C. (1976). Quantitative requirements for exponential growth of *Alcaligenes eutrophus*. *Applied and Environmental Microbiology*, *32*(4), 585–591. https://doi.org/10.1128/aem.32.4.585-591.1976

Rittmann, B. E., & McCarty, P. L. (2001). Environmental biotechnology: principles and applications. McGraw-Hill Education (USA).

Ryu, H. W., Cho, K. S., Goodrich, P. R., & Park, C. H. (2008). Production of polyhydroxyalkanoates by Azotobacter vinelandii UWD using swine wastewater: Effect of supplementing glucose, yeast extract, and inorganic salts. *Biotechnology and Bioprocess Engineering*, *13*(6), 651–658. https://doi.org/10.1007/s12257-008-0072-x

Schmieman, E. A., Yonge, D. R., Rege, M. A., Petersen, J. N., Turick, C. E., Johnstone, D. L., & Apel, W. A. (1998). Comparative kinetics of bacterial reduction of chromium. *Journal of Environmental Engineering*, *124*(5), 449–455. https://doi.org/10.1061/(asce)0733-9372(1998)124:5(449)

Sin, G., Guisasola, A., de Pauw, D. J. W., Baeza, J. A., Carrera, J., & Vanrolleghem, P. A. (2005). A new approach for modelling simultaneous storage and growth processes for activated sludge systems under aerobic conditions. *Biotechnology and Bioengineering*, *92*(5), 600–613. https://doi.org/10.1002/bit.20741

Sohn, Y. J., Son, J., Jo, S. Y., Park, S. Y., Yoo, J. I., Baritugo, K.-A., Na, J. G., Choi, J., Kim, H. T., Joo, J. C., & Park, S. J. (2021). Chemoautotroph *Cupriavidus necator* as a potential game-changer for global warming and plastic waste problem: A review. *Bioresource Technology*, *340*, 125693. https://doi.org/https://doi.org/10.1016/j.biortech.2021.125693

Sugimoto, T., Tsuge, T., Tanaka, K., & Ishizaki, A. (1999). Control of acetic acid concentration by pH-stat continuous substrate feeding in heterotrophic culture phase of two-stage cultivation of *Alcaligenes eutrophus* for production of P (3HB) from CO_2, H_2, and O_2 under non-explosive conditions. *Biotechnology and Bioengineering*, *62*(6), 625–631.

Takeshita, T., & Ishizaki, A. (1996). Influence of hydrogen limitation on gaseous substrate utilization in autotrophic culture of *Alcaligenes eutrophus* ATCC 17697T. *Journal of Fermentation and Bioengineering*, *81*(1), 83–86. https://doi.org/https://doi.org/10.1016/0922-338X(96)83127-8

Tanadchangsaeng, N., & Yu, J. (2012). Microbial synthesis of polyhydroxybutyrate from glycerol: Gluconeogenesis, molecular weight and material properties of biopolyester. *Biotechnology and Bioengineering*, *109*(11), 2808–2818. https://doi.org/https://doi.org/10.1002/bit.24546

Tiemeyer, A., Link, H., & Weuster-Botz, D. (2007). Kinetic studies on autohydrogenotrophic growth of Ralstonia eutropha with nitrate as terminal electron acceptor. *Applied Microbiology and Biotechnology*, *76*(1), 75–81. https://doi.org/10.1007/s00253-007-0983-z

Tiquia-Arashiro, S. M. (2018). Lead absorption mechanisms in bacteria as strategies for lead bioremediation. *Applied Microbiology and Biotechnology*, *102*(13), 5437–5444. https://doi.org/10.1007/s00253-018-8969-6

van Aalst-van Leeuwen, M. A., Pot, M. A., Van Loosdrecht, M. C. M., & Heijnen, J. J. (1997). Kinetic modeling of poly(β-hydroxybutyrate) production and consumption by *Paracoccus pantotrophus* under dynamic substrate supply. *Biotechnology and Bioengineering*, *55*(5), 773–782. https://doi.org/10.1002/(SICI)1097-0290(19970905)55:5<773::AID-BIT7>3.0.CO;2-8

Verlinden, R. A. J., Hill, D. J., Kenward, M. A., Williams, C. D., Piotrowska-Seget, Z., & Radecka, I. K. (2011). Production of polyhydroxyalkanoates from waste frying oil by cupriavidus necator. *AMB Express*, *1*(1), 1–8. https://doi.org/10.1186/2191-0855-1-11

Volova, T. G., Kalacheva, G. S., & Altukhova, O. v. (2002). Autotrophic synthesis of polyhydroxyalkanoates by the bacteria *Ralstonia eutropha* in the presence of carbon monoxide. *Applied Microbiology and Biotechnology*, *58*(5), 675–678. https://doi.org/10.1007/s00253-002-0941-8

Wen, Q., Chen, Z., Wang, C., & Ren, N. (2012). Bulking sludge for PHA production: Energy saving and comparative storage capacity with well-settled sludge. *Journal of Environmental Sciences*, *24*(10), 1744–1752. https://doi.org/https://doi.org/10.1016/S1001-0742(11)61005-X

Woraittinun, N., & Suwannasilp, B. B. (2017). polyhydroxyalkanoate production from different carbon substrates using sludge from a wastewater treatment plant: Microbial communities, polymer compositions, and thermal characteristics. *Environmental Progress and Sustainable Energy*, *36*(6), 1754–1764. https://doi.org/10.1002/ep.12645

2. Isolation of Pb(II)-reducing bacteria and demonstration of biological Pb(II) reduction to metallic Pb

Lead (Pb) is a major environmental pollutant found in industrial wastewater and mining areas. Pb causes major health problems to humans and is highly toxic to microorganisms. The current removal methods apply chemical treatment methods which produce large amounts of highly concentrated sludge. In this study, we isolated several bacterial species that can reduce Pb(II) to metallic Pb^0. The isolated bacteria were investigated for the ability to grow on acetate as the electron donor and Pb(II) as the only terminal electron acceptor under anaerobic conditions. Biological Pb(II) reduction can efficiently be applied in the remediation of groundwater and water streams contaminated with Pb(II).

The following published journal article is included in this chapter:

- Amer, A., and Kim, Y. (2022). Isolation of Pb (II)-reducing bacteria and demonstration of biological Pb (II) reduction to metallic Pb. Journal of Hazardous Materials, 423, 126975.

The co-author's contributions include:

- Supervision.
- Funding acquisition and conceptulization.
- Manuscript revision.

Abstract

Pb(II) contamination imposes serious threats to human health and the environment. Biological reduction of Pb(II) to metallic Pb is an attractive method for remediation of Pb(II)-contaminated water and sediments. In this study, Pb(II)-reducing microorganisms were isolated by the dilution-to-extinction (DTE) and streak-plate methods. As a result, *Delftia acidovorans*, *Azonexus caeni*, and *Comamonas testosteroni* were successfully isolated. At a high lead concentration (10 mg-Pb(II)/L), each of the isolated *D. acidovorans* strain Pb11 and *A. caeni* strain Pb2 cultures showed successful utilization of Pb(II), resulting in a 5.15- and 8.14-fold growth in 3 days, respectively. Pb(II) reduction to metallic Pb by *D. acidovorans* strain Pb11 and *A. caeni* strain Pb2 was confirmed using scanning electron microscopy and energy dispersive X-ray spectroscopy (SEM-EDS) was coupled with X-ray photoelectron spectroscopy (XPS). This strategic analysis was necessary to confirm the formation of metallic Pb separately from lead phosphate precipitates which are inevitable in the biological Pb(II) removal experiments. Among the 3 isolated microbes, *C. testosteroni* strain Pb3 did not leave immobile and detectable Pb solids in SEM-EDS analyses. *D. acidovorans* and *A. caeni* are recommended for engineered remediation of Pb(II)-contaminated wastewater and sediments.

Keywords

Bioremediation; Heavy metal contamination; Lead phosphate precipitation; Lead reduction; Metallic Pb formation

2.1. Introduction

Lead (Pb) pollution of water and wastewater streams is a serious environmental concern as Pb has toxic effects on human health (Abadin et al., 2007b; Igiri et al., 2018). In aquatic environments, Pb(II) is considered more toxic than other inorganic Pb forms as Pb(II) is highly soluble and mobile. Biological Pb(II) reduction to metallic Pb is an attractive treatment method

because $Pb^{(0)}$ is not available for metabolic uptake and metallic Pb particles can readily be separated from polluted environments (Jing & Kjellerup, 2018). Microbial Pb(II) reduction by mixed cultures has been demonstrated in previous studies (Colantonio & Kim, 2016b; Kabutey et al., 2019). Under anaerobic conditions, microorganisms can gain energy by oxidizing acetate and reducing Pb(II) to metallic Pb (Eq. 2.1).

$$CH_3COO^- + 4Pb^{2+} + 4\,H_2O \rightarrow 4Pb^0 + 2HCO_3^- + 9H^+ \quad (2.1)$$

This biological Pb(II) reduction reaction is spontaneous (ΔG=-50.3 KJ/mol) under common concentrations of reactants and products ($[CH_3COO^-]$= 12.2 mM; $[Pb^{2+}]$ = 24.13 µM (5 mg/L); $[HCO^{3-}]$ = 0.12 mM; $[H^+]$ = 10^{-7} M; and T = 30˚C, Appnedix A1) (Arnold & Brezonik, 2009). Based on the free energy calculations with the thermodynamic model, the theoretical biomass yield on Pb(II) is estimated to be 12.62 g-cells per mole Pb(II) (Appendix A) (Bruce & McCarty, 2020; McCarty, 2007). Microbial Pb(II) reduction to $Pb^{(0)}$ was previously reported in microbial electrolysis cells (MECs) at the anode chamber under open circuit conditions (Colantonio & Kim, 2016b). A subsequent study successfully utilized an enriched MEC anode to reduce and remove Pb(II) from synthetic wastewater (Jannati, 2019). A microbial consortium originally collected from Pb-batteries recycle plant could reduce and remove 90-99% of elevated Pb(II) concentrations (80-1000 ppm) under anaerobic conditions (Brink et al., 2017; Peens et al., 2018). Although biological Pb(II)-reduction was previously reported in the literature (Brink et al., 2017, 2020a; Colantonio & Kim, 2016b; Jannati, 2019; Peens et al., 2018), none of the previous studies enriched, isolated, or identified Pb(II)-reducing microorganisms. Therefore, the main goal of this study is to isolate microbial species that can reduce Pb(II) to metallic Pb.

Lead phosphate precipitation is known to be a common obstacle to demonstrating biological Pb(II) removal in research studies as lead phosphate salts are insoluble in water (Eq.

2.2 and 2.3) (Stumm & Morgan, 1996; Tiquia-Arashiro, 2018); as a result, Pb(II) removed by lead phosphate precipitation can hardly be separated from other targeted Pb forms in research experiments.

$$3\,Pb^{2+} + 2\,(PO_4)^{3-} \leftrightarrow \quad Pb_3(PO_4)_{2\,(S)} \qquad K_{SP} = 10^{-43.5} \tag{2.2}$$

$$Pb^{2+} + H^{+} + \,(PO_4)^{3-} \quad \leftrightarrow \quad PbHPO_{4\,(S)} \qquad K_{SP} = 10^{-23.8} \tag{2.3}$$

In this study, the confirmation of metallic Pb formation by Pb(II)-reducing bacteria was also a serious challenge because lead phosphate precipitates and metallic $Pb^{(0)}$ co-existed in the experimental samples. Thus, we aimed to confirm the presence of metallic Pb by applying the analytical approach developed by Brink and coauthors (Brink et al., 2020a). The specific objectives of this study were to: (1) isolate Pb(II)-reducing bacteria; (2) demonstrate metallic Pb formation separately from lead phosphate precipitation; and (3) investigate the microbial growth of the isolated microbes using Pb(II) as a terminal electron acceptor.

2.2. Materials and Methods

2.2.1. Source of microorganisms and growth solution

Samples for the isolation of potential Pb(II)-reducing microbes were effluent from a healthy lab-scale microbial electrolysis cell (MEC) fed with Pb(II). The growth solution used for all isolation and subsequent growth experiments was prepared using: 1.0 g/L of $NaCH_3COO$; 0.031 g/L NH_4Cl; 0.215 g/L NaH_2PO_4; 0.864 g/L Na_2HPO_4-$7H_2O$; 0.013 g/L KCl; and a trace amount of minerals and vitamins (Colantonio & Kim, 2016a). Acetate concentration was sufficiently high to ensure that Pb(II) was the limiting factor in the experiment. Designated Pb(II) concentrations (0.50 mg-Pb(II)/L (2.41 µM), 5.0 mg-Pb(II)/L (24.13 µM), and 10.0 mg-Pb(II)/L (48.26 µM)) were achieved by adding lead acetate ($Pb(CH_3COO)_2$) (Fisher Scientific, Canada) in the growth solution. The resulting pH of the growth solution was always between 7.0 and 7.50 in all experiments in this study (SevenMulti,

Mettler-Toledo International Inc., OH). All experiments (isolation and growth) were conducted at 30°C. For all experiments in this study, the growth solution (including Pb(II)) was purged with N_2 gas for at least 5 min to establish anaerobic conditions. The dissolved oxygen concentration was always below the detection limit (YSI 5000 dissolved oxygen instrument, OH). The purged solution was aliquoted into Hungate tubes using sterilized syringes to avoid oxygen contamination and then autoclaved before injecting microbial cultures.

2.2.2. Microbial isolation by dilution-to-extinction (DTE)

Samples from the MEC were taken and serially diluted in the growth solution with 0.50 and 5.0 mg-Pb(II)/L and kept in 10-mL electrode-free glass tubes. After 5 days of incubation, the highest diluted tube with bacterial growth was selected for the next round of the serial dilution experiment (DTE method) (Xing et al., 2010; Zuo et al., 2008). The DTE isolation experiment was performed in duplicate and repeated over four rounds. After the 4th round of DTE, the isolated microorganisms were identified based on 16S-rDNA gene sequences in Sanger sequencing.

2.2.3. Microbial isolation by streak plate method

The streak plate method was also employed for microbial isolation from the MEC effluent. The agar medium was prepared with 0.50 or 5.0 mg-Pb(II)/L in addition to the growth solution in 1.5% agar. Agar plates were streaked with MEC effluent and incubated for 5 days in a sealed jar system with an anaerobic indicator strip (VWR, Canada) (Nagy et al., 2018; Tortora et al., 2015). During the incubation, an anaerobic gas generator sachet (Oxoid™ AnaeroGen™, Thermofisher) was added into the jar to maintain anerobic conditions so that Pb(II) can be used as the only TEA in the agar medium. After the incubation, colonies on the agar plates were selected based on their shapes and colors and then transferred to anaerobic tubes with 10-mL growth solution and 0.50 or 5.0 mg-Pb(II)/L. The anaerobic tubes were incubated for 5 days before isolates were identified based on 16S rDNA gene sequences in

Sanger sequencing. It should be noted that the isolated bacteria were then transferred and cultured under anaerobic conditions with Pb(II) so that Pb(II) can only be available as the terminal electron acceptor.

2.2.4. Identification of isolated microbes

The samples from the isolation experiments (streak plate and DTE methods) were prepared for 16S rDNA gene sequencing using the colony PCR procedure (Surette Laboratory, McMaster University, Canada) (Sim et al., 2012). The PCR reaction was performed with Veriti thermal cycler (Applied Biosystems, USA) with a pair of universal bacterial primers: 8f (AGAGTTTGATCCTGGCTCAG) and 1482r (GGTTACCTTGTTACGACTT) (Caccavo et al., 1994; Xing et al., 2010). The reaction tube included: 5 µL of DNA template; 1 µL of 10 µM forward and reverse primers; 0.25 µL of Taq polymerase; 5 µL of 10x PCR buffer; 1 µL of 10 mM dNTPs ;1.5 µL of 50 mM $MgCl_2$; and dH_2O to a final volume of 50 µL. The PCR program included one cycle of heating to 94°C for 2 sec followed by 29 cycles (94°C for 30 sec, 56 °C for 30 sec, 72°C for 1 min) and a final cycle at 72°C for 10 min. In addition, Sanger sequencing was performed with the ABI BigDye™ v1.1 terminator chemistry on 3730 DNA Analyzer (Applied Biosystems, Foster City, CA, USA) (Mobix Lab, McMaster University, Canada). Sequencing results were viewed and modified by Finchtv program (Digital World Biology, Seattle, USA) and merged using the EMBOSS merger tool (Singh & Bhatia, 2016). The obtained merged sequences were tested against NCBI BLAST database to identify the isolated bacteria (available in GenBank under accession numbers from MW309863 to MW309869) (McGinnis & Madden, 2004).

2.2.5. Pb deposition on carbon fibers

Each of the isolated bacteria was further examined for its Pb(II)-reducing capability in glass tubes filled with 5-mL growth solution at 5.0 mg-Pb(II)/L. Several pieces of carbon fibers (10 µm diameter and ~2 cm long; Zoltek, USA) were added in the tubes to check if the microbes

can deposit reduced Pb on the surface of the carbon fibers. After 5-day incubation, the solution was analyzed to measure the residual Pb(II) concentrations in ICP-OES. The carbon fibers were collected and cleaned with 70% ethanol (for 60 min) and distilled water (for 30 min) for 3 times to remove attached microbial cells and then examined in scanning electron microscopy and energy dispersive X-ray spectroscopy (SEM-EDS) (JEOL JSM-6610LV, Japan) to investigate how Pb(II) was removed by the microbes (Colantonio & Kim, 2016a, 2016c). It should be noted that SEM-EDS analysis cannot distinguish between different Pb forms and was applied here to prove the microbial Pb deposition on the carbon fibers (Grimes et al., 1995; Naik et al., 2013b; Naik & Dubey, 2011b).

2.2.6. Pb(II) concentration measurement

Pb(II) concentration was measured in inductively coupled plasma-optical emission spectrometry (ICP-OES) (Vista Pro, Varian Inc., USA) according to EPA Method 200.7. A 5-mL sample was filtered (0.45 µm syringe filters, Pall Ltd., Canada), and the filtrate was acidified by adding 0.2 mL of HNO_3 (30 % v/v) prior to the ICP-OES analysis.

2.2.7. Microbial growth on Pb(II)

The capability of the isolates to utilize Pb(II) as a terminal electron acceptor was examined in an additional test (no carbon fibers in this test). Lower concentrations of *Delftia acidovorans* strain Pb11 and *Azonexus caeni* strain Pb2 (the optical density at 600 nm was ~0.001 to 0.005) were injected in glass tubes filled with 10-mL of the growth solution at different Pb(II) concentrations (0 to 10 mg/L). The initial biomass was minimized to avoid Pb(II) absorption into bacteria cells. After 3 days of incubation, samples were collected and analysed with qPCR to quantify the growth of the microbes on Pb(II) by comparing the number of 16S rDNA gene copies after 3 days of incubation to the initial number of genes. DNA was extracted using Instagene™ Matrix (Bio-Rad, Canada). Specific 16S rDNA primers for *A. caeni* strain Pb2 (CAACCCTGATCCAGCCAT and CATGCAGGGTATTAGCCCAC; 77 bp) and *D.*

acidovorans strain Pb11 (GTAACAGGTCTTCGGACGCT and GAGAAGCCTTTTCGTTCCGT; 374 bp) were designed as previously described (Lorenz, 2012) and synthesized by Life Technologies Inc., Canada. The qPCR reaction matrix contained: 10 µL of 2x iTaq™ Universal SYBR® Green Supermix; 1 µL of 10 µM forward and reverse primers; 2 µL of DNA template; and 6 µL dH_2O per reaction well. The qPCR program consisted of 40 cycles (94°C for 5 sec and 60°C for 30 sec) followed by the melt curve analysis (65-95°C with 0.5°C increments at 5 sec/step). Samples were run in triplicate on a 96-well plate with Bio-Rad CFX 96 Real-time detection system (Bio-Rad, Canada). The standard curve (Fig. A1) was prepared for serially diluted extracted DNA templates from the isolated bacteria (Arya et al., 2005). The ratio between the number of 16S rDNA gene copies in the final and initial samples was determined based on the qPCR threshold number (C_q) using the comparative C_T method (Schmittgen & Livak, 2008).

$$Fold\ change\ in\ bacterial\ population\ = \frac{Final\ 16s\ rDNA\ gene\ copies}{Initial\ 16s\ rDNA\ gene\ copies} = 2^{C_{q,initial} - C_{q,final}} \qquad (2.4)$$

2.2.8. Strategic analyses for confirming metallic Pb formation

D. acidovorans strain Pb11 and *A. caeni* strain Pb2 were injected into glass tubes with 15-mL of the growth solution. Pb(II) was injected into the tubes (5 mg-Pb(II)/L for each injection), and the injection was repeated every 2-3 days over two weeks (total 30 mg-Pb(II)/L). After 2 weeks, the solution was analyzed both in ICP-OES and X-ray photoelectron spectroscopy (XPS) to confirm Pb(II) reduction to metallic Pb by the microbes as previously described (Chastain & King Jr, 1992; Grimes et al., 1995; L. K. Wang et al., 2006). The final solution was pre-treated by adding ethanol (30% v/v), and the samples were kept overnight for the lysis of bacterial cells. The samples were then filtered using 0.20 µm Acrodisc® syringe filters (Pall Ltd., Canada). The filter membranes were manually extracted from the syringe filters and analysed in XPS (Quantera II Scanning XPS Microprobe, PHI, USA) to identify the composition of removed Pb on their surfaces (Brink et al., 2020b; A. Y. Lee et al., 2002). The

X-ray photoelectron spectroscopy (XPS) analysis was applied to confirm Pb(II) reduction to metallic Pb by the microbes as previously described (Chastain & King Jr, 1992; Grimes et al., 1995; L. K. Wang et al., 2006).

2.3. Results and Discussion

2.3.1. Isolation of Pb(II)-reducing bacteria

Delftia acidovorans and *Azonexus caeni* were successfully isolated by streaking the MEC effluent on agar plates while *Comamonas testosteroni* and *A. caeni* were isolated from the MEC effluent after 4 rounds of DTE (Table 2.1 and Fig. A1.2). *D. acidovorans* was isolated by the streak plate method at both the low (0.50 mg/L) and high (5.0 mg/L) Pb(II) concentrations. For the isolated colony from the 5.0 mg-Pb(II)/L plate, 3 species within the *Delftia* genus were identified with similar 16S rDNA identities: *Delftia tsuruhatensis* strain NBRC 16741 (99.44%); *Delftia lacustris* 332^T (99.44%); and *Delftia acidovorans* strain NBRC 14950 (98.89%). The isolate was named as *Delftia acidovorans* strain Pb11. *Delftia* species were reported in previous studies to use Cr(VI) and Se(IV) as terminal electron acceptors (Garavaglia et al., 2010; Morel et al., 2011; Prakash et al., 2010). *Azonexus caeni* was isolated both in the streak plate method (5.0 mg-Pb(II)/L) (named as *Azonexus caeni* strain Pb2) and the DTE technique (0.50 and 5.0 mg-Pb(II)/L) (named as *Azonexus caeni* strain Pb21 and strain Pb22) (Table 2.1), indicating that *A. caeni* can be isolated with either the aqueous or agar mediums. *A. caeni* was previously reported to utilize different terminal electron acceptors such as O_2 and NO_3^- (Quan et al., 2006). *Comamonas testosteroni* strain was isolated by the DTE method at both 0.50 and 5.0 mg-Pb(II)/L (Table 2.1) (named as *Comamonas testosteroni* strain Pb3 and strain Pb31). *C. testosteroni* was previously isolated from heavy-metal contaminated sites and reported to resist Cu(II), Cd(II), and As(III) and reduce both Se(IV) and Se(VI) to Se^0 (Willems & Gillis, 2015; Zheng et al., 2014).

Table 2.1. List of species isolated by applying the streak plate and dilution-to-extinction (1:100 dilution factor) methods. Pb(II) was added as 0.50 or 5.0 mg/L in both broth and agar mediums. Experiments were run in duplicate. The isolation procedure is summarized in Fig. A1.2.

Isolation procedure	Pb(II) conc.	Highest identified species	Designated strains [a]	Identity
Streak plate method	0.50 mg/L	*Delftia tsuruhatensis* strain NBRC 16741	*Delftia acidovorans* strain Pb1	95.69%
		Delftia lacustris strain 332^{T}		95.42%
		Delftia acidovorans strain NBRC 14950		95.40%
	5.0 mg/L	*Delftia tsuruhatensis* strain NBRC 16741	*Delftia acidovorans* strain Pb11[b]	99.44%
		Delftia lacustris strain 332^{T}		99.44%
		Delftia acidovorans strain NBRC 14950		98.89%
		Azonexus caeni strain Slu-05	*Azonexus caeni* strain Pb2[b]	99.24%
4 rounds of 1:100 DTE	0.50 mg/L	*Azonexus caeni* strain Slu-05	*Azonexus caeni* strain Pb21	96.46%
		Comamonas testosteroni strain KS 0043	*Comamonas testosteroni* strain Pb3	96.59%
	5.0 mg/L	*Azonexus caeni* strain Slu-05	*Azonexus caeni* strain Pb22	96.58%
		Comamonas testosteroni strain KS 0043	*Comamonas testosteroni* strain Pb31[b]	98.30%

[a] The sequences were submitted to the NCBI genebank database under accession numbers: MW309863 to MW309869.

[b] These isolates were used for the remaining investigations and experiments.

2.3.2. Pb(II) removal and deposition on carbon fibers

In the Pb deposition tests with carbon fibers with the isolated bacteria, *D. acidovorans* strain Pb11 showed 80.13±3.62% of Pb(II) removal (from 5.0 to 0.99 mg-Pb(II)/L). In addition, *D. acidovorans* strain Pb11 was found to form relatively thick deposits on the carbon fiber surfaces where the deposits were proven to contain Pb in a solid form in the SEM-EDS analysis (Figs. 2.1A and 2.1B). Similarly, *A. caeni* strain Pb2 was found to remove Pb(II) by 83.04±6.30% (from 5.0 to 0.85 mg-Pb(II)/L), and Pb in a solid form was detected in the SEM-EDS analysis (Figs. 2.1C and 2.1D). However, among the 3 isolates, *C. testosteroni* strain Pb31 did not leave immobile and detectable Pb solids on the carbon fiber surfaces, as shown in the

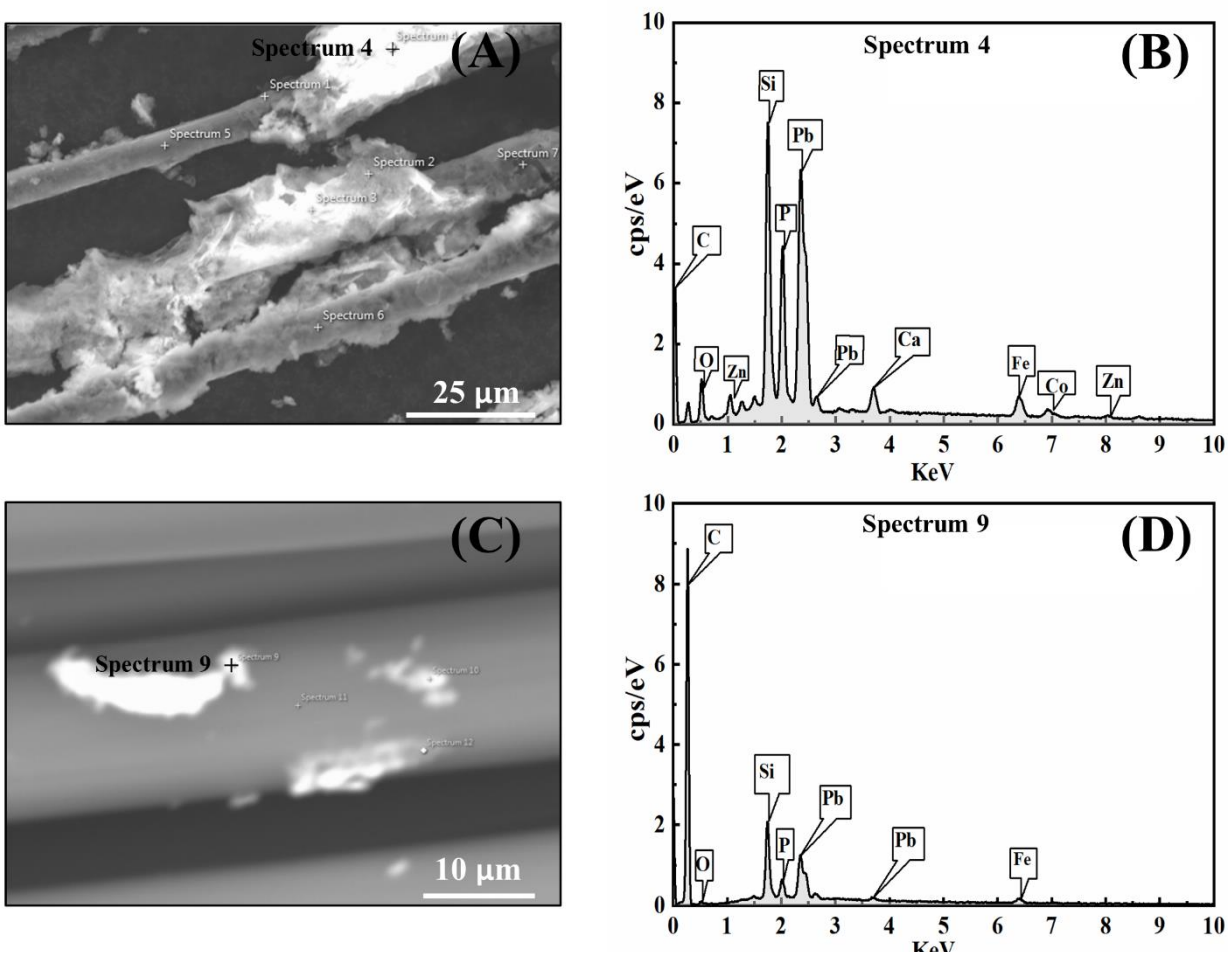

Fig. 2.1. Pb deposition on graphite fibers by isolated microbes: (**A** and **B**) Pb accumulation by *D. acidovorans* strain Pb11; (**C** and **D**) Pb accumulation by *A. caeni* strain Pb2. All fibers were thoroughly cleaned with ethanol to remove biofilms prior to the SEM-EDS analysis.

SEM-EDS analysis (Fig. A1.3), suggesting that *C. testosteroni* strain Pb31 cannot be applied in the same manner for Pb(II)-remediation applications.

2.3.3. Bacterial growth with Pb(II)

Both *D. acidovorans* strain Pb11 and *A. caeni* strain Pb2 were found to utilize Pb(II) as an electron acceptor and grow more rapidly at the higher Pb(II) concentrations, as proven by the qPCR analysis (Fig. 2.2). After incubation for 72 hrs, the population of *D. acidovorans* strain Pb11 has increased by 4.7, 6.8, and 9.8 times for the initial Pb(II) concentrations of 0, 5, and 10 mg/L, respectively (Fig. 2.2A). Similar outcomes were obtained for *A. caeni* strain Pb2 where the bacterial population increased by 4.1, 8.3, and 12.6 times for 0, 5, and 10 mg-Pb(II)/L, respectively. Because the acetate concentration was sufficiently high (12.2 mM), the microbial growth was limited by Pb(II) concentrations (< 0.05 mM), resulting in a greater fold increase in 16S rDNA gene copies for the higher initial Pb(II) concentrations.

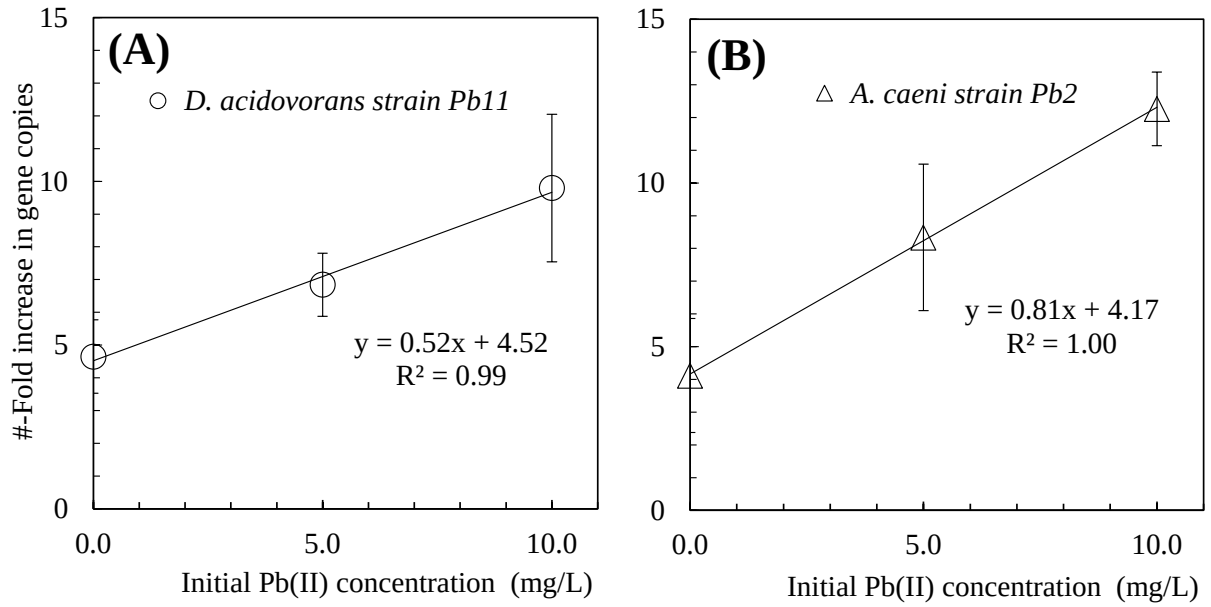

Fig. 2.2. qPCR analysis results for the microbial growth of (**A**) *D. acidovorans* strain Pb11 and (**B**) *A. Caeni* strain Pb2 samples at different initial Pb(II) concentrations. Samples were incubated for 3 days (n=4; duplicated experiment with 2 qPCR samples per experiment).

2.3.4. Confirmation of Metallic Pb formation

In the XPS analysis, particles of *D. acidovorans* strain Pb11 (95.8% Pb(II) removal from 30.0 to 1.13 mg-Pb(II)/L) and *A. caeni* strain Pb2 (98.9% Pb(II) removal from 30.0 to 0.28 mg-Pb(II)/L) were found to contain lead oxide (PbO) and lead phosphate. The samples with *D. acidovorans* strain Pb11 and *A. caeni* strain Pb2 showed Pb 4f peaks at 138 eV (Figs. 2.3C and 2.3E) and O 1s peaks at 530 eV (Figs. 2.3D and 2.3F), which signify the existence of PbO (Kloprogge & Wood, 2020; A. Y. Lee et al., 2002). It should be noted that PbO was not observed in the abiotic control experiments (Fig. 2.3B). Formation of PbO during the experiment was not feasible because a complete anaerobic condition was maintained. In addition, the isolated bacteria (*D. acidovorans* strain Pb11 and *A. caeni* strain Pb2) did not remove Pb(II) in the presence of oxygen, indicating that PbO was not created by aerobic reactions (Fig. A1.5). Also, the potential PbO formation reactions from Pb(II) or $Pb^{(0)}$ and H_2O cannot be driven with positive free energy values (Eqs. 2.4 and 2.5).

$$Pb^{2+} + H_2O \rightarrow PbO + 2H^{+} \qquad \Delta G = +19.2 \text{ kJ/mol} \qquad (2.4)$$

$$Pb^{(0)} + H_2O \rightarrow PbO + H_2 \qquad \Delta G = +12.85 \text{ kJ/mol} \qquad (2.5)$$

Thus, the only explanation for PbO detection is the formation of metallic $Pb^{(0)}$ particles during the anaerobic experiment. $Pb^{(0)}$ was then oxidized to PbO when the sample solution was filtered, and the filters were dried for the XPS analysis as described in a previous study on Pb detection in biological samples using XPS (Brink et al., 2020b). It should be noted that the surface of metallic lead (e.g., recently cut) is rapidly oxidized upon exposure to air to form a PbO layer protecting $Pb^{(0)}$ from further oxidation, which proves the possibility of $Pb^{(0)}$ oxidation in air (Abadin et al., 2007a; Schoenung, 2008). Another important challenge for the demonstration of biological Pb(II) removal is the abiotic Pb(II) partial removal as a result of lead phosphate precipitation (Stumm & Morgan, 1996). It should be noted that lead phosphate

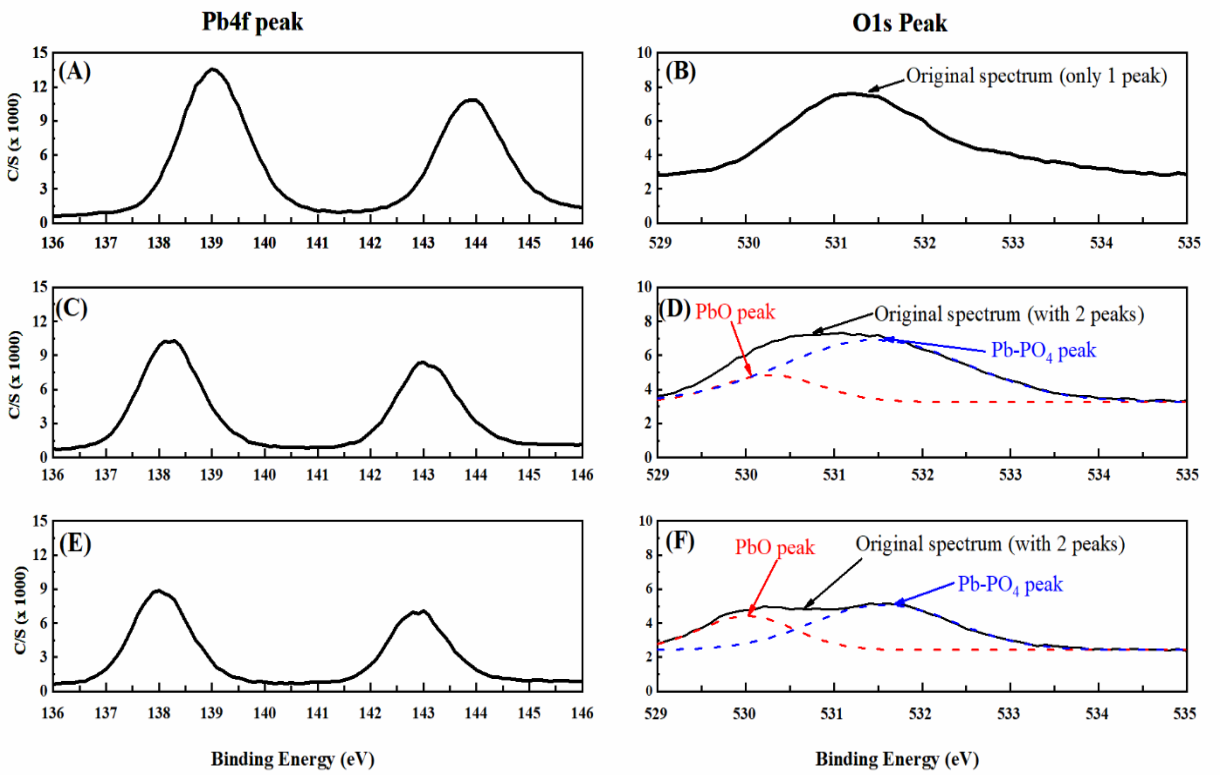

Fig. 2.3. XPS spectrums for Pb 4f (left) and O 1s (right) peaks for: Control (**A**, **B**); *D. acidovorans* strain Pb11 (**C**, **D**); and *A. caeni* strain Pb2 (**E**, **F**) samples. The O 1s spectrums showed two peaks (PbO: red dash lines; Pb-PO4 precipitants: blue dash lines) in the biotic samples (**D**, **F**); and one O 1s peak for Pb-PO4 in the control sample (**B**). All peaks were referenced to the adventitious C1s peak at 284.8 eV.

is highly insoluble in water with very low solubility products (e.g., K_{SP} of $Pb_3(PO_4)_2$ is $10^{-43.5}$) (Stumm & Morgan, 1996). In our XPS analysis results, lead phosphate was detected in both control (without bacteria) and biotic samples where there were a second O 1s peak at 531.5 eV (Fig. 2.3) and a P 2p peak at 132.2 eV (Fig. A1.4).

2.4. Conclusions

This study examined two isolation methods (solid- and liquid-medium based) for Pb(II)-reducing microorganisms. *D. acidovorans* and *A. caeni* were isolated by the solid-medium method (streak plate) while *A. caeni* and *C. testosteroni* were separated by the liquid-medium method (dilution-to-extinction). In the further experiments with the isolated species,

D. acidovorans strain Pb11 and *A. caeni* strain Pb2 were found to utilize Pb(II) and reduce it to metallic Pb. We also demonstrated that the XPS in combination with SEM-EDS analyses are essential to prove the microbial Pb(II) reduction because of lead phosphate precipitation. Our experimental results imply that *D. acidovorans* strain Pb11 and *A. caeni* strain Pb2 are competitive candidates for biological Pb(II) remediation. Future work should further examine their capability to remove Pb(II) in natural environments, such as Pb(II)-contaminated sediments and wastewater. The capability of the isolated bacteria to reduce other potential metal TEAs should be investigated in a separate study.

Acknowledgments

This study was supported by Natural Sciences and Engineering Research Council of Canada (Discovery Grants, RGPIN-2019-06747 and Discovery Accelerator Supplement, RGPAS-2019-00102), Canada Foundation for Innovation (Leaders Opportunity Fund, 31604), and Ontario Ministry of Research and Innovation (Early Researcher Awards, ER16-12-126 and Ontario Research Fund-Research Infrastructure, 31604).

References

Abadin, H., Ashizawa, A., Llados, F., & Stevens, Y.-W. (2007). *Toxicological profile for lead*. Agency for Toxic Substances and Disease Registry (Atlanta, USA).

Arnold, W., & Brezonik, P. (2009). Water chemistry: an Introduction to the chemistry of natural and engineered aquatic systems. In *Introduction to Environmental Management*. Oxford University Press.

Arya, M., Shergill, I. S., Williamson, M., Gommersall, L., Arya, N., & Patel, H. R. H. (2005). Basic principles of real-time quantitative PCR. *Expert Review of Molecular Diagnostics*, *5*(2), 209–219. https://doi.org/10.1586/14737159.5.2.209

Brink, H. G., Hörstmann, C., & Peens, J. (2020). Microbial Pb(II)-precipitation: the influence of oxygen on Pb(II)-removal from aqueous environment and the resulting precipitate identity. *International Journal of Environmental Science and Technology*, *17*(1), 409–420. https://doi.org/10.1007/s13762-019-02502-4

Brink, H. G., Lategan, M., Naude, K., & Chirwa, E. M. N. (2017). Microbial precipitation of lead (II) by industrially obtained consortia. *International Conference on Energy, Environment and Climate Change (ICEECC 2017), Mauritius.*

Bruce, E. R., & McCarty, P. L. (2020). *Environmental biotechnology: principles and applications* (2nd edition). McGraw-Hill Education.

Caccavo, F., Lonergan, D. J., Lovley, D. R., Davis, M., Stolz, J. F., & McInerney, M. J. (1994). Geobacter sulfurreducens sp. nov., a hydrogen- and acetate-oxidizing dissimilatory metal-reducing microorganism. *Applied and Environmental Microbiology*, *60*(10), 3752–3759. https://doi.org/10.1128/aem.60.10.3752-3759.1994

Chastain, J., & King Jr, R. C. (1992). Handbook of X-ray photoelectron spectroscopy. *Perkin-Elmer Corporation*, *40*, 221.

Colantonio, N., & Kim, Y. (2016a). Cadmium (II) removal mechanisms in microbial electrolysis cells. *Journal of Hazardous Materials*, *311*, 134–141. https://doi.org/10.1016/j.jhazmat.2016.02.062

Colantonio, N., & Kim, Y. (2016b). Lead(II) Removal at the Bioanode of Microbial Electrolysis Cells. *ChemistrySelect*, *1*(18), 5743–5748. https://doi.org/10.1002/slct.201601539

Garavaglia, L., Cerdeira, S. B., & Vullo, D. L. (2010). Chromium (VI) biotransformation by β- and γ-Proteobacteria from natural polluted environments: A combined biological and chemical treatment for industrial wastes. *Journal of Hazardous Materials*, *175*(1–3), 104–110. https://doi.org/10.1016/j.jhazmat.2009.09.134

Grimes, S. M., Johnston, S. R., & Batchelder, D. N. (1995). Lead carbonate-phosphate system: Solid-dilute solution exchange reactions in aqueous systems. *The Analyst*, *120*(11), 2741–2746. https://doi.org/10.1039/AN9952002741

Igiri, B. E., Okoduwa, S. I. R., Idoko, G. O., Akabuogu, E. P., Adeyi, A. O., & Ejiogu, I. K. (2018). Toxicity and Bioremediation of Heavy Metals Contaminated Ecosystem from Tannery Wastewater: A Review. *Journal of Toxicology*, *2018*, 2568038. https://doi.org/10.1155/2018/2568038

Jannati, M. (2019). Bio-Electrochemical Removal of Lead by Exoelectrogens and Phosphate Removal using Zeolite for Potential Industrial Wastewater Treatment (Master dissertation).

Jing, R., & Kjellerup, B. V. (2018). Biogeochemical cycling of metals impacting by microbial mobilization and immobilization. *Journal of Environmental Sciences*, *66*, 146–154. https://doi.org/https://doi.org/10.1016/j.jes.2017.04.035

Kabutey, F. T., Antwi, P., Ding, J., Zhao, Q., & Quashie, F. K. (2019). Enhanced bioremediation of heavy metals and bioelectricity generation in a macrophyte-integrated cathode sediment microbial fuel cell (mSMFC). *Environmental Science and Pollution Research*, *26*(26), 26829–26843. https://doi.org/10.1007/s11356-019-05874-9

Kloprogge, J. T., & Wood, B. J. (2020). Sulphides. In *Handbook of Mineral Spectroscopy* (pp. 23–67). Elsevier. https://doi.org/10.1016/b978-0-12-804522-0.00002-x

Lee, A. Y., Blakeslee, D. M., Powell, C. J., & Rumble, Jr., J. R. (2002). Development of the web-based NIST X-ray Photoelectron Spectroscopy (XPS) Database. *Data Science Journal*, *1*, 1–12. https://doi.org/10.2481/dsj.1.1

Lorenz, T. C. (2012). Polymerase chain reaction: Basic protocol plus troubleshooting and optimization strategies. *Journal of Visualized Experiments*, *63*, e3998. https://doi.org/10.3791/3998

McGinnis, S., & Madden, T. L. (2004). BLAST: at the core of a powerful and diverse set of sequence analysis tools. *Nucleic Acids Research*, *32*(suppl_2), W20–W25. https://doi.org/10.1093/nar/gkh435

McCarty, P. L. (2007). Thermodynamic electron equivalents model for bacterial yield prediction: modifications and comparative evaluations. *Biotechnology and Bioengineering*, *97*(2), 377–388.

Morel, M. A., Ubalde, M. C., Braña, V., & Castro-Sowinski, S. (2011). *Delftia* sp. JD2: A potential Cr(VI)-reducing agent with plant growth-promoting activity. *Archives of Microbiology*, *193*(1), 63–68. https://doi.org/10.1007/s00203-010-0632-2

Nagy, E., Boyanova, L., & Justesen, U. S. (2018). How to isolate, identify and determine antimicrobial susceptibility of anaerobic bacteria in routine laboratories. *Clinical Microbiology and Infection*, *24*(11), 1139–1148. https://doi.org/https://doi.org/10.1016/j.cmi.2018.02.008

Naik, M. M., & Dubey, S. K. (2011). Lead-enhanced siderophore production and alteration in cell morphology in a Pb-resistant Pseudomonas aeruginosa strain 4EA. *Current Microbiology*, *62*(2), 409–414.

Naik, M. M., Khanolkar, D., & Dubey, S. K. (2013). Lead-resistant *Providencia alcalifaciens* strain 2 EA bioprecipitates Pb+ 2 as lead phosphate. *Letters in Applied Microbiology*, *56*(2), 99–104.

Peens, J., Wu, Y. W., & Brink, H. G. (2018). Microbial Pb(II) precipitation: The influence of elevated Pb(II) Concentrations. *Chemical Engineering Transactions*, *64*, 583–588. https://doi.org/10.3303/CET1864098

Prakash, D., Pandey, J., Tiwary, B. N., & Jain, R. K. (2010). Physiological adaptations and tolerance towards higher concentration of selenite (Se^{+4}) in Enterobacter sp. AR-4, *Bacillus* sp. AR-6 and *Delftia tsuruhatensis* AR-7. *Extremophiles*, *14*(3), 261–272. https://doi.org/10.1007/s00792-010-0305-8

Quan, Z. X., Im, W. T., & Lee, S. T. (2006). *Azonexus caeni* sp. nov., a denitrifying bacterium isolated from sludge of a wastewater treatment plant. *International Journal of Systematic and Evolutionary Microbiology*, *56*(5), 1043–1046. https://doi.org/10.1099/ijs.0.64019-0

Schmittgen, T. D., & Livak, K. J. (2008). Analyzing real-time PCR data by the comparative CT method. *Nature Protocols*, *3*(6), 1101–1108. https://doi.org/10.1038/nprot.2008.73

Schoenung, J. M. (2008). Lead compounds. *Ceramic and Glass Materials: Structure, Properties and Processing*, 151–167. https://doi.org/10.1007/978-0-387-73362-3_9

Sim, K., Cox, M. J., Wopereis, H., Martin, R., Knol, J., Li, M. S., Cookson, W. O. C. M., Moffatt, M. F., & Kroll, J. S. (2012). Improved detection of bifidobacteria with optimised 16S rRNA-gene based pyrosequencing. *PLoS ONE*, *7*(3), e32543. https://doi.org/10.1371/journal.pone.0032543

Singh, A., & Bhatia, P. (2016). Automated Sanger Analysis Pipeline (ASAP): a tool for rapidly analyzing Sanger sequencing data with minimum user interference. *Journal of Biomolecular Techniques: JBT*, *27*(4), 129.

Stumm, W., & Morgan, J. J. (1996). Aquatic chemistry. In *Aquatic chemistry. 3rd ed. John Wiley & Sons, New York.* (Vol. 126). John Wiley & Sons.

Tiquia-Arashiro, S. M. (2018). Lead absorption mechanisms in bacteria as strategies for lead bioremediation. *Applied Microbiology and Biotechnology*, *102*(13), 5437–5444. https://doi.org/10.1007/s00253-018-8969-6

Tortora, G. J., Funke, B. R., & Case, C. L. (2015). Microbiology: An Introduction, Global Edition. In *USA: Pearson Education*.

Wang, L. K., Hung, Y.-T., & Shammas, N. K. (2006). *Handbook of Environmental Engineering: Advanced Physicochemical Treatment Processes; Volume 4*. Humana Press.

Willems, A., & Gillis, M. (2015). Comamonas. *Bergey's Manual of Systematics of Archaea and Bacteria*, 1–17.

Xing, D., Cheng, S., Logan, B. E., & Regan, J. M. (2010). Isolation of the exoelectrogenic denitrifying bacterium *Comamonas denitrificans* based on dilution to extinction. *Applied Microbiology and Biotechnology*, *85*(5), 1575–1587. https://doi.org/10.1007/s00253-009-2240-0

Zheng, S., Su, J., Wang, L., Yao, R., Wang, D., Deng, Y., Wang, R., Wang, G., & Rensing, C. (2014). Selenite reduction by the obligate aerobic bacterium *Comamonas testosteroni* S44 isolated from a metal-contaminated soil. *BMC Microbiology*, *14*(1), 204. https://doi.org/10.1186/s12866-014-0204-8

Zuo, Y., Xing, D., Regan, J. M., & Logan, B. E. (2008). Isolation of the exoelectrogenic bacterium *Ochrobactrum anthropi* YZ-1 by using a U-tube microbial fuel cell. *Applied and Environmental Microbiology*, *74*(10), 3130–3137. https://doi.org/10.1128/AEM.02732-07

3. Theoretical estimation for the yield coefficients for microbial polyhydroxyalkanoate production

Polyhydroxyalkanoates (PHA) are internally stored polymers that can be used to produce biodegradable plastics. In commercial PHA production, PHA accumulators are cultivated to produce significant amounts of PHA under distinct cultivation conditions. Thus, the estimation of theoretical PHA yields from organic and inorganic carbon substrates can assist with optimizing the cultivation conditions for efficient PHA production. In this work, thermodynamic energetics were applied to predict the yield coefficients for PHA and bacterial cells. The applied model enabled to obtain stochiometric reactions for PHA and cell synthesis reactions for PHA accumulators. Consequently, theoretical PHA and cell yield coefficients were estimated under autotrophic and heterotrophic cultivation conditions and compared to observed yield coefficients in the literature.

The paper was prepared for future journal publication.

- Amer, A., and Kim, Y. Theoretical estimation of the yield coefficients for microbial polyhydroxyalkanoate production.

The co-author's contributions include:

- Funding acquisition
- Supervision and technical support
- Manuscript revision

Abstract

Polyhydroxyalkanoates (PHAs) are a group of biodegradable polymers that include several monomers such as poly(3-hydroxybutyrate) (PHB) and poly(3-hydroxyvalerate) (PHV). A variety of microorganisms can store PHA granules inside their cells under heterotrophic or autotrophic conditions. In this work, the thermodynamic electron equivalents model (TEEM1) was applied to calculate theoretical PHA and cell yields for PHA accumulators. Based on the thermodynamic characteristics of reactants and products, stochiometric balanced equations for cell and PHB synthesis reactions can be constructed. As a result, the theoretical PHB yields on several organic substrates were estimated at standard conditions. For example, the true PHB yield on acetate was calculated as 0.66 $g_{PHB}/\ g_{acetate}$. Similarly, the true PHB yield under autotrophic conditions (i.e., using CO_2, H_2, and O_2) was also estimated using the TEEM1 as 2.97 g_{PHB}/mol_{H_2}. Along with PHB yield calculations, the heterotrophic (e.g., 0.34 $g_{cells}/g_{acetate}$) and autotrophic (4.11 g_{cells}/mol_{H_2}) cell yields were calculated for *Cupriavidus necator*, a representative of PHA accumulators that accumulate PHA up to 90% (w/w). The theoretical PHB and cell yields estimated by the TEEM1 were compared to the reported values in experimental studies. Based on the current findings, the TEEM1 can be used to predict theoretical PHA yields under distinct cultivation conditions without the need to conduct time-consuming experimental studies.

Keywords:

Thermodynamic energy; Free energy; Polyhydroxybutyrate; PHA accumulation; Autotrophic conditions; Heterotrophic growth

3.1. Introduction

Polyhydroxyalkanoates (PHAs) are biodegradable bioplastics produced by a variety of microorganisms as internally stored polymers (Khatami et al., 2021). PHA polymers consist of major monomers such as poly-3-hydroxybutrate (PHB) and poly-3-hydroxyvalerate (PHV) in addition to other minor constituents such as 3-hydroxyhexanoate (3HHx) (Kumar et al., 2020). PHAs are classified into short chain length (scl), medium chain length (mcl), or long chain length (lcl) according to the number of carbon atoms in the side chain (Raza et al., 2018). PHAs can be composed of homo (e.g., PHB, PHV) or copolymers (e.g., PHB-PHV)) (Raza et al., 2018). The composition of PHA polymers depends mainly on the provided substrate (Raza et al., 2018). For instance, PHB and PHV were accumulated when acetate and propionate were provided individually, while a mixture of PHB/PHV was formed when both acetate and propionate were supplied together (Jiang et al., 2011). Although PHA polymers have been widely studied, the free energy of formation (ΔG_f^0) values of different PHA polymers were not reported in the literature. Thus, in this study, we estimated ΔG_f^0 values for PHB, PHV, and PHB-PHV so that their reduction half-reactions ($\Delta G^{0\prime}$, $KJ/e^-\ eq$) can be constructed.

PHA can be accumulated under heterotrophic or autotrophic conditions (Khosravi-Darani et al., 2013; J. Lee et al., 2021; Volova et al., 2002; Yu, 2018). Heterotrophic PHA accumulators utilize organic substrates as the energy and carbon sources for microbial growth and PHA accumulation (Tiemeyer et al., 2007). Under autotrophic conditions, several PHA accumulators (e.g., *Cupriavidus necator*) can grow and accumulate PHA by utilizing CO_2 as the carbon source, O_2 as the terminal electron acceptor, and H_2 as the electron donor (Do et al., 2007; Ishizaki et al., 2001). In addition, the highest reported PHA amounts (~ 90% (w/w) of cell dry weight) were accumulated under nutrient-limited conditions, in which one of the essential growth nutrients is omitted from the culture medium to maximize PHA accumulation (Biglari et al., 2020; Jiang et al., 2011; Jiang, Marang, et al., 2011b; Johnson et al., 2009;

Marang et al., 2013). Therefore, in this work, we focused on the estimation of theoretical PHA yields under autotrophic and heterotrophic conditions without simultaneous microbial growth.

Under heterotrophic or autotrophic conditions, the carbon source (i.e., an organic substrate or CO_2) is first converted to an intermediate organic compound (e.g., acetyl-CoA), and then the latter is used to synthesize PHA monomers or new cells (Jiang et al., 2011; van Aalst-van Leeuwen et al., 1997). Thus, cell and PHA yields can be estimated by applying the same procedure. Several approaches were suggested to estimate theoretical cell yields in the literature (Dias et al., 2005; van Aalst-van Leeuwen et al., 1997). Rittmann and McCarty (2001) introduced the Thermodynamic Electron Equivalents Model (TEEM1) to predict bacterial cell yields based on electron equivalents (Rittmann & McCarty, 2001). The TEEM1 uses reduction half-reactions for electron donors, terminal electron acceptors, and cell synthesis to obtain balanced stoichiometric equations for microbial growth and substrate utilization, which can be used to predict cell yields (McCarty, 2007; Rittmann & McCarty, 2001). Thus, in this study, we applied the TEEM1 to estimate theoretical PHA yields under autotrophic and heterotrophic accumulation conditions. The TEEM1 was also applied to estimate cell yields of *Cupriavidus necator* as a representative of PHA accumulators that can accumulate PHA up to 90% (w/w) under autotrophic or heterotrophic conditions (Grothe & Chisti, 2000; Hänggi, 1990; S. Y. Lee, 1996).

3.2. Methods

3.2.1. Energetic model development

The TEEM1 utilizes three half-reactions: electron donor oxidation (R_d); electron acceptor reduction (R_a); and cell or PHB synthesis (R_C) reactions (Bruce & McCarty, 2020; McCarty, 2007). The amount of energy required to synthesize cell or PHB is defined as *A* equivalents of the electron donor,

$$A = -\frac{\frac{\Delta G_p}{\varepsilon^n} + \frac{\Delta G_{pc}}{\varepsilon}}{\varepsilon\,(\Delta G_r)} \tag{3.1}$$

ΔG_p is the energy required to convert the carbon source to an intermediate component (e.g., activated acetate). ΔG_p is calculated as the difference between the free energy of activated acetate and carbon source half-reactions,

$$\Delta G_p = \Delta G^{0'}_{AcCoA} - \Delta G^{0'}_{e^- donor} = 30.90 - \Delta G^{0'}_{e^- donor} \qquad (KJ/e^- eq) \tag{3.2}$$

The energy required to convert the activated acetate into cellular carbon is defined as (Bruce & McCarty, 2020),

$$\Delta G_{pc-cells} = \Delta G^{0'}_{cells} - \Delta G^{0'}_{AcCoA} = 18.8 \qquad (KJ/e^- eq) \tag{3.3}$$

Similarly, the energy required for PHB synthesis from activated acetate can be estimated as,

$$\Delta G_{pc-PHB} = \Delta G^{0'}_{PHB} - \Delta G^{0'}_{AcCoA} = 33.84 - 30.9 = 2.94 \quad (KJ/e^- eq) \tag{3.4}$$

In addition, ΔG_r is the difference between the half-reactions of electron acceptor reduction and electron donor oxidation,

$$\Delta G_r = \Delta G^{0'}_{e^- acceptor} - \Delta G^{0'}_{e^- donor} \quad (KJ/e^- eq) \tag{3.5}$$

In equation 3.1, ε is electron transfer efficiency (= 0.38 for aerobic reactions and $0.55 - 0.70$ for chemoautotrophic reactions). The exponent *n* equals +1 if $\Delta G_p > 0$, and −1 if $\Delta G_p < 0$ (Bruce & McCarty, 2020). The portions of donor used to obtain energy (f_e^0) and synthesize PHA monomers (f_s^0) are defined as,

$$f_s^o = \frac{1}{1+A} \tag{3.6}$$

$$f_e^o = \frac{A}{1+A} \tag{3.7}$$

A balanced stoichiometric equation can be written for the total reaction ($f_s^o R_c + f_e^o R_a - R_d$) for either cell synthesis or PHB formation reactions, and thus the theoretical yields can be estimated.

3.2.2. Change in free energy of formation (ΔG_f^0) for PHA polymers

The Joback method was applied to determine the change in free energy of formation ($\Delta G_{f,298}^0$) for several PHA polymers such as PHB, PHV, and PHB-PHV (Fig. 3.1). The free energy of formation of an organic compound can be estimated using the following equation (Joback & Reid, 1987),

$$\Delta G_{f,298}^0 = 53.88 + \sum \Delta G_{f,298}^0{}_{for\ all\ functional\ groups}\ (Kj/mole) \quad (3.8)$$

$\Delta G_{f,298}^0{}_{for\ all\ functional\ groups}$ is the sum of the free energy of formation of the contributing functional groups in each polymer (e.g., $-CH_3$) (Joback & Reid, 1987). The free energy of formation for common reactants and products are listed in Tables A2.1 and A2.2 (Bruce & McCarty, 2020; Madigan et al., 2009; McCarty, 2007; Pedley, 2012). To illustrate, PHB polymer ($C_4H_8O_3$) has the following functional groups: $-CH_3$; $-CH-$; $-CH_2-$; $-COOH-$; and $-OH-$ (Fig. 3.1). The Gibbs free energy change of PHB can be estimated as,

$$\Delta G_{f,PHB}^0 = 53.88 + \left[\left(\Delta G_{f,-CH_3}^0\right) + \left(\Delta G_{f,-CH}^0\right) + \left(\Delta G_{f,-CH_2-}^0\right) + \left(\Delta G_{f,-COOH}^0\right) + \left(\Delta G_{f,-OH}^0\right)\right]$$

$$= 53.88 + [-43.96 + 58.36 + 8.42 - 387.87 - 189.20] = -500.37\ (KJ/mole) \quad (3.9)$$

Similarly, the $\Delta G_{f,298}^0$ values for PHV and PHB-PHV polymers were estimated as -492.25 and -554.25 (kJ/mole), respectively. The half-reaction equations for PHB and PHV synthesis reactions (R_C) can be written as,

$$\frac{4}{18}CO_2 + H^+ + e^- \rightarrow \frac{1}{18}C_4H_8O_3 + \frac{5}{18}H_2O \qquad \Delta G_{PHB}^{0\prime} = 33.84\ (kJ/e^-\ eq) \quad (3.10)$$

$$\frac{5}{24}\mathrm{CO_2} + \mathrm{H^+} + \mathrm{e^-} \rightarrow \frac{1}{24}\mathrm{C_5H_{10}O_3} + \frac{7}{24}\mathrm{H_2O} \qquad \Delta G_{PHV}^{0\prime} = 32.40\ (kJ/e^-\ eq) \quad (3.11)$$

Since the half-reactions of PHB and PHV have similar $\Delta G^{0\prime}$ values, we only considered PHB yields in this work.

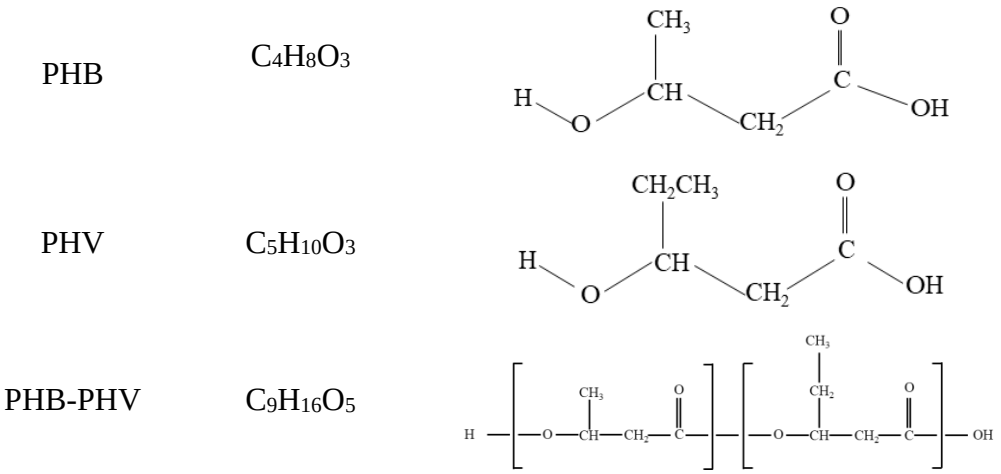

Fig. 3.1. Chemical formula for common PHA polymers. Number of monomeric units in a PHA polymer ranges between 100-30,000 monomers (S. Y. Lee, 1996; Raza et al., 2018).

3.2.3. Calculations for non-standard conditions

The impact of ambient conditions (i.e., the prevailing environmental conditions) on PHB yield calculations was studied. Several parameters such as substrate concentration, pH, temperature, and dissolved oxygen concentration were investigated. The ΔG_r values at ambient conditions were calculated using the following formula (Arnold & Brezonik, 2009; Madigan et al., 2009),

$$\Delta G = \Delta G^{0\prime} + RT\ ln\ (Q) \tag{3.12}$$

Where, $\Delta G^{0\prime}$ is the reduction half-reaction at standard conditions (1 molar concentration of reactant and products, 1 atmospheric pressure of gaseous components, pH 7, and 298.15°F); R is the universal gas constant (8.31 J/mole.K); T is the temperature in Kelvin; and Q is the reaction quotient (Mihelcic et al., 2014).

In addition to the environmental conditions, the impact of the number of monomers in PHB polymers was also investigated. At standard conditions (Eq. 3.9), PHB monomer was assumed to compose of only one monomeric unit. Thus, we calculated the $\Delta G_r^{0\prime}$ for PHB reduction half-reaction with monomeric units in the range of 1 – 30,000, as previously reported for PHA polymers (S. Y. Lee, 1996; Raza et al., 2018).

3.3. Results and discussions

3.3.1. PHB yields on organic substrates

The theoretical PHB yields on acetate, glucose and glycerol were estimated. To illustrate the TEEM1 calculations, the PHB yield using acetate as the carbon and energy source is explained in detail. The three half-reactions involved in PHB synthesis from acetate are: acetate oxidation (R_d; Eq. 3.13); oxygen reduction (R_a; Eq. 3.14); and PHB synthesis reaction (R_c; Eq. 3.10):

R_d $\quad \frac{1}{4}CO_2 + H^+ + e^- \rightarrow \frac{1}{8}CH_3COOH + \frac{1}{4}H_2O \qquad \Delta G^{0\prime}_{Acetate} = 32.99\ (kJ/e^-\ eq)$ (3.13)

R_a $\quad \frac{1}{4}O_2 + H^+ + e^- \rightarrow \frac{1}{2}H_2O \qquad \Delta G^{0\prime}_{O_2} = -78.72\ (kJ/e^-\ eq)$ (3.14)

By applying equations 3.1 – 3.6, the model constants A, f_e^0, and f_s^0 were estimated as 0.14; 0.12; and 0.88, respectively. The model results indicate that 88% acetate are used to synthesize PHB is 88% while only 12% are used to obtain energy. The stoichiometric balanced reaction for PHB production on acetate could be obtained by applying the overall reaction equation ($f_s^o R_c + f_e^o R_a - R_d$),

$$0.125\ CH_3COOH + 0.035\ O_2 \rightarrow 0.048\ C_4H_8O_3 + 0.059\ H_2O + 0.059\ CO_2 \qquad (3.15)$$

The theoretical PHA yield ($Y_{PHB-true}$) on acetate is 0.66 $g_{PHB}/\ g_{acetate}$ (0.76 $Cmol_{PHB}/\ Cmol_{acetate}$), which is higher than observed PHA yields (0.28 – 0.51 $g_{PHB}/\ g_{acetate}$) (Fig. 3.2) (Estévez-Alonso, Van Loosdrecht, et al., 2021; Sruamsiri et al., 2020). Dias et al. (2005) estimated the theoretical PHB yield on acetate as 0.74 $Cmol_{PHB}/\ Cmol_{acetate}$ using a

metabolic model, which agrees well with the TEEM1 results (Dias et al., 2005). Similarly, the true PHB yields on glucose and glycerol were also estimated to be 0.84 and 0.94 $g_{PHB}/\ g_{substrate}$, respectively (Fig. 3.2) (half-reactions and stochiometric balanced equations

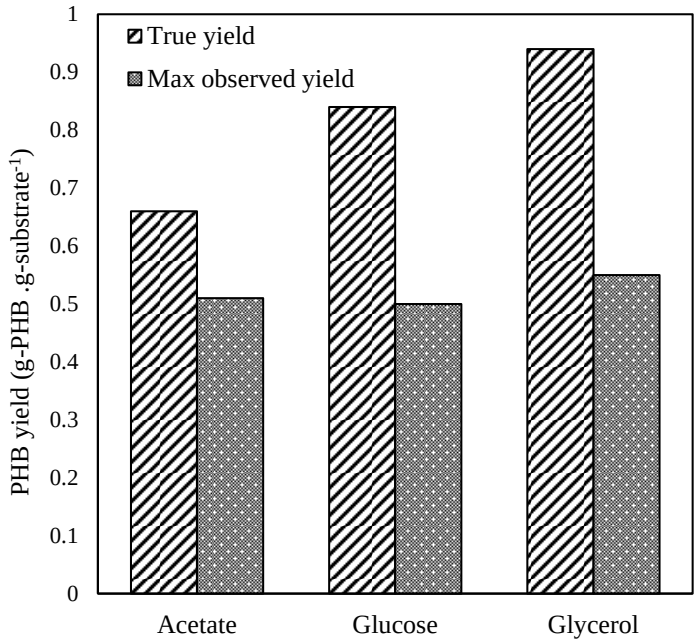

Fig. 3.2. True and maximum observed PHB yields on acetate, glucose, and glycerol.

for glucose and glycerol are shown in Table A2.2 and A2.3, respectively). The highest reported values for observed PHB yields on glucose and glycerol were 0.50 (Biglari et al., 2020) and 0.55 $g_{PHB}/\ g_{substrate}$ (Mozumder, Goormachtigh, et al., 2014), respectively. The difference between theoretical and observed PHB yields can be attributed to the maintenance requirements on organic substrates (Van Loosdrecht & Henze, 1999).

3.3.2. Impact of non-standard conditions

The impact of common environmental conditions (e.g., substrate concentration, pH, Temperature) on theoretical PHB yields on acetate was investigated (Fig. 3.3). At 1.0 – 20.0 g/L of acetate, the true PHB yields (0.78 – 0.84 $Cmol_{PHB}/\ Cmol_{acetate}$) are analogous to the PHB yield values at standard conditions ($Y_{PHB\text{-}acetate}$ = 0.76 $Cmol_{PHB}/\ Cmol_{acetate}$; Eq. 3.14). Similar results were found for other studied parameters such as pH (Fig. 3.3B), temperature (Fig. 3.3C), and dissolved oxygen concentrations (Fig. 3.3D), which had no significant impact

on the true PHB yields. These results suggest that the standard conditions can be applied to estimate theoretical PHB yields without the need to correct for actual operational conditions (Bruce & McCarty, 2020; Madigan et al., 2009).

In addition to the environmental conditions, the impact of the number monomeric units in synthesized PHA polymers was also investigated. For instance, PHB polymers were estimated to compose of up to 30,000 monomer units (S. Y. Lee, 1996a; Raza et al., 2018).

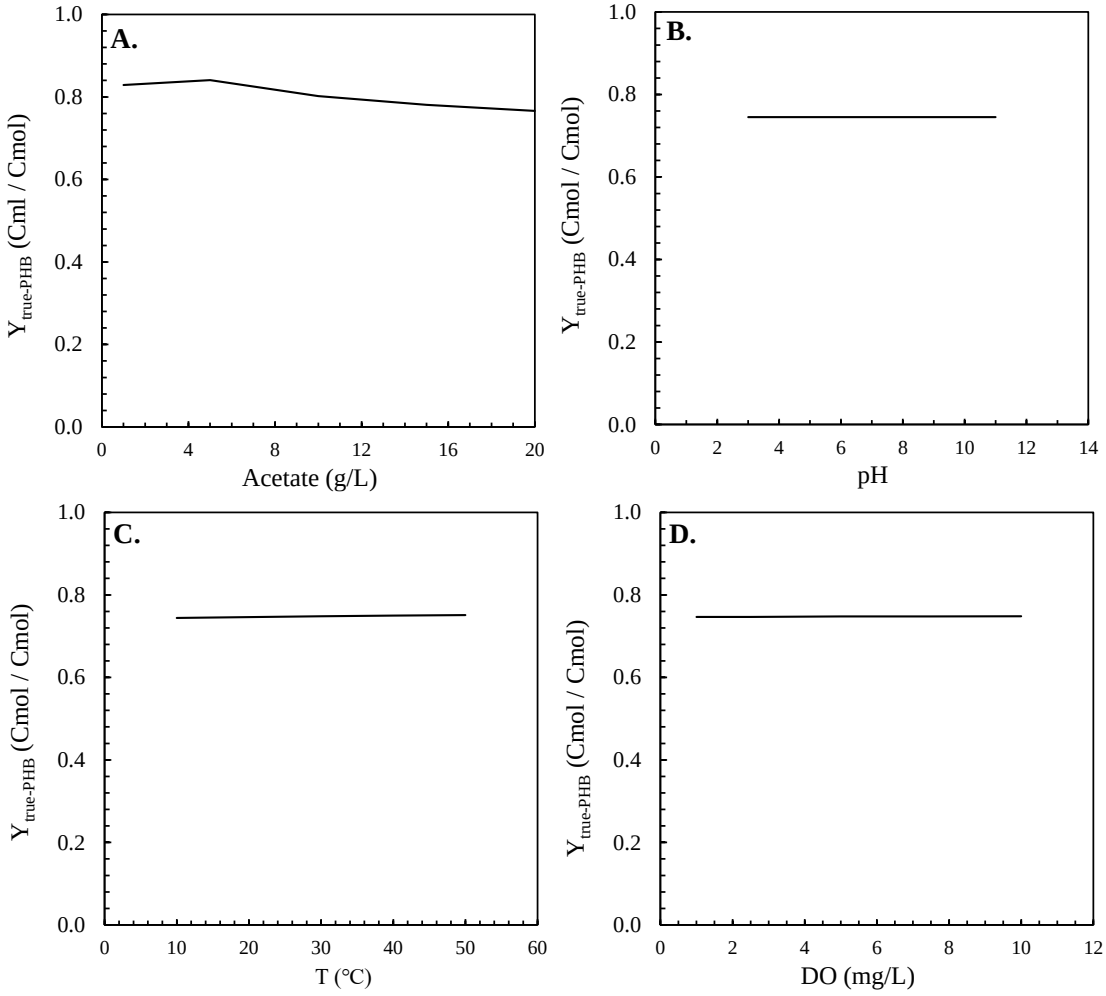

Fig. 3.3. Impact of non-standard conditions on true PHB yield estimation. **A.** Impact of acetate concentration on PHB yield (pH 7; T=25°C; [DO] = 1 M). B. Impact of pH on theoretical PHB yields ([Acetate] = 1 M; T=25°C; [DO] = 1 M). C. Impact of Temperature on PHB yields ([Acetate] = 1 M; pH 7; [DO] = 1 M). D. Impact of dissolved oxygen on PHB yield ([Acetate] = 1 M; pH 7 T=25°C). All other reactants and products were set at the standard values.

The TEEM1 estimated the true PHB yields to be 0.76 – 0.80 $Cmol_{PHB}/mol_{acetate}$ for PHB polymers with 100 – 30,000 monomer units (Table 3.1), indicating that the number of monomeric units do not significantly impact the PHB yield values.

Table 3.1. Free energy of formation and true PHB yields for different monomer units

No of monomers	$\Delta G^0_{f,\ PHB}$ $(KJ/mole)$	$\Delta G^{0'}_{PHB}$ for half-reaction $(kJ/e^-\ eq)$	$Y_{PHB-true}$ $(Cmol_{PHB}/\ Cmol_{acetate})$
1	-500	33.84	0.76
10	-3013	33.05	0.80
100	-28134	33.04	0.80
1000	-279351	32.96	0.80
10000	-2791521	32.95	0.80
30000	-8374121	32.95	0.80

3.3.3. Autotrophic PHB yield

In the autotrophic PHB synthesis, the CO_2 conversion into activated acetate has a ΔG_p value of 109.6 kJ/e^- eq (Rittmann & McCarty, 2001). The three half-reactions involved in autotrophic PHB production are: hydrogen oxidation (R_d, Eq. 3.16); oxygen reduction (R_a; Eq. 3.14) and PHB synthesis (R_c; Eq. 3.10).

R_d $$H^+ + e^- \rightarrow \frac{1}{2} H_2 \qquad \Delta G^{0'}_{H_2} = 39.87\ (kJ/e^-\ eq) \qquad (3.16)$$

Assuming $\varepsilon = 0.60$ (for chemolithoautotrophic reactions), A is estimated to be 2.63. As a result, only 28% of hydrogen is consumed to produce PHB ($f_e^o = 0.28$; Eq. 3.6) while the remaining portion (72%; Eq. 3.5) is used to obtain energy. Thus, the stoichiometric PHB production reaction under autotrophic conditions can be written as,

$$4\ CO_2 + 11.8\ O_2 + 32.7\ H_2 \rightarrow C_4H_8O_3 + 28.7\ H_2O \qquad (3.17)$$

The $Y_{PHB-true}$ is 3.18 $g_{PHB}/\ mol_{H_2}$. Ishizaki and Tanaka (1991) proposed a similar equation for the autotrophic PHB production from experimental results (Ishizaki & Tanaka, 1991). The reported autotrophic $Y_{PHB-observed}$ values were 2.60 – 3.44 $g_{PHB}/\ mol_{H_2}$ (Ishizaki & Tanaka, 1991; Schlegel et al., 1961).

3.3.4. Impact of gas composition on autotrophic PHB yields

The impact of the ratio between H_2, O_2, and CO_2 in the gas mixture on true PHB yields was investigated in an arbitrary scenario with 200-mL culture and 0 – 2.0 L of a gas mixture with different fractions of H_2, O_2, CO_2, and N_2 (for balancing) (Fig. 3.4; Appendix A2). In

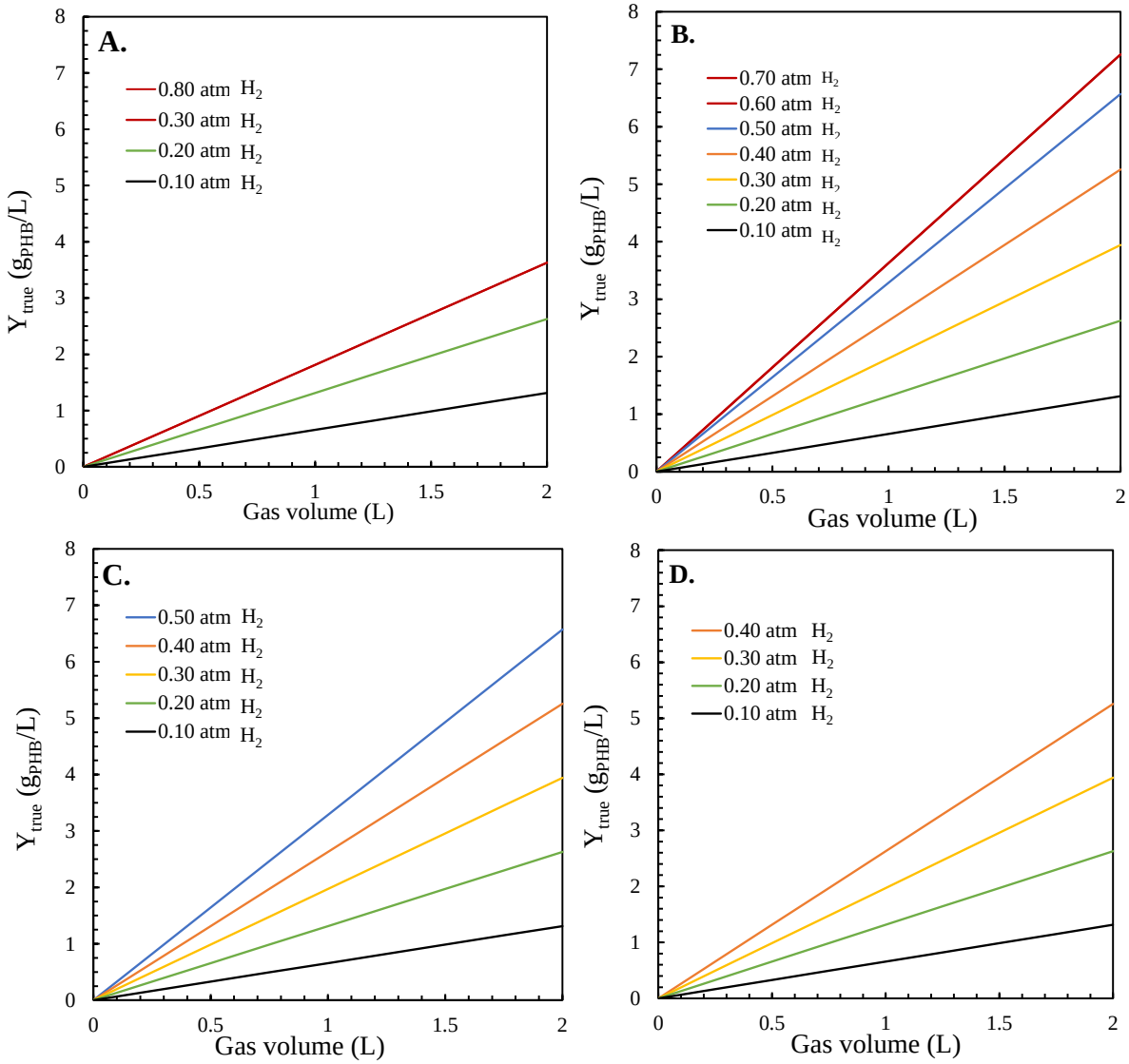

Fig. 3.4. The impact of gas composition on true PHB yield estimation. The solution volume was assumed to be 200 mL, while the gas volume changed from 0 to 2.0 L. CO_2 was assumed to be 0.10 atm in all scenarios. **A.** The gas mixtures included: O_2 = 0.10 atm; H_2 = 0.1 to 0.80. **A.** The gas mixtures included: O_2 = 0.20 atm; H_2 = 0.10 to 0.70. **C.** The gas mixtures included: O_2 = 0.40 atm; H_2 = 0.10 to 0.50. **D.** The gas mixtures included: O_2 = 0.50 atm; H_2 = 0.10 to 0.30. N2 was assumed to balance the gas fractions to have 1.0 atm as a total headspace gas pressure. A detailed calculation example is shown in Appendix 2.

figure 3.4, the PHB yields were limited by low oxygen concentrations (at $P_{O_2} \leq 0.10$ atm, Fig. 3.4A). Thus, increasing the H_2 partial pressure more than 0.30 did not improve PHB yield (Fig. 3.4A). The highest PHB yields were achieved at $P_{O_2} = 0.20$ atm with a ratio of H_2: O_2: CO_2 = 7: 2: 1 (Fig. 3.4A), which was previously reported as the optimal gas composition to attain sufficient cell growth and avoid gas limitation (Ishizaki et al., 2001; Mozumder et al., 2015). Increasing $P_{O_2} \geq 0.20$ atm does not improve PHB yields (Figs. 3.4C and 3.4D) because H_2 was limited at these elevated oxygen concentrations. According to these results, a gas mixture of a ratio of H_2, O_2, and CO_2 = 7: 2: 1 is suggested as the optimal ratio to attain high PHB yields.

3.3.5. Heterotrophic cell yield

The theoretical heterotrophic cell yields of *C. necator* were estimated. The elementary composition of *C. necator* was previously estimated to have a formula of $C_{4.09}H_{7.13}O_{1.89}N_{0.76}$ (Ishizaki & Tanaka, 1990). Therefore, the cell synthesis half-reaction *for C. necator* can be written as,

$$\text{R}_c \quad 0.191\ CO_2 + 0.044\ NH_4^+ + 0.044\ HCO_3 + H^+ + e^- \rightarrow 0.057\ C_{4.09}H_{7.13}O_{1.89}N_{0.76} + 0.404\ H_2O \qquad \Delta G^{0'}_{Cells} = 49.70\ (kJ/e^-\ eq) \qquad (3.18)$$

The other two half-reactions involved in the cell synthesis reaction are acetate oxidation (R_d; Eq. 3.9) and oxygen reduction (R_a; Eq. 3.13). Assuming ε is equal to 0.38, the model parameters A, f_e^0, and f_s^0 were calculated as 1.15; 0.53; and 0.47, respectively. The balanced equation for cell synthesis reaction could be written as,

$$0.125\ CH_3COOH + 0.020\ NH_4^+ + 0.134\ O_2 + 0.020\ HCO_3 \rightarrow 0.027\ C_{4.09}H_{7.13}O_{1.89}N_{0.76} + 0.205\ H_2O + 0.161\ CO_2 \qquad (3.19)$$

The $Y_{cells-true}$ on acetate is 0.43 $Cmol_{cells}/\ Cmol_{substrate}$ (0.34 $g_{cells}/\ g_{substrate}$), which is higher than the observed cell yield (0.20 $g_{cells}/\ g_{substrate}$) (Jawed et al., 2022). The same procedure was applied to calculate the cell yields on glucose and glycerol (Tables A2.2

and A2.3). The true cell yields on glucose is 0.37 $g_{cells}/\,g_{glucose}$ which is close to the previously reported values (0.37 – 0.45 $g_{cells}/\,g_{glucose}$) (Belfares et al., 1995; Marudkla et al., 2018; Mozumder, de Wever, et al., 2014; Shang et al., 2007; Tanadchangsaeng & Yu, 2012). Similarly, the true cell yield of *C. necator* on glycerol (0.41 $g_{cells}/\,g_{glycerol}$) is analogous to the previously reported observed yield range (0.41 – 0.48 $g_{cells}/\,g_{glycerol}$) (Mozumder, Goormachtigh, et al., 2014; Mozumder, de Wever, et al., 2014; Tanadchangsaeng & Yu, 2012), signifying the robustness of the energetic model to estimate heterotrophic cell yields.

3.3.6. Autotrophic cell yield

The true autotrophic cell yields for *C. necator* were also estimated. The three half-reactions required for the model are: hydrogen oxidation (R_d, Eq. 3.17); oxygen reduction (R_a; Eq. 3.13); and cell synthesis (R_c; Eq. 3.18). The model parameters A, f_e^0, and f_s^0 values were estimated as 2.21; 0.31; and 0.69, respectively. As a result, 69% of H_2 are oxidized to supply the energy required to reduce oxygen while only 31% are utilized to fix CO_2, indicating the high energy cost required for autotrophic cell synthesis (Bruce & McCarty, 2020). The balanced equation for autotrophic cell synthesis can be written as,

$$3.35\,CO_2 + 7.42\,O_2 + 23.62\,H_2 + 0.77\,NH_3^+ + 0.77\,HCO_3^- \rightarrow C_{4.09}H_{7.13}O_{1.89}N_{0.76} + 21.94\,H_2O \quad (3.20)$$

The autotrophic $Y_{Cells-true}$ is estimated to be 4.11 $g_{cells}/\,mol_{H_2}$. The stochiometric cell synthesis reaction for *C. necator* was previously determined using experimental lab-scale experimental results as (Ishizaki & Tanaka, 1990),

$$4.09\,CO_2 + 6.21\,O_2 + 21.36\,H_2 + 0.76\,NH_3^+ \rightarrow C_{4.09}H_{7.13}O_{1.89}N_{0.76} + 18.70\,H_2O \quad (3.21)$$

The observed cell yield of *C. necator* (4.54 $g_{cells}/\,mol_{H_2}$.) under autotrophic conditions is analogous to the true yield estimated using the TEEM1. According to the stoichiometric equations, the autotrophic $Y_{Cells-true}$= 29 $g_{cells}/\,Cmol_{CO_2}$. (Eq. 3.21) is approximately three

times the heterotrophic cell yield on acetate (10.31 $g_{cells}/\ Cmol_{acetate}$; Eq. 3.19), signifying higher carbon utilization efficiency under autotrophic conditions.

3.4. Conclusions

The TEEM1 was applied to calculate the theoretical PHA and cell yields under autotrophic and heterotrophic conditions. The free energy of formation and half-reactions for several PHA monomers such as PHB, PHV, and PHB-PHV were estimated. The theoretical PHB yields on acetate, glucose, and glycerol were calculated to be 0.76, 0.84, and 0.94 $Cmol_{PHB}/Cmol_{susbtrate}$ at standard conditions. When the ambient conditions and number of monomeric units in PHB polymers were investigated, there was no significant impact on theoretical PHB yields. Similarly, the number of monomeric units in PHA polymers does not affect the PHB yield calculations. In addition to heterotrophic conditions, the TEEM1 was also applied to calculate the true PHB yield (3.18 $g_{PHB}/\ mol_{H_2}$) under autotrophic conditions. The model results indicated that the ratio of H_2: O_2: CO_2 = 7: 2: 1 attained the highest PHB yields. Along with theoretical PHB yield estimation, the heterotrophic and autotrophic cell yields for *C. necator* were determined to be 0.34 $g_{cells}/\ g_{acetate}$ and 4.11 $g_{cells}/\ mol_{H_2}$, respectively. Based on these results, the thermodynamic energetic model could be applied to drive important insights into the autotrophic and heterotrophic PHA and cell yields.

References:

Arnold, W., & Brezonik, P. (2009). Water chemistry: An introduction to the chemistry of natural and engineered aquatic systems. In *Introduction to Environmental Management*. Oxford University Press.

Belfares, L., Perrier, M., Ramsay, B. A., Ramsay, J. A., Jolicoeur, M., & Chavarie, C. (1995). Multi-inhibition kinetic model for the growth of *Alcaligenes eutrophus*. *Canadian Journal of Microbiology*, *41*(13), 249–256.

Biglari, N., Orita, I., Fukui, T., & Sudesh, K. (2020). A study on the effects of increment and decrement repeated fed-batch feeding of glucose on the production of poly(3-hydroxybutyrate) [P(3HB)] by a newly engineered *Cupriavidus necator* NSDG-GG mutant in batch fill-and-draw fermentation. *Journal of Biotechnology*, *307*, 77–86. https://doi.org/https://doi.org/10.1016/j.jbiotec.2019.10.013

Bruce, E. R., & McCarty, P. L. (2020). *Environmental biotechnology: principles and applications* (2nd edition). McGraw-Hill Education (USA).

Dias, J. M. L., Serafim, L. S., Lemos, P. C., Reis, M. A. M., & Oliveira, R. (2005). Mathematical modelling of a mixed culture cultivation process for the production of polyhydroxybutyrate. *Biotechnology and Bioengineering*, *92*(2), 209–222. https://doi.org/10.1002/bit.20598

Do, Y. S., Smeenk, J., Broer, K. M., Kisting, C. J., Brown, R., Heindel, T. J., Bobik, T. A., & DiSpirito, A. A. (2007). Growth of *Rhodospirillum rubrum* on synthesis gas: Conversion of CO to H_2 and poly-β-hydroxyalkanoate. *Biotechnology and Bioengineering*, *97*(2), 279–286. https://doi.org/10.1002/bit.21226

Estévez-Alonso, Á., Van Loosdrecht, M. C. M., Kleerebezem, R., & Werker, A. (2021). Simultaneous nitrification and denitrification in microbial community-based polyhydroxyalkanoate production. *Bioresource Technology*, 125420. https://doi.org/https://doi.org/10.1016/j.biortech.2021.125420

Grothe, E., & Chisti, Y. (2000). Poly(β-hydroxybutyric acid) thermoplastic production by *Alcaligenes latus*: Behavior of fed-batch cultures. *Bioprocess Engineering*, *22*(5), 441–449. https://doi.org/10.1007/s004490050757

Hänggi, U. J. (1990). Pilot scale production of PHB with *Alcaligenes latus*. In *Novel Biodegradable Microbial Polymers* (pp. 65–70). Springer. https://doi.org/10.1007/978-94-009-2129-0_6

Ishizaki, A., & Tanaka, K. (1990). Batch culture of *Alcaligenes eutrophus* ATCC 17697T using recycled gas closed circuit culture system. *Journal of Fermentation and Bioengineering*, *69*(3), 170–174. https://doi.org/https://doi.org/10.1016/0922-338X(90)90041-T

Ishizaki, A., & Tanaka, K. (1991). Production of poly-β-hydroxybutyric acid from carbon dioxide by Alcaligenes eutrophus ATCC 17697T. *Journal of Fermentation and Bioengineering*, *71*(4), 254–257. https://doi.org/https://doi.org/10.1016/0922-338X(91)90277-N

Ishizaki, A., Tanaka, K., & Taga, N. (2001). Microbial production of poly-D-3-hydroxybutyrate from CO_2. *Applied Microbiology and Biotechnology*, *57*(1–2), 6–12.

Jawed, K., Irorere, V. U., Bommareddy, R. R., Minton, N. P., & Kovács, K. (2022). Establishing mixotrophic growth of *Cupriavidus necator* H16 on CO_2 and Volatile Fatty Acids. In *Fermentation* (Vol. 8, Issue 3). https://doi.org/10.3390/fermentation8030125

Jiang, Y., Dimitry, Y., Kleerebezem, R., Muyzer, G., & Van Loosdrecht, M. (2011). *Plasticicumulans acidivorans* gen. nov., sp. nov., a polyhydroxyalkanoate-accumulating gammaproteobacterium from a sequencing-batch bioreactor. *International Journal of Systematic and Evolutionary Microbiology*, *61*(9), 2314–2319. https://doi.org/10.1099/ijs.0.021410-0

Jiang, Y., Hebly, M., Kleerebezem, R., Muyzer, G., & Van Loosdrecht, M. C. M. (2011). Metabolic modeling of mixed substrate uptake for polyhydroxyalkanoate (PHA) production. *Water Research*, *45*(3), 1309–1321. https://doi.org/10.1016/j.watres.2010.10.009

Jiang, Y., Marang, L., Kleerebezem, R., Muyzer, G., & Van Loosdrecht, M. C. M. (2011). Polyhydroxybutyrate production from lactate using a mixed microbial culture. *Biotechnology and Bioengineering*, *108*(9), 2022–2035. https://doi.org/10.1002/bit.23148

Joback, K. G., & Reid, R. C. (1987). Estimation of pure-component properties from group-contributions. *Chemical Engineering Communications*, *57*(1–6), 233–243. https://doi.org/10.1080/00986448708960487

Johnson, K., Jiang, Y., Kleerebezem, R., Muyzer, G., & Van Loosdrecht, M. C. M. (2009). Enrichment of a mixed bacterial culture with a high polyhydroxyalkanoate storage capacity. *Biomacromolecules*, *10*(4), 670–676. https://doi.org/10.1021/bm8013796

Khatami, K., Perez-Zabaleta, M., Owusu-Agyeman, I., & Cetecioglu, Z. (2021). Waste to bioplastics: How close are we to sustainable polyhydroxyalkanoates production? *Waste Management*, *119*, 374–388. https://doi.org/https://doi.org/10.1016/j.wasman.2020.10.008

Khosravi-Darani, K., Mokhtari, Z. B., Amai, T., & Tanaka, K. (2013). Microbial production of poly(hydroxybutyrate) from C1 carbon sources. *Applied Microbiology and Biotechnology*, *97*(4), 1407–1424. https://doi.org/10.1007/s00253-012-4649-0

Kumar, M., Rathour, R., Singh, R., Sun, Y., Pandey, A., Gnansounou, E., Lin, K.-Y. A., Tsang, D. C. W., & Thakur, I. S. (2020). Bacterial polyhydroxyalkanoates: Opportunities, challenges, and prospects. *Journal of Cleaner Production*, 121500.

Lee, J., Park, H. J., Moon, M., Lee, J.-S., & Min, K. (2021). Recent progress and challenges in microbial polyhydroxybutyrate (PHB) production from CO_2 as a sustainable feedstock: A state-of-the-art review. *Bioresource Technology*, 125616.

Lee, S. Y. (1996). Plastic bacteria? Progress and prospects for polyhydroxyalkanoate production in bacteria. *Trends in Biotechnology*, *14*(11), 431–438.

Madigan, M. T., Martinko, J. M., Stahl, D. A., & Clark, D. P. (2009). Brock Biology of Microorganisms 13th Edition. In *Benjamin Cummings* (Vol. 53, Issue 3). Benjamin Cummings. http://www.mdpi.com/1996-1073/2/3/556/

Marang, L., Jiang, Y., Van Loosdrecht, M. C. M., & Kleerebezem, R. (2013). Butyrate as preferred substrate for polyhydroxybutyrate production. *Bioresource Technology*, *142*, 232–239. https://doi.org/10.1016/j.biortech.2013.05.031

Marudkla, J., Lee, W.-C., Wannawilai, S., Chisti, Y., & Sirisansaneeyakul, S. (2018). Model of acetic acid-affected growth and poly(3-hydroxybutyrate) production by *Cupriavidus necator* DSM 545. *Journal of Biotechnology*, *268*, 12–20. https://doi.org/https://doi.org/10.1016/j.jbiotec.2018.01.004

McCarty, P. L. (2007). Thermodynamic electron equivalents model for bacterial yield prediction: modifications and comparative evaluations. *Biotechnology and Bioengineering*, *97*(2), 377–388.

Mihelcic, J. R., Zimmerman, J. B., & Auer, M. T. (2014). *Environmental engineering: Fundamentals, sustainability, design* (Vol. 1). Wiley Hoboken, NJ.

Mozumder, M. S. I., Garcia-Gonzalez, L., de Wever, H., & Volcke, E. I. P. (2015). Poly (3-hydroxybutyrate)(PHB) production from CO_2: model development and process optimization. *Biochemical Engineering Journal*, *98*, 107–116.

Mozumder, M. S. I., Goormachtigh, L., Garcia-Gonzalez, L., de Wever, H., & Volcke, E. I. P. (2014). Modeling pure culture heterotrophic production of polyhydroxybutyrate (PHB). *Bioresource Technology*, *155*, 272–280. https://doi.org/10.1016/j.biortech.2013.12.103

Mozumder, Md. S. I., de Wever, H., Volcke, E. I. P., & Garcia-Gonzalez, L. (2014). A robust fed-batch feeding strategy independent of the carbon source for optimal polyhydroxybutyrate production. *Process Biochemistry*, *49*(3), 365–373. https://doi.org/https://doi.org/10.1016/j.procbio.2013.12.004

Pedley, J. B. (2012). *Thermochemical data of organic compounds*. Springer Science & Business Media.

Raza, Z. A., Abid, S., & Banat, I. M. (2018). Polyhydroxyalkanoates: Characteristics, production, recent developments and applications. *International Biodeterioration & Biodegradation*, *126*, 45–56.

Rittmann, B. E., & McCarty, P. L. (2001). *Environmental biotechnology: principles and applications*. McGraw-Hill Education.

Schlegel, H. G., Gottschalk, G., & von Bartha, R. (1961). Formation and utilization of poly-β-hydroxybutyric acid by Knallgas bacteria (Hydrogenomonas). *Nature*, *191*(4787), 463–465.

Shang, L., Kim, M. il, & Chang, H. N. (2007). Modeling of poly (3-hydroxybutyrate) production by high cell density fed-batch culture of *Ralstonia eutropha*. *Biotechnology and Bioprocess Engineering*, *12*(4), 417–423.

Sruamsiri, D., Thayanukul, P., & Suwannasilp, B. B. (2020). In situ identification of polyhydroxyalkanoate (PHA)-accumulating microorganisms in mixed microbial cultures under feast/famine conditions. *Scientific Reports*, *10*(1), 1–10. https://doi.org/10.1038/s41598-020-60727-7

Tanadchangsaeng, N., & Yu, J. (2012). Microbial synthesis of polyhydroxybutyrate from glycerol: Gluconeogenesis, molecular weight and material properties of biopolyester. *Biotechnology and Bioengineering*, *109*(11), 2808–2818. https://doi.org/https://doi.org/10.1002/bit.24546

Tiemeyer, A., Link, H., & Weuster-Botz, D. (2007). Kinetic studies on autohydrogenotrophic growth of *Ralstonia eutropha* with nitrate as terminal electron acceptor. *Applied Microbiology and Biotechnology*, *76*(1), 75–81. https://doi.org/10.1007/s00253-007-0983-z

Van Aalst-van Leeuwen, M. A., Pot, M. A., Van Loosdrecht, M. C. M., & Heijnen, J. J. (1997). Kinetic modeling of poly(β-hydroxybutyrate) production and consumption by *Paracoccus pantotrophus* under dynamic substrate supply. *Biotechnology and Bioengineering*, *55*(5), 773–782. https://doi.org/https://doi.org/10.1002/(SICI)1097-0290(19970905)55:5<773::AID-BIT7>3.0.CO;2-8

Van Loosdrecht, M. C. M., & Henze, M. (1999). Maintenance, endogenous respiration, lysis, decay and predation. *Water Science and Technology*, *39*(1), 107–117. https://doi.org/10.1016/S0273-1223(98)00780-X

Volova, T. G., Kalacheva, G. S., & Altukhova, O. v. (2002). Autotrophic synthesis of polyhydroxyalkanoates by the bacteria *Ralstonia eutropha* in the presence of carbon monoxide. *Applied Microbiology and Biotechnology*, *58*(5), 675–678. https://doi.org/10.1007/s00253-002-0941-8

Yu, J. (2018). Fixation of carbon dioxide by a hydrogen-oxidizing bacterium for value-added products. *World Journal of Microbiology and Biotechnology*, *34*(7), 89. https://doi.org/10.1007/s11274-018-2473-0

4. Minimizing the lag phase of *Cupriavidus necator* growth under autotrophic, heterotrophic, and mixotrophic conditions

Cupriavidus necator has been extensively studied for the ability to accumulate high amounts of polyhydroxyalkanoates (PHAs), a promising alternative to chemical plastics that cause sever impacts on the environment. Depending on environmental conditions, *C. necator* can grow under autotrophic and/or heterotrophic conditions. In the current work, we investigated the microbial growth of *C. necator* under several cultivation conditions (e.g., autotrophic, heterotrophic, or mixotrophic growth). The effect of growth conditions on the lag phase length of *C. necator* was examined. The bacterium was also cultivated in two-stage systems in which *C. necator* was grown autotrophically or heterotrophically and then switched to other growth modes.

The following manuscript was prepared for future journal publication.

- Amer, A., and Kim, Y. Minimizing the lag phase of *Cupriavidus necator* growth under autotrophic, heterotrophic, and mixotrophic conditions**.**

The co-author's contributions include:

- Funding acquisition.
- Supervision and technical support.
- Manuscript revision.

Abstract

Cupriavidus necator has unique metabolic capabilities as it can grow under heterotrophic, autotrophic, or mixotrophic conditions. In the current work, we examined the effect of growth conditions on the metabolic responses of *C. necator*. In lab-scale experiments, the autotrophic growth was rapid with a short lag phase as the exponential growth stage was initiated in 6 – 12 h. The lag phase increased significantly (>22 h) at elevated O_2 and CO_2 partial pressures, while the lag phase was independent of increased H_2 or N_2 partial pressures. Under heterotrophic conditions with acetate as the organic substrate, the lag phase length was short (<12 h), but it increased with increasing acetate concentration. When glucose and glycerol were provided as the organic substrate, the lag phase was consistently long (> 12 h) regardless of the examined substrate concentrations (up to 10.0 g/L). In the transition experiments, *C. necator* showed rapid transitions from autotrophic to heterotrophic growth in less than 12 h and vice versa. Our experimental results indicate that *C. necator* can rapidly grow with both autotrophic and heterotrophic substrates, while the lag time substantially increases with non-acetate organic substrates (e.g., glucose or glycerol), high acetate concentration, and high O_2 and CO_2 partial pressures.

Keywords:

Ralstonia eutropha; PHA-accumulating bacteria; lag phase; inhibition by high substrate; mixotrophic growth

4.1. Introduction

Biodegradable plastics are gaining an increasing attention as a sustainable alternative to petroleum-based chemical plastics because of their biodegradability in the environment. Polyhydroxyalkanoates (PHA) is a biodegradable polymer produced by various microorganisms with thermoplastic properties comparable to petrochemical plastics (J. Lee et al., 2021). Among over 300 identified PHA accumulators, only a few microorganisms, such as *Cupriavidus necator* (previously *Alcaligenes eutrophus* (Kärst & Friedrich 1984; Repaske & Repaske, 1976) and *Ralstonia eutropha* (Cramm, 2009; Müller et al., 2013; Tiemeyer et al., 2007; Volova et al., 2002)), can be employed for commercial and large-scale PHA production (Jawed et al., 2022; Sohn et al., 2021) for the high PHA accumulation capabilities. For instance, *C. necator* can accumulate up to 90% (w/w) of the cell dry weight as PHA (Jawed et al., 2022; López-Cuellar et al., 2011; Passanha et al., 2013).

Cupriavidus necator can utilize inorganic carbon sources such as CO_2 and CO, as well as organic substrates (Khosravi-Darani et al., 2013; J. Lee et al., 2021; Przybylski et al., 2015). As a hydrogen-oxidizing bacterium, *C. necator* can obtain the energy required for CO_2 fixation by oxidizing H_2 (i.e., the electron donor) and reducing O_2 (i.e., the terminal electron acceptor) (Ishizaki et al., 2001; Khosravi-Darani et al., 2013). The recommended gas mixture composition to attain sufficient cell growth has a volume-based ratio of H_2: O_2: CO_2 = 7: 2: 1 (Ishizaki et al., 2001). O_2 concentrations above 0.30 atm are known to inhibit cell growth (Ishizaki & Tanaka, 1990). Also, hydrogen concentrations lower than 0.04 atm resulted in low biomass yields (Miyahara et al., 2020). Although the inhibition effects of the gaseous substrates on the cell growth were previously reported, the inhibition on the microbial adaption (i.e., lag phase) has not been investigated in previous literature. Therefore, one of the main objectives of the current work is to examine how the partial pressure of individual gases (e.g., O_2, CO_2, H_2, N_2) affects the lag phase so that we can propose strategic methods to improve the

autotrophic biomass yields such as optimal gas-to-solution ratios and the frequency of injecting gaseous substrates.

C. necator can also grow and accumulate PHA by utilizing organic substrates as the energy and carbon sources (Belfares et al., 1995; Repaske & Repaske, 1976; Roy, 1962). *C. necator* was examined to grow and accumulate PHA on various organic substrates such as acetate (Marudkla et al., 2018; Sugimoto et al., 1999), glucose (Biglari et al., 2020), glycerol (Mothes et al., 2007; Tanadchangsaeng & Yu, 2012), valerate (Kumar et al., 2020), and other waste organics (Kumar et al., 2020; Pavan et al., 2019). The elevated concentrations of organic substrates may inhibit the heterotrophic growth of *C. necator*. For example, acetic acid concentrations higher than 0.50 g/L were previously reported to cease the microbial growth (Marudkla et al., 2018). Additionally, the lag phase increased significantly with increasing the concentrations of volatile fatty acids (Jawed et al., 2022). Therefore, we investigated the concentration effect of several organic substrates (e.g., glucose, glycerol, and organic mixtures) on the lag phase lengths and biomass yields of *C. necator*.

C. necator can also consume organic and inorganic carbon substrates simultaneously (Jawed et al., 2022; Kärst & Friedrich 1984). In previous studies, *C. necator* mixotrophic growth on lactate was more rapid than individual autotrophic or heterotrophic growth, and the mixotrophic biomass yields were significantly higher than in the heterotrophic experiments for the same consumed lactate (Rittenberg et al., 1969). However, *C. necator* was not able to grow mixotrophically on some substrates such as pyruvate (Yu, 2018). Thus, another research objective of this study was to evaluate the mixotrophic growth of *C. necator* on several organic substrates (i.e., acetate, glucose, and glycerol). In this work, we also investigated the ability of *C. necator* to transit between the metabolic pathways (i.e., subsequent transition from autotrophic to heterotrophic or vice versa) with a focus on the lag time (i.e., adaption time).

4.2. Materials and Methods

4.2.1. Bacterial strain

C. necator Makkar and Casida 17697 was purchased from the American Type Culture Collection (ATCC) (Cedarlane Cor., Burlington, Canada). The bacterium was revived on agar solid media and subsequently cultured in liquid mediums (section 4.2.2) according to the supplier instructions. For the revival, the agar medium was prepared using 3.0 g/L of beef extract, 5.0 g/L of soybean peptone, and 15.0 g/L of agar.

4.2.2. Growth solutions and organic substrates

The autotrophic growth solution included: 2.30 g/L KH_2PO_4; 2.9 g/L $Na_2HPO_4.2H_2O$; 1.0 g/L $NaHCO_3$; 0.30 g/L NH_4Cl; and trace amounts of minerals and vitamins. The initial pH of the autotrophic growth solution was 7.4 (SevenMulti, Mettler-Toledo International Inc., OH). For the heterotrophic and mixotrophic growth experiments, the same autotrophic growth solution composition was used in addition to acetate (provided as CH_3COONa), glucose, glycerol, or mixed substrates (33.3% acetate + 33.3% glucose + 33.3% glycerol) at various concentrations (1 – 10 g/L). It should be noted that the four substrates have the same carbon load per the same concentration (e.g., 1.0 g/L of acetate, glucose, glycerol, or mixed substrates has 33 – 34 Cmmol/L). For the autotrophic growth conditions, there was no organic substrate added in the experiments.

All experiments were conducted at 30°C in 17-mL Hungate glass vials with 14-mL headspace volume and 3-mL solution volume unless mentioned otherwise. The vials were placed horizontally in a mechanical shaker (150 rpm) to increase the contact surface area between the medium solution and headspace gas. The growth solution and vials were autoclaved at 121°C for 20 min before the experiments.

4.2.3. Gas composition in the headspace

For the autotrophic and mixotrophic experiments, the headspace air was replaced (using gas-tight syringes) with a gas mixture containing H_2 (0.70 atm), O_2 (0.20 atm), and CO_2 (0.10 atm) (Table 4.1) (Ishizaki et al., 2001; Repaske & Repaske, 1976; Roy, 1962). In the inhibition experiments by gaseous substrates, we examined the impact of various partial pressures of individual H_2, O_2, CO_2, and N_2 on *C. necator* autotrophic growth (Table 4.1). In the heterotrophic experiments, the headspace volume contained air only.

4.2.4. Transition between autotrophic and heterotrophic growth conditions

The transition between heterotrophic and autotrophic conditions was examined in this study. For the transition from heterotrophic to autotrophic growth, *C. necator* was initially cultivated under heterotrophic conditions (1.0 g/L of acetate) before injecting 1.0 atm of standard gas composition (Table 4.1) at 12, 24, or 36 h. For the transition from autotrophic to heterotrophic growth conditions, the experiment was started identically to the autotrophic growth experiment (Table 4.1) while 1.0 g-acetate/L was injected at 12, 24, or 36 h (Table 4.1).

Table 4.1. Summary of the autotrophic gas mixture compositions applied in this study

Experiment	Partial pressure (atm) in the vial headspace			
	H_2	O_2	CO_2	N_2
Autotrophic, mixotrophic, and transition experiments	0.70	0.20	0.10	0
Inhibition by gaseous substrates	0.70	0.20 – 2.20	0.10	0
	0.70	0.20	0.10 – 2.10	0
	0.70 – 2.70	0.20	0.10	0
	0.70	0.20	0.10	0 – 2.0

4.2.5. Experimental Analyses

Microbial growth was monitored by measuring the optical density (OD) at 600 nm (DR3000, Hach, US). The biomass yield was determined by measuring the net total chemical oxygen demand (COD) (Method 8000, Hach, US). pH was measured using SevenMulti (Mettler-Toledo International Inc., OH).

Samples were collected at the end of experiments and tested for contamination using 16S rDNA gene Sanger sequencing. The 16S rDNA gene sequencing using the colony PCR procedure was performed, as previously described (Amer & Kim, 2022a). In brief, the PCR reaction was performed with the universal bacterial primer 8f (Caccavo et al., 1994; Xing et al., 2010). The PCR reaction mixture included: 1 µL of 10 mM dNTPs; 0.25 µL of Taq polymerase; 5 µL of DNA template; 5 µL of 10x PCR buffer; 1.5 µL of 50 mM $MgCl_2$; 1 µL of 10 µM forward and reverse primers; and dH_2O to a final volume of 50 µL. The PCR program started with heating to 94ºC for 2 sec and them 29 cycles (94ºC for 30 sec, 56 ºC for 30 sec, 72ºC for 1 min) followed by a final cycle at 72ºC for 10 min. Then, Sanger sequencing was conducted on 3730 DNA Analyzer (Applied Biosystems, Foster City, CA, USA) (Mobix Lab, McMaster University, Canada). Sequencing results were viewed and modified by Finchtv program (Digital World Biology, Seattle, USA) (Singh & Bhatia, 2016). The obtained merged sequences were checked using the NCBI BLAST tool to identify the bacteria (McGinnis & Madden, 2004). Based on Sanger sequencing results, *C. necator* was identified for all samples collected at the end of the current experiments, indicating that there was no contamination in all experiments. Thus, the OD results reported in this work can be used as a representative for the growth of *C. necator*.

4.3. Results and Discussion

4.3.1. Autotrophic growth

C. necator grew rapidly with short lag phases (< 12 h) when cultivated with the standard gas mixture (H_2: O_2: CO_2 = 7: 2: 1) (Fig. 4.1A). The highest optical densities were achieved in 22 h, indicating fast fixation of carbon dioxide. In addition, the biomass yields were dependent on the provided gas volumes (Fig. 4.1B). As a result, the biomass yield at 24 h was 510 ± 25 g-COD/L at the highest ratio between the gas (14 mL) and growth solution (3 mL) volumes. Also, the total biomass was linearly correlated to the provided gas volumes (Fig. 4.1C), signifying the dependence of microbial growth on gas mixture volumes.

Higher optical densities were also achieved by increasing the frequency of gas addition to the headspace (Fig. A3.1). However, the additional injections of an individual gas (i.e., H_2, O_2, or CO_2) did not enhance the biomass yield substantially (Fig. A3.1), indicating the necessity to maintain specific gas ratios to attain the highest cell productivity and avoid gas limitation (Garcia-Gonzalez et al., 2015; Morinaga et al., 1978; Volova et al., 2013).

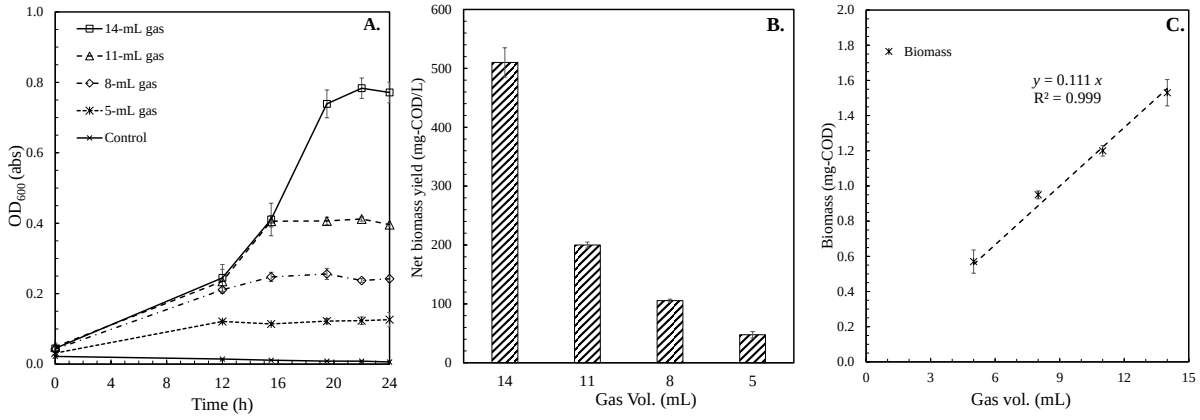

Fig. 4.1. A. Autotrophic *C. necator* growth at different ratios between gas (14 – 5 mL) and growth solution (3 – 12 mL) volumes (n = 2). **B.** Maximum autotrophic biomass yield at different gas volumes after 24 h. **C.** The relation between autotrophic biomass (= yield (mg-COD/L) *x* solution volume (mL)) and the supplied gas volumes (3 – 12 mL). In the control vials, the autotrophic growth solution was used under the gas mixture (H_2 : O_2 : CO_2 = 7 : 2 : 1) without microbial seed.

4.3.2. Impact of individual gas partial pressures on autotrophic growth

Higher oxygen and carbon dioxide partial pressures severely inhibited the autotrophic growth of *C. necator* and resulted in longer lag phases (Fig. 4.2). The highest optical density (OD_{600} = 0.78) was achieved with the standard gas mixture at a total pressure of 1 atm, indicating that the standard gas composition (H_2: O_2: CO_2 = 7: 2: 1) and pressure were optimal for autotrophic growth. *C. necator* growth was suppressed when P_{O_2} exceeded 0.70 atm (Fig. 4.2A), signifying the inhibiting influence of higher oxygen concentrations (Ishizaki & Tanaka, 1990). Similarly, P_{CO_2} greater than 0.10 atm resulted in slower *C. necator* growth with longer lag phases (> 12 h) (Fig. 4.2B). For example, the lag phase (37 h) at P_{CO_2} = 2.10 atm was much longer than at P_{CO_2} = 0.10 atm (< 12 h). In addition, the highest OD_{600} at P_{CO_2} = 2.10 atm (after 60 h) was 58% lower than at P_{CO_2} = 0.10 atm (after 22 h). It should be noted that the lowest pH was 6.02 at P_{CO_2} = 2.10 atm at the end of the experiments (Fig. A3.2), indicating that pH did not inhibit the autotrophic growth (Roy, 1962).

Applying high H_2 or N_2 partial pressures (up to 2.0 atm) did not impact the lag phases (~ 12 h) (Fig. 4.2C, D). Although H_2 was the limiting growth factor (Fig. A3.3), applying P_{H_2} higher than 0.70 atm reduced the optical densities by ~25% (Fig. 4.2C). In addition, elevated nitrogen partial pressures did not influence the attained optical densities (Fig. 4.2D), suggesting that *C. necator* cells can survive under high nitrogen pressures without impacting the autotrophic growth.

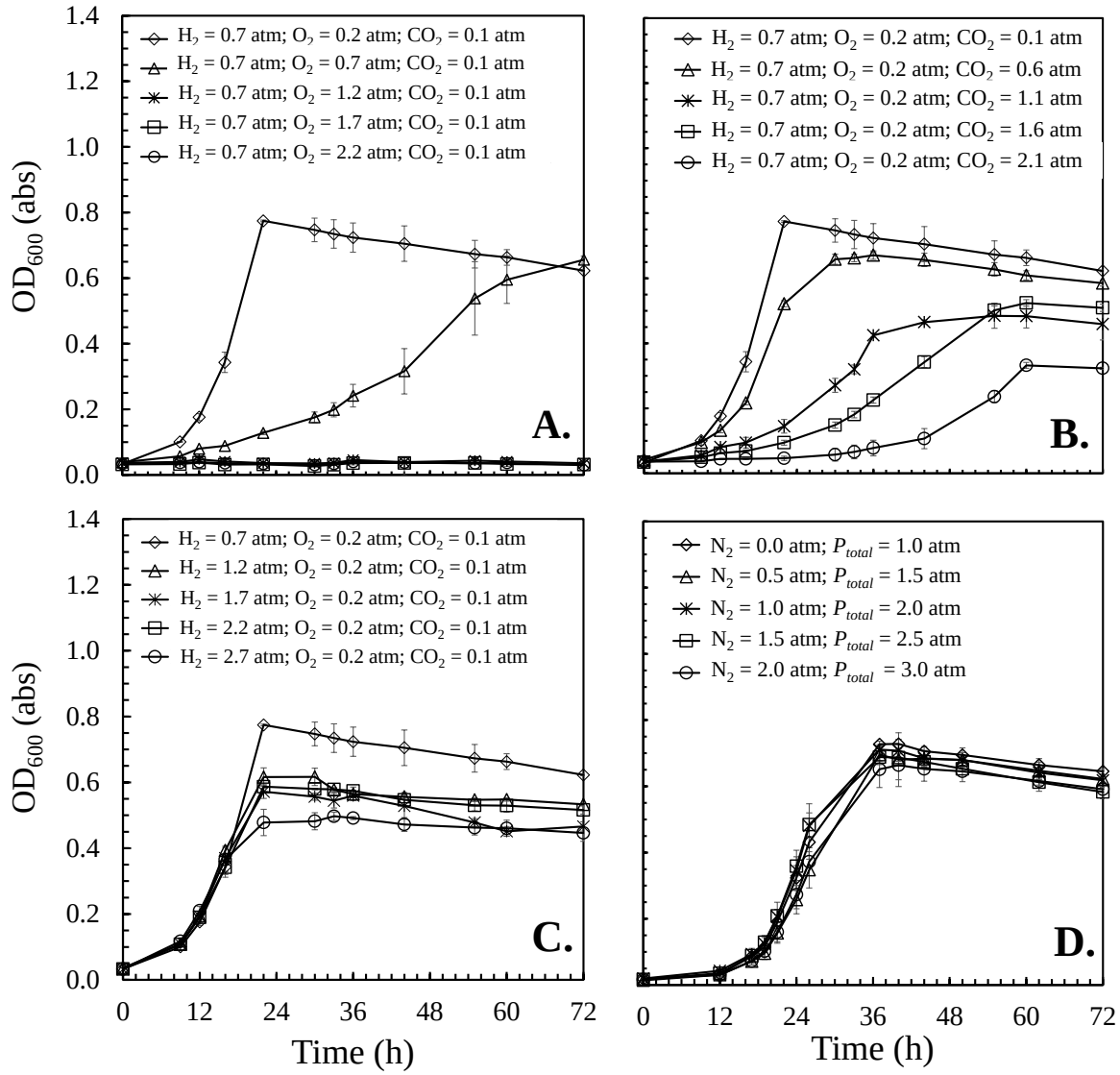

Fig. 4.2. Impact of individual gas pressures on *C. necator* autotrophic growth. The initial gas mixture was $H_2 : O_2 : CO_2 = 7 : 2 : 1$, and then the headspace pressure was increased up to 3.0 atm using: O_2 **(A)**; CO_2 **(B)**; H_2 (**C);** or N_2 **(D)** (n = 2). In the control vials, the autotrophic growth solution was used under 1.0 atm of the gas mixture ($H_2 : O_2 : CO_2 = 7 : 2 : 1$) without microbial seed.

4.3.3. Substrate inhibition for heterotrophic growth

C. necator growth under heterotrophic conditions was examined with acetate, glucose, glycerol, and mixed organic substrates (Fig. 4.3). The microbial growth was fast with a short lag phase (< 6 h) at 1 – 2.50 g/L of acetate (Fig. 4.3A). However, elevated acetate

concentrations (≥ 5.0 g/L) resulted in extended lag times (24 – 48 h) (Fig. 4.3A), indicating growth inhibition by elevated acetic acid concentrations (Garcia-Gonzalez & de Wever, 2018; Jawed et al., 2022; Sugimoto et al., 1999). In addition, the lag phase lengths (< 12 h) were not impacted at 1.0 – 10.0 g/L of mixed substrates (Fig. 4.3B), glycerol (Fig. 4.3C), or glucose (Fig. 4.3D). However, the increases in the optical densities were not consistent with the increase in substrate concentrations. For instance, the optical densities at 10.0 g/L of organic substrates were only 4 – 40 % higher than at 1.0 g/L. According to these results, lower organic substrate concentrations (≤ 2.50 g/L) are recommended for efficient heterotrophic growth.

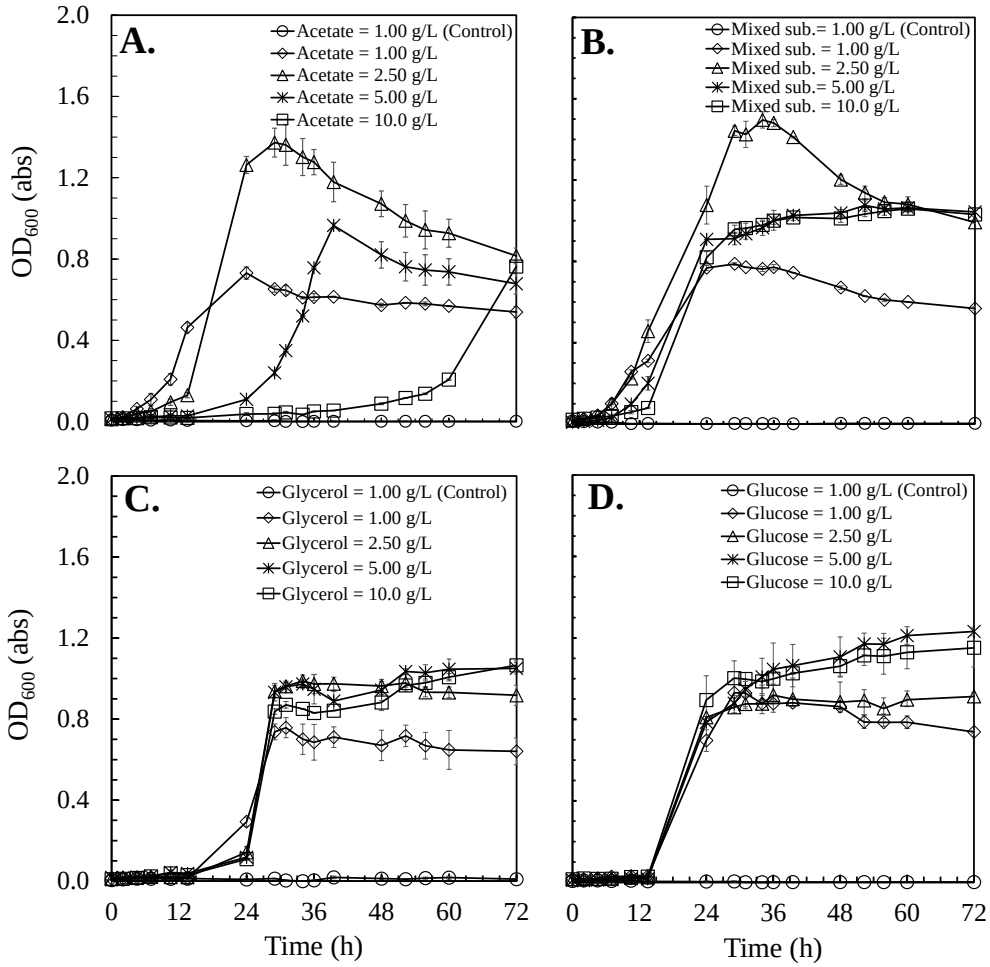

Fig. 4.3. Heterotrophic growth of *C. necator* on: (**A)** acetate; **(B)** mixed substrates (i.e., 33.3% of acetate + 33.3% of glucose + 33.3% of glycerol); **(C)** glycerol; and **(D)** glucose **(D** (n=2). In the control vials, the growth solution with 1.0 g/L of the organic substrate was used without microbial seed.

4.3.4. Organic substrates for mixotrophic growth

The mixotrophic growth (Fig. 4.4) was more rapid than individual heterotrophic (Fig. 4.3) or autotrophic growth (Fig. 4.1) for similar substrate and gas conditions. The lag phases during the mixotrophic growth on acetate and glucose (~5 h) were shorter than on using glycerol or mixed substrates (~12 h) (Fig. 4.4). Also, the mixotrophic optical densities were greater than individual heterotrophic or autotrophic ones. For instance, the highest OD with 1.0 g/L of mixed substrates under mixotrophic (1.23; Fig. 4.4) was greater than under heterotrophic (0.77; Fig. 4.3B) or autotrophic conditions (0.78; Fig. 4.1). These results suggested that *C. necator* can utilize acetate, glucose, or glycerol as the main carbon and energy source and CO_2 and H_2 as additional carbon and energy sources (Rittenberg et al., 1969; Jawed et al., 2022; Kärst & Friedrich, 1984).

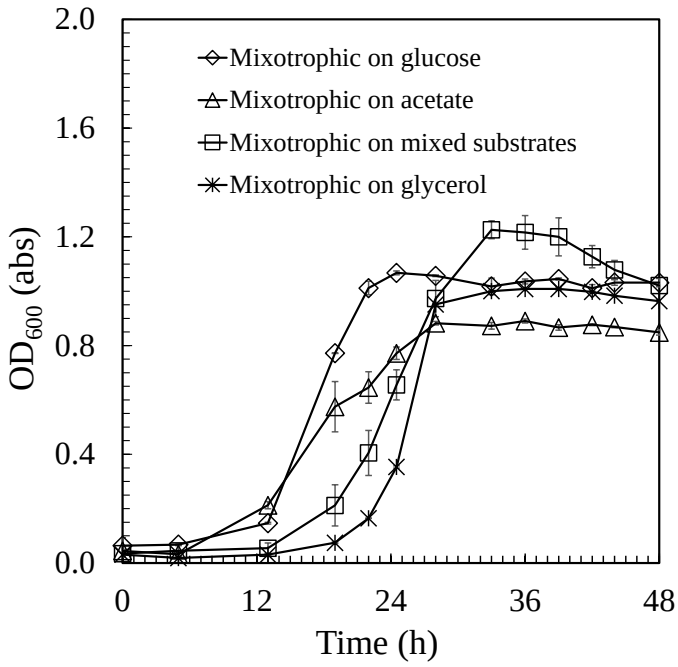

Fig. 4.4. *C. necator* mixotrophic growth on 1.0 g/L of acetate, glucose, glycerol, or mixed substrates (0.33 g-acetate/L + 0.33 g-glucose/L, and 0.33 g-glycerol/L)**.** The headspace was replaced with the standard gas mixture (H_2: O_2 : CO_2 = 7: 2: 1) (n=2).

4.3.5. Hysteresis in two-stage cultivation

C. necator can change the metabolic pathways from heterotrophic to autotrophic/mixotrophic condition very rapidly as it takes less than 12 h for the complete transition (Fig. 4.5A – C). Consistently high optical densities (1.17 – 1.24) were attained when the heterotrophic conditions were switched to mixotrophic conditions at different substrate conditions (i.e., with existing acetate (Fig. 4.5A); after acetate consumption (Fig. 4.5B); or under starvation conditions (Fig. 4.5C)).

In addition, the transition from autotrophic to heterotrophic/mixotrophic growth was also rapid, taking 12 h or less (Fig. 4.5D – F). Similarly, the transition occurred at three different growth stages (i.e., during the exponential phase (Fig. 4.5D); at the end of the exponential phase (Fig. 4.5E); and after the steady state phase (Fig. 4.5F)). However, the higher optical density

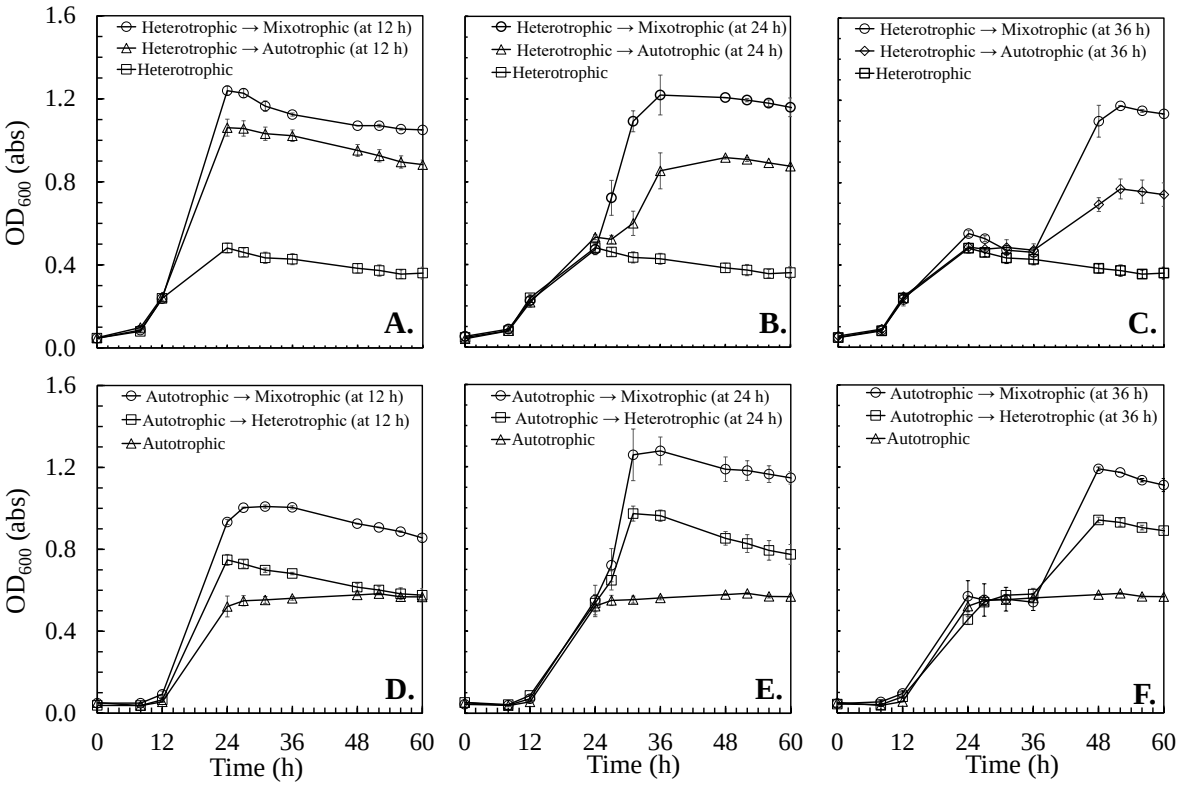

Fig. 4.5. *C. necator* growth in two-stage cultivation systems. In **A**, **B**, and **C**, the bacterium was first grown aerobically on 1.0 g-acetate/L before switching to mixo- or autotrophic conditions after 12 h (**A**), 24 h (**B**), or 36 h (**C**) (n = 2). *C. necator* was first cultivated autotrophically (H_2: O_2: CO_2 = 7:2:1) before switching to other conditions after 12 h (**D**), 24 h (**E**), or 36 h (**F**) (n = 2)

was observed when the second stage was initiated after the end of the exponential phase (> 24 h). According to our results, the two-stage cultivation system with initial heterotrophic growth followed by mixotrophic or autotrophic conditions can achieve higher optical densities in a short cultivation time (< 24 h).

4.4. Conclusions

The impacts of cultivation conditions on the metabolic responses of *C. necator* were investigated. Under autotrophic conditions, the lag phases were short (< 12 h) when a mixture of H_2: O_2: CO_2 = 7: 2: 1 was used. When the partial pressure of O_2 was greater than 0.70 atm, the autotrophic growth was totally inhibited. Similarly, increasing P_{CO_2} higher than 0.6 atm resulted in longer lag phases (> 16 h) and severely impacted the optical densities. The elevated partial pressures of hydrogen (up to 2.7 atm) or nitrogen (up to 2.0 atm) had no impact on the lag phase lengths. Under heterotrophic conditions, the lag phase lengths (< 12 h) were not affected at 1.0 – 10.0 g/L of glucose, glycerol, or mixed substrates; however, acetate concentrations ≥ 5.0 g/L resulted in longer lag periods (> 24 h). The concentration of organic substrates is recommended to be in the lower range (≤ 5.0 g/L) to decrease the lag phase time. With dual substrates, the mixotrophic optical densities were always better than individual autotrophic or heterotrophic optical densities for the same substrate conditions. In two-stage cultivation systems, *C. necator* could completely switch between the three metabolic pathways in less than 12 h. The highest optical densities (1.17 – 1.24) were achieved in two-stage systems with initial heterotrophic conditions followed by mixotrophic or autotrophic conditions. The current results can improve the application of *C. necator* in large-scale industrial systems for biological CO_2 fixation. In future work, the impacts of the metabolic conditions on PHA accumulation by *C. necator* need to be investigated.

Acknowledgement

This study was supported by Natural Sciences and Engineering Research Council of Canada (Discovery Grants, RGPIN-2019-06747 and Discovery Accelerator Supplement, RGPAS-2019-00102), and Ontario Ministry of Research and Innovation (Early Researcher Awards, ER16-12-126 and Ontario Research Fund-Research Excellence, RE09-077).

References

Amer, A., & Kim, Y. (2022). Isolation of Pb(II)-reducing bacteria and demonstration of biological Pb(II) reduction to metallic Pb. *Journal of Hazardous Materials*, *423*, 126975. https://doi.org/https://doi.org/10.1016/j.jhazmat.2021.126975

Belfares, L., Perrier, M., Ramsay, B. A., Ramsay, J. A., Jolicoeur, M., & Chavarie, C. (1995). Multi-inhibition kinetic model for the growth of *Alcaligenes eutrophus*. *Canadian Journal of Microbiology*, *41*(13), 249–256.

Biglari, N., Orita, I., Fukui, T., & Sudesh, K. (2020). A study on the effects of increment and decrement repeated fed-batch feeding of glucose on the production of poly(3-hydroxybutyrate) [P(3HB)] by a newly engineered *Cupriavidus necator* NSDG-GG mutant in batch fill-and-draw fermentation. *Journal of Biotechnology*, *307*, 77–86. https://doi.org/https://doi.org/10.1016/j.jbiotec.2019.10.013

Rittenberg, S. C., & Goodman, N. S. (1969). Mixotrophic Growth of *Hydrogenomonas eutropha*. *Journal of Bacteriology*, *98*(2), 617–622. https://doi.org/10.1128/jb.98.2.617-622.1969.

Caccavo, F., Lonergan, D. J., Lovley, D. R., Davis, M., Stolz, J. F., & McInerney, M. J. (1994). *Geobacter sulfurreducens* sp. nov., a hydrogen- and acetate-oxidizing dissimilatory metal-reducing microorganism. *Applied and Environmental Microbiology*, *60*(10), 3752–3759. https://doi.org/10.1128/aem.60.10.3752-3759.1994

Cramm, R. (2009). Genomic View of Energy Metabolism in *Ralstonia eutropha* H16. *Microbial Physiology*, *16*(1–2), 38–52. https://doi.org/10.1159/000142893

Garcia-Gonzalez, L., & de Wever, H. (2018). Acetic acid as an indirect sink of CO_2 for the synthesis of polyhydroxyalkanoates (PHA): comparison with PHA production processes directly using CO_2 as feedstock. *Applied Sciences*, *8*(9), 1416.

Garcia-Gonzalez, L., Mozumder, M. S. I., Dubreuil, M., Volcke, E. I. P., & de Wever, H. (2015). Sustainable autotrophic production of polyhydroxybutyrate (PHB) from CO_2 using a two-stage cultivation system. *Catalysis Today*, *257*(Part 2), 237–245. https://doi.org/10.1016/J.CATTOD.2014.05.025

Grothe, E., & Chisti, Y. (2000). Poly(β-hydroxybutyric acid) thermoplastic production by Alcaligenes latus: Behavior of fed-batch cultures. *Bioprocess Engineering*, *22*(5), 441–449. https://doi.org/10.1007/s004490050757

Hänggi, U. J. (1990). Pilot scale production of PHB with *Alcaligenes latus*. In *Novel Biodegradable Microbial Polymers* (pp. 65–70). Springer. https://doi.org/10.1007/978-94-009-2129-0_6

Ishizaki, A., & Tanaka, K. (1990). Batch culture of *Alcaligenes eutrophus* ATCC 17697T using recycled gas closed circuit culture system. *Journal of Fermentation and Bioengineering*, *69*(3), 170–174. https://doi.org/https://doi.org/10.1016/0922-338X(90)90041-T

Ishizaki, A., Tanaka, K., & Taga, N. (2001). Microbial production of poly-D-3-hydroxybutyrate from CO_2. *Applied Microbiology and Biotechnology*, *57*(1–2), 6–12.

Jawed, K., Irorere, V. U., Bommareddy, R. R., Minton, N. P., & Kovács, K. (2022). Establishing Mixotrophic Growth of *Cupriavidus necator* H16 on CO_2 and Volatile Fatty Acids. In *Fermentation* (Vol. 8, Issue 3). https://doi.org/10.3390/fermentation8030125

Kärst, U. W. E., & Friedrich, C. G. (1984). Mixotrophic Capabilities of *Alcaligenes eutrophus*. *Microbiology*, *130*(8), 1987–1994. https://doi.org/10.1099/00221287-130-8-1987

Khosravi-Darani, K., Mokhtari, Z. B., Amai, T., & Tanaka, K. (2013). Microbial production of poly(hydroxybutyrate) from C1 carbon sources. *Applied Microbiology and Biotechnology*, *97*(4), 1407–1424. https://doi.org/10.1007/s00253-012-4649-0

Kumar, M., Rathour, R., Singh, R., Sun, Y., Pandey, A., Gnansounou, E., Lin, K.-Y. A., Tsang, D. C. W., & Thakur, I. S. (2020). Bacterial polyhydroxyalkanoates: Opportunities, challenges, and prospects. *Journal of Cleaner Production*, 121500.

Lee, J., Park, H. J., Moon, M., Lee, J.-S., & Min, K. (2021). Recent progress and challenges in microbial polyhydroxybutyrate (PHB) production from CO_2 as a sustainable feedstock: A state-of-the-art review. *Bioresource Technology*, 125616.

Lee, S. Y. (1996). Plastic bacteria? Progress and prospects for polyhydroxyalkanoate production in bacteria. *Trends in Biotechnology*, *14*(11), 431–438.

McGinnis, S., & Madden, T. L. (2004). BLAST: at the core of a powerful and diverse set of sequence analysis tools. *Nucleic Acids Research*, *32*(suppl_2), W20–W25. https://doi.org/10.1093/nar/gkh435

Marudkla, J., Lee, W.-C., Wannawilai, S., Chisti, Y., & Sirisansaneeyakul, S. (2018). Model of acetic acid-affected growth and poly(3-hydroxybutyrate) production by *Cupriavidus necator* DSM 545. *Journal of Biotechnology*, *268*, 12–20. https://doi.org/https://doi.org/10.1016/j.jbiotec.2018.01.004

Miyahara, Y., Yamamoto, M., Thorbecke, R., Mizuno, S., & Tsuge, T. (2020). Autotrophic biosynthesis of polyhydroxyalkanoate by *Ralstonia eutropha* from non-combustible gas mixture with low hydrogen content. *Biotechnology Letters*, *42*(9), 1655–1662. https://doi.org/10.1007/s10529-020-02876-3

Morinaga, Y., Yamanaka, S., Ishizaki, A., & Hirose, Y. (1978). Growth Characteristics and Cell Composition of *Alcaligenes Eutrophus* in Chemostat Culture. *Agricultural and Biological Chemistry*, *42*(2), 439–444. https://doi.org/10.1271/bbb1961.42.439

Mothes, G., Schnorpfeil, C., & Ackermann, J. (2007). Production of PHB from crude glycerol. *Engineering in Life Sciences*, *7*(5), 475–479.

Müller, J., MacEachran, D., Burd, H., Sathitsuksanoh, N., Bi, C., Yeh, Y. C., Lee, T. S., Hillson, N. J., Chhabra, S. R., Singer, S. W., & Beller, H. R. (2013). Engineering of *Ralstonia eutropha* H16 for autotrophic and heterotrophic production of methyl ketones. *Applied and Environmental Microbiology*, *79*(14), 4433–4439. https://doi.org/10.1128/AEM.00973-13

Pavan, F. A., Junqueira, T. L., Watanabe, M. D. B., Bonomi, A., Quines, L. K., Schmidell, W., & de Aragao, G. M. F. (2019). Economic analysis of polyhydroxybutyrate production by *Cupriavidus necator* using different routes for product recovery. *Biochemical Engineering Journal*, *146*, 97–104. https://doi.org/https://doi.org/10.1016/j.bej.2019.03.009

Przybylski, D., Rohwerder, T., Dilßner, C., Maskow, T., Harms, H., & Müller, R. H. (2015). Exploiting mixtures of H_2, CO_2, and O_2 for improved production of methacrylate precursor 2-hydroxyisobutyric acid by engineered *Cupriavidus necator* strains. *Applied Microbiology and Biotechnology*, *99*(5), 2131–2145. https://doi.org/10.1007/s00253-014-6266-6

Repaske, R., & Repaske, A. C. (1976). Quantitative requirements for exponential growth of *Alcaligenes eutrophus*. *Applied and Environmental Microbiology*, *32*(4), 585–591. https://doi.org/10.1128/aem.32.4.585-591.1976

Roy, R. (1962). Nutritional requirements for *Hydrogenonomonas eutropha*. *Journal of Bacteriology*, *83*(2), 418–422. https://doi.org/10.1128/jb.83.2.418-422.1962

Singh, A., & Bhatia, P. (2016). Automated Sanger Analysis Pipeline (ASAP): a tool for rapidly analyzing Sanger sequencing data with minimum user interference. *Journal of Biomolecular Techniques: JBT*, *27*(4), 129.

Sohn, Y. J., Son, J., Jo, S. Y., Park, S. Y., Yoo, J. I., Baritugo, K.-A., Na, J. G., Choi, J., Kim, H. T., Joo, J. C., & Park, S. J. (2021). Chemoautotroph *Cupriavidus necator* as a potential game-changer for global warming and plastic waste problem: A review. *Bioresource Technology*, *340*, 125693. https://doi.org/https://doi.org/10.1016/j.biortech.2021.125693

Sugimoto, T., Tsuge, T., Tanaka, K., & Ishizaki, A. (1999). Control of acetic acid concentration by pH-stat continuous substrate feeding in heterotrophic culture phase of two-stage cultivation of *Alcaligenes eutrophus* for production of P (3HB) from CO_2, H_2, and O_2 under non-explosive conditions. *Biotechnology and Bioengineering*, *62*(6), 625–631.

Tanadchangsaeng, N., & Yu, J. (2012). Microbial synthesis of polyhydroxybutyrate from glycerol: Gluconeogenesis, molecular weight and material properties of biopolyester. *Biotechnology and Bioengineering*, *109*(11), 2808–2818. https://doi.org/https://doi.org/10.1002/bit.24546

Tiemeyer, A., Link, H., & Weuster-Botz, D. (2007). Kinetic studies on autohydrogenotrophic growth of *Ralstonia eutropha* with nitrate as terminal electron acceptor. *Applied Microbiology and Biotechnology*, *76*(1), 75–81. https://doi.org/10.1007/s00253-007-0983-z

Volova, T. G., Kalacheva, G. S., & Altukhova, O. v. (2002). Autotrophic synthesis of polyhydroxyalkanoates by the bacteria *Ralstonia eutropha* in the presence of carbon

monoxide. *Applied Microbiology and Biotechnology*, *58*(5), 675–678. https://doi.org/10.1007/s00253-002-0941-8

Volova, T. G., Kiselev, E. G., Shishatskaya, E. I., Zhila, N. O., Boyandin, A. N., Syrvacheva, D. A., Vinogradova, O. N., Kalacheva, G. S., Vasiliev, A. D., & Peterson, I. v. (2013). Cell growth and accumulation of polyhydroxyalkanoates from CO_2 and H_2 of a hydrogen-oxidizing bacterium, *Cupriavidus eutrophus* B-10646. *Bioresource Technology*, *146*, 215–222. https://doi.org/https://doi.org/10.1016/j.biortech.2013.07.070

Xing, D., Cheng, S., Logan, B. E., & Regan, J. M. (2010). Isolation of the exoelectrogenic denitrifying bacterium *Comamonas denitrificans* based on dilution to extinction. *Applied Microbiology and Biotechnology*, *85*(5), 1575–1587. https://doi.org/10.1007/s00253-009-2240-0

Yu, J. (2018). Fixation of carbon dioxide by a hydrogen-oxidizing bacterium for value-added products. *World Journal of Microbiology and Biotechnology*, *34*(7), 89. https://doi.org/10.1007/s11274-018-2473-0

5. Modeling the growth of diverse microorganisms during feast-famine enrichment

Polyhydroxyalkanoates (PHAs) are an eco-friendly alternative to chemical plastics that have severe impacts on the environment. The current PHA production utilizes pure cultures that require sophisticated cultivation conditions which increase the commercial production costs. The utilization of mixed microbial cultures (MMCs) in PHA production can reduce the higher PHA production cost as MMCs do not require sterilization conditions. In this work, we developed and calibrated a comprehensive mathematical model for the competition between PHA accumulators and non-PHA accumulators in mixed cultures. The model was calibrated and validated using published lab-scale experimental data. The model can be used to optimize the cultivation conditions for the successful enrichment of PHA accumulators in mixed cultures. The model can also be applied to simulate PHA production by the enriched cultures.

The paper was submitted for journal publication.

- Amer, A., and Kim, Y. (2022). A numerical model for the cultivation of *Plasticicumulans acidivorans* and the importance of microbial diversity in feast-famine enrichments (under review).

The co-author's contributions include:

- Funding acquisition.
- Supervision and technical support.
- Manuscript revision.

Abstract

Polyhydroxyalkanoates (PHAs) are biodegradable polymers that can decrease the severe environmental pollution of petroleum plastics. PHA production by mixed microbial communities has been extensively studied to lower the high PHA prices. In this work, we developed a mathematical model for the competition between PHA accumulators and non-PHA accumulators in the feast-famine enrichment strategy. The developed model successfully simulated published lab-scale experimental data for *Plasticicumulans acidivorans*, a well-studied PHA accumulator that can store PHA up to 90% of the cell weight. The growth kinetics for both PHA and non-PHA accumulators were estimated and compared to the values in the literature. The uncertainties in the model kinetics were studied by expanding the model to include additional sub-biomass components for each heterotrophic group. As a result, the microbial diversity of microbial communities was observed to influence the enrichment of PHA accumulators in mixed cultures. Additionally, the calibrated model was applied to investigate the cultivation conditions such as cycle lengths, carbon-to-nitrogen ratio, and solids retention time for successful *P. acidivorans* enrichment in mixed cultures. The developed model can be applied to control the cultivation and enrichment of PHA accumulators in large-scale PHA production systems.

Keywords: *Plasticicumulans acidivorans*; Polyhydroxyalkanoates; Microbial mixed cultures; PHA accumulation; Mathematical modeling; Sensitivity analysis.

5.1. Introduction

Polyhydroxyalkanoates (PHAs) are biodegradable polyesters that can substitute conventional petrochemical plastics. Currently, commercial PHA production utilizes pure cultures that require strict cultivation conditions and expensive organic substrates (Argiz et al., 2020; Korkakaki et al., 2016). PHA production using mixed microbial cultures (MMCs) is gaining increased attention because MMCs can utilize cheap feedstocks without the

requirements for sterilized conditions (Fang et al., 2019; Kumar et al., 2020; Oliveira et al., 2017). In mixed cultures, heterotrophic microorganisms are classified into PHA-accumulating and non-PHA-accumulating microbes (Chen et al., 2016). PHA accumulators can be enriched using a dynamic feeding strategy known as feast-famine enrichment. In the feast stage, PHA accumulators feed on external organic substrates to simultaneously grow and store PHA inside their cells. PHA accumulators utilize the stored PHA as a source of carbon and energy when the external carbon substrate is substantially consumed in the famine stage. This ecological advantage enables PHA accumulators to strongly compete with other heterotrophs and eventually dominate the cultures (Chen et al., 2016; Fang et al., 2019).

The competition between PHA accumulators and non-PHA accumulators in the enrichment process was not demonstrated in previous mathematical models (Fang et al., 2019; Marang et al., 2015; Mozumder et al., 2020). The Activated Sludge Model No. 3 (ASM3) was used to develop several models to describe the storage and utilization of internal products such as PHA (Henze et al., 2000; Ni et al., 2009, 2010; Ni & Yu, 2007, 2008). However, the ASM3 assumed that all heterotrophic microorganisms convert organic substrates into internally stored products, without differentiating between PHA and non-PHA accumulators (Gujer et al., 1999; Henze et al., 2000; Ni et al., 2009, 2010; Ni & Yu, 2007, 2008). As a result, the ASM3 cannot be applied to simulate feast-famine enrichment (Sin et al., 2005). Thus, one of the main objectives of this work was to develop and calibrate a mathematical model that can comprehensively describe the competition between PHA accumulators and non-PHA accumulators in feast-famine enrichment.

Plasticicumulans acidivorans can accumulate high PHA fractions when utilizing organic substrates such as acetate or lactate (~90% w/w) (Jiang et al., 2011; Jiang, Marang, et al., 2011b; Johnson et al., 2009; Marang et al., 2013) or complex waste feedstocks (~70% w/w) (Marang et al., 2016; Tamang et al., 2019; Tamis et al., 2014). *P. acidivorans* was successfully

inoculated into mixed cultures and dominated the microbial community (>80%) in seven days (Jiang, Marang, et al., 2011a), suggesting the ability to use the bacterium in commercial production without sterilization. Therefore, the developed model was calibrated and verified using previous experimental results for enriching *P. acidivorans* in mixed microbial cultures . In previous studies, PHA accumulators were modeled as a single component assuming an average metabolic activity for all individual species existing in mixed cultures. However, the microbial diversity in mixed cultures could impact the enrichment of PHA accumulators (Ramirez et al., 2009). Consequently, the impact of microbial diversity on the enrichment of PHA accumulators was also investigated. In addition, we studied the influence of the uncertainty in model kinetics on the enrichment of PHA accumulators. Another objective of this work was to investigate the effect of operational parameters such as solids retention time (SRT), carbon-to-nitrogen (C/N) ratio, and cycle length on the enrichment of PHA accumulators in mixed cultures.

5.2. Methods

5.2.1. Model development

A non-steady-state model with nine components was developed to describe the competition between PHA accumulators (X_{PA}) and non-PHA accumulators (X_{NA}) in the feast-famine enrichment and PHA accumulation by X_{PA} (Table 5.1). The developed model was based on the ASM3 and other published models for PHA storage and utilization (Fang et al., 2019; Henze et al., 2000; Mozumder et al., 2020; Ni & Yu, 2008; Sin et al., 2005). The microbial consortium was assumed to contain heterotrophs only as the feast-famine strategy reduces the populations of other microorganisms (e.g., autotrophs) significantly (Dias et al., 2005). X_{PA} biomass was assumed to consist of active biomass and PHA while X_{NA} had active biomass only. In addition to X_{PA} and X_{NA}, other particulate components are polyhydroxyalkanoates (X_{PHA}), slowly biodegradable solids (X_S), and inert solids (X_I) (Henze et al., 2000; Ni & Yu, 2008). The soluble components are external organic substrate (S_S), Oxygen (S_O), nitrogen (S_N),

and phosphorus (S_P), included in microbial growth kinetics (Eq. 5.3, 5.4, and 5.9) as Monod equations (Johnson, Kleerebezem, et al., 2010b, 2010a; Korkakaki et al., 2017). S_N is assumed to be assimilated for microbial growth only because nitrification is usually suppressed by using chemicals (e.g., allylthiourea) in feast-famine enrichments (Marang et al., 2018).

The main microbial reactions described in the model are microbial growth on S_S (Eq. 5.3 and 5.9); PHA-storage (Eq. 5.2); growth on X_{PHA} (Eq. 5.4); maintenance on S_S (Eq. 5.5 and 5.10); maintenance on X_{PHA} (Eq. 5.6); X_S hydrolysis (Eq. 5.1 and 5.8); and cell decay (Eq. 5.7 and 5.11) under feast and famine conditions. In the feast stage, X_{PA} grow on external S_S (Eq. 5.3) along with storing X_{PHA} (Eq. 5.2) while X_{NA} grow without storing any X_{PHA} (Eq. 5.9). The stored X_{PHA} amount depends on available substrate concentrations, polymer storage rate (k_{sto}), and the maximum PHA-storage fraction ($f_{(PHA)}max$) (Eq. 5.2) (Amini et al., 2020; Oshiki et al., 2011a; Porras et al., 2018). PHA storage may occur under aerobic, anoxic, or anaerobic conditions and thus the oxygen term was not included in the PHA-storage kinetics (Eq. 5.2) (Vjayan & Vadivelu, 2017; X. Wang et al., 2017, 2019). After the depletion of external carbon sources (i.e., the famine stage), only X_{PA} could synthesize new cells and maintain their cells by utilizing the stored X_{PHA} (Eqs. 5.4 and 5.6). An inverted Monod term $\left(\frac{K_{S,PA}}{K_{S,PA}+S_S}\right)$ was included in the equations of microbial growth and maintenance on PHA to allow the transition from the feast to famine stages (Eq. 5.4 and 5.5).

5.2.2. Numerical solution and model calibration

Nine non-steady-state ordinary differential equations were prepared and numerically approximated by the Crank-Nicolson method. The discretized mass-balance equations were then solved by the fixed-point iteration method with a convergence tolerance < 10^{-5}. The simulations were performed using the Visual Basic for Application (VBA) tool in Microsoft Excel.

The model coefficients were calibrated and validated by simulating published experimental data for enriching *P. acidivorans* in mixed cultures and PHA accumulation under various operational conditions (Jiang et al., 2011; Jiang, Marang, et al., 2011a, 2011b; Johnson et al., 2009; Johnson, Kleerebezem, et al., 2010a; Korkakaki et al., 2017; Marang et al., 2013, 2016, 2018). The experimental data from these studies were extracted using an online tool (WebPlotDigitizer, California, USA) and then fitted by minimizing the differences between the data points and the model-simulated results. The initial conditions for these published results are summarized in Table 5.2. The model kinetic constants and stoichiometric coefficients were then estimated and compared to the reported ranges in previous studies (Table 5.3) (Jiang, Marang, et al., 2011a; Johnson, Jiang, et al., 2009; Johnson, Kleerebezem, et al., 2010a; Korkakaki et al., 2017; Marang et al., 2016, 2018; Henze et al., 2000; Ni et al., 2009, 2010; Ni & Yu, 2007, 2008).

5.2.3.Sensitivity analysis

A parameter sensitivity analysis was performed to identify the highly sensitive parameters that impact the model results. The average sensitivity value (δ) of a variable (y) with respect to a model parameter (θ) (Table 5.3) was calculated (Mozumder et al., 2014),

$$\delta = \frac{\sum_{i=1}^{t}\left(\frac{\partial y_i(t)}{\partial \theta}.\frac{\theta_0}{y_i(t)}\right)}{n} \cong \frac{\sum_{i=1}^{t}\left(\frac{y_{(t,\theta+\Delta\theta)}-y_{(t,\theta-\Delta\theta)}}{2\Delta\theta}.\frac{\theta}{y_i(t)}\right)}{n} \qquad (5.12)$$

Where, Δθ is ±1% change in the average model parameter (θ) value (Δθ = ±0.01 θ), and n is the number of the time steps ((simulation time (τ))/(time step (10 Sec))). The sensitivity analysis was conducted for the X_{PA} enrichment scenario in which y was defined as X_{PA} fraction (f_{PA}) in the mixed culture. In another scenario for PHA accumulation, the sensitivity of X_{PA} parameters was studied by defining y as X_{PHA}.

5.2.4. Extended model to study uncertainty in kinetics

The main model was expanded to investigate the impact of the diversity of individual microbes on X_{PA} enrichment and PHA accumulation by studying the uncertainties in model parameters (Ramirez et al., 2009). Three active biomass sub-components were included for each microbial group: $X_{PA_1} = X_{PA_2} = X_{PA_3}$= 3.33 g-COD$_X$.m^{-3}; and X_{NA_1}=$X_{NA_2} = X_{NA_3}$ = 330 g-COD$_X$.m^{-3} (Table A4.1). It is noted that PHA accumulators (X_{PA} = 10 g-COD$_X$.m^{-3}) and non PHA accumulators (X_{NA} = 990 g-COD$_X$.m^{-3}) were defined as single components in the single-X model (Table 5.1). In the extended model simulations, only one parameter (e.g., $\mu_{XPA,S}$) for the same sub-components ($X_{PA_{1-3}}$or $X_{NA_{1-3}}$) was changed by ±20 and 50% while other kinetic constants were assumed to be constant

Table 5.1. Stoichiometric and kinetic matrix for the model

Reaction	*Soluble Components*				*Particulate Components*					*Reaction rate*	
	S_O	S_s	S_N	S_p	X_I	X_S	X_{NA}	X_{PA}	X_{PHA}		
PHA accumulators (X_{PA}):											
Hydrolysis by X_{PA}		1				−1				$k_H \cdot \frac{X_S/X_{PA}}{K_X + (X_S/X_{PA})} X_{PA}$	(5.1)
PHA storage	$1 - \frac{1}{Y_{PHA,S}}$	$\frac{-1}{Y_{PHA,S}}$							1	$k_{sto} \cdot \frac{S_S}{K_{S,PA} + S_S} \cdot \left(1 - \frac{X_{PHA}/X_{PA}}{f_{(PHA)}max}\right) X_{PA}$	(5.2)
Growth on S_s	$1 - \frac{1}{Y_{PA,S}}$	$\frac{-1}{Y_{PA,S}}$	-i_{NBM}	-i_{PBM}				1		$\mu_{PA,S} \cdot \frac{S_S}{K_{S,PA} + S_S} \frac{S_N}{K_N + S_N} \frac{S_P}{K_P + S_P} \frac{S_{O2}}{K_{O2} + S_{O2}} X_{PA}$	(5.3)
Growth on PHA	$1 - \frac{1}{Y_{PA,S}}$		-i_{NBM}	-i_{PBM}				1	$\frac{-1}{Y_{PA,PHA}}$	$\mu_{PA,PHA} \cdot \frac{K_{S,PA}}{K_{S,PA} + S_S} \frac{S_N}{K_N + S_N} \frac{S_P}{K_P + S_P} \frac{S_{O2}}{K_{O2} + S_{O2}} \frac{X_{PHA}/X_{PA}}{K_{PHA} + X_{PHA}/X_{PA}}$	(5.4)
Maintenance on S_S		−1								$m_{PA,S} \cdot \frac{S_S}{K_{S,PA} + S_S} \cdot X_{PA}$	(5.5)
Maintenance on PHA									−1	$m_{PA,PHA} \cdot \frac{K_{S,PA}}{K_{S,PA} + S_S} \cdot \frac{X_{PHA}/X_{PA}}{K_{PHA} + X_{PHA}/X_{PA}} X_{PA}$	(5.6)
Decay	−(1- f_I)		i_{NBM} - f_I*i_{NXI}	i_{PBM} - f_I*i_{PXI}	f_I	1- f_I		−1		$b_{PA} \cdot \frac{K_{PHA}}{K_{PHA} + X_{PHA}/X_{PA}} X_{PA}$	(5.7)
Non-PHA accumulators (X_{NA}):											
Hydrolysis by X_{NA}		1				−1				$k_H \cdot \frac{X_S/X_{NA}}{K_X + (X_S/X_{NA})} X_{NA}$	(5.8)
Growth on S_s	$1 - \frac{1}{Y_{NA,S}}$	$\frac{-1}{Y_{NA,S}}$	-i_{NBM}	-i_{PBM}			1			$\mu_{NA,S} \cdot \frac{S_S}{K_{S,NA} + S_S} \cdot \frac{S_N}{K_N + S_N} \frac{S_P}{K_P + S_P} \frac{S_O}{K_O + S_O} X_{NA}$	(5.9)
Maintenance on S_S		-1								$m_{NA,S} \cdot \frac{S_S}{K_{S,NA} + S_S} \cdot X_{NA}$	(5.10)
Decay	-(1- f_I)		i_{NBM} - f_I*i_{NXI}	i_{PBM} - f_I* i_{PXI}	f_I	1- f_I	−1			$b_{NA} \cdot X_{NA}$	(5.11)

Table 5.2. Summary of initial conditions for figures in this study

Figure/Table	Simulated lab-scale experimental results	Substrate	$S_{O,0}$ ($g\text{-}O_2.m^{-3}$)	$S_{S,0}$ ($g\text{-}COD.m^{-3}$)	$S_{N,0}$ ($g\text{-}N.m^{-3}$)	$S_{P,0}$ ($g\text{-}P.m^{-3}$)	$X_{I,0}$ ($g\text{-}COD.m^{-3}$)	$X_{S,0}$ ($g\text{-}COD.m^{-3}$)	$X_{NA,0}$ ($g\text{-}COD.m^{-3}$)	$X_{PA,0}$ ($g\text{-}COD.m^{-3}$)	$X_{PHA,0}$ ($g\text{-}COD.m^{-3}$)
Fig. 5.1A	(Jiang, Marang, et al., 2011a)	Acetate	5.0	1600	95	77	0	0	540	6	0
Fig. 5.1B	(Jiang, Marang, et al., 2011b)			20280	23	77	0	0	0	864	30
Fig. 5.1C	(Jiang, Marang, et al., 2011b)			1572	102	77	0	0	0	655	0
Fig. A4.1A	(Johnson et al., 2009)			2000	113	77	0	0	0	700	0
Fig. A4.1B	(Johnson et al., 2009)			114600	1184	200	0	0	0	630	40
Fig. A4.2A	(Johnson, Kleerebezem, et al., 2010a)			22700	14200	1000	0	0	0	1000	40
Fig. A4.2B	(Johnson, Kleerebezem, et al., 2010a)			1630	160	9.7	0	0	0	1100	0
Fig. A4.3	(Korkakaki et al., 2017)			2166	138	80	0	0	0	1086	0
Fig. A4.4A	(Marang et al., 2018)			5902	16	80	0	0	0	120	0
Fig. A4.4B	(Marang et al., 2018)			8500	5	85	0	0	0	1485	0
Fig. A4.5A	(Marang et al., 2016)			0	120	77	0	8.92	0	386	1244
Fig. A4.5B	(Marang et al., 2016)			1077	120	77	0	0	0	770	0
Fig. A4.6A	(Marang et al., 2013)	Butyrate		8972	5	77	0	0	0	750	74
Fig. A4.6B	(Marang et al., 2013)			1207	142	77	0	0	0	560	0
Fig. A4.6C	(Jiang et al., 2011)	Propionate		13050	32.5	77	0	0	0	1100	0
Fig. A4.6D	(Jiang et al., 2011)			1750	85	77	0	0	10	990	0
Figs. 5.2A, 2B, 5.3, 5.4, 5.5, 5.6				10000	0	446	0	0	0	1000	0
Table A4.1											

Table 5.3. Summary of estimated and previously reported kinetic constants for model parameters (at 30°C)

Parameter	Definition (units)	Estimated in this study (Θ)*	Reported range
PHA-accumulators (X_{PA}):			
$\mu_{PA,S}$	Specific growth rate for X_{PA} on S_S (h^{-1})	0.20	0.08-0.234 (Johnson, Kleerebezem, et al., 2010a; Korkakaki et al., 2017; Marang et al., 2016)
$\mu_{PA,PHA}$	Specific growth rate for X_{PA} on X_{PHA} (h^{-1})	0.40	0.04-2.0 (Fang et al., 2019; Jiang, Marang, et al., 2011b; Marang et al., 2016; Mozumder et al., 2020)
$Y_{PA,S}$	Yield coefficient for X_{PA} on S_S (g-COD_X.g-COD_S^{-1})	0.65	0.04-0.63 (Henze et al., 2000; Mozumder et al., 2020; Ni et al., 2010; Ni & Yu, 2007)
$Y_{PA,PHA}$	Yield coefficient for X_{PA} growth on X_{PHA} (g-COD_X. g-COD_{PHA}^{-1})	0.90	0.67-0.85 (Mozumder et al., 2020; Ni et al., 2010; Ni & Yu, 2007)
$Y_{PHA,S}$	Yield coefficient for PHA storage on S_S (g-COD_{PHA}.g-COD_S^{-1})	0.70	0.59-0.91 (Jiang, Marang, et al., 2011b; Johnson, van Geest, et al., 2010; Marang et al., 2016, 2018)
ksto	PHA storage rate (g-COD_{PHA}.g-COD_X^{-1}.h^{-1})	2.50	0.71-3.3 (Jiang, Marang, et al., 2011b; Johnson, Kleerebezem, et al., 2010a; Marang et al., 2016)
PHA storage	Maximum accumulated PHA ratio in cells ($\frac{X_{PHA}}{X_{PHA}+X_{PA}}$) (%)	67	37-70[a] 69-89[b] (Jiang, Marang, et al., 2011b; Johnson et al., 2009; Johnson, Kleerebezem, et al., 2010a; Korkakaki et al., 2017; Marang et al., 2016, 2018)
$f_{(PHA)}^{max}$	Maximum ratio of PHA to active biomass $\left(\frac{X_{PHA}}{X_{PA}} = \left(\frac{100}{PHA\ storage\ (\%)} - 1\right)^{-1}\right)$	2.0	0.59-2.33[a] 2.23-8.30[b] (Jiang, Marang, et al., 2011b; Johnson et al., 2009; Johnson, Kleerebezem, et al., 2010a; Korkakaki et al., 2017; Marang et al., 2016, 2018)
$K_{S,PA}$	Half-saturation constant for X_{PA} on S_S (g-COD_S. m^{-3})	9.8	9.8 (Henze et al., 2000)
b_{PA}	Decay rate coefficient for X_{PA} (h^{-1})	0.017	0.0083-0.052 (Marang et al., 2018; Ni & Yu, 2008)
$K_{PHA,PA}$	PHA half-saturation constant for X_{PA} (g-COD_{PHA}. g-COD_X^{-1})	2.0	0.9-1.0 (Fang et al., 2019; Henze et al., 2000; Ni & Yu, 2008)
$m_{PA,PHA}$	Maintenance coefficient for X_{PA} on X_{PHA} (h^{-1})	0.0044	0.0044-0.01 (Henze et al., 2000; Ni & Yu, 2007, 2008)
$K_{N,PA}$	N affinity constant for X_{PA} (g-N.m^{-3})	0.50	0.01-0.50 (Marang et al., 2018; Ni & Yu, 2008)

Table 5.3 cont.: Summary of estimated and previously reported kinetic constants for model parameters (at 30°C)

$K_{P,\,PA}$	P affinity constant for X_{PA} (g-P.m^{-3})	0.01	0.01 (Fang et al., 2019; Henze et al., 2000; Ni et al., 2009; Ni & Yu, 2007)
$K_{O,\,PA}$	Oxygen affinity constant for X_{PA} (g-O_2.m^{-3})	0.20	0.20 (Ni et al., 2010; Ni & Yu, 2007, 2008)
$m_{PA,S}$	Maintenance coefficient for X_{PA} on S_S (h^{-1})	0.0066	0.0066-0.01 (Fang et al., 2019; Henze et al., 2000; Mozumder et al., 2020)
Non-PHA accumulators (X_{NA}):			
$\mu_{NA,\,S}$	Maximum growth rate for X_{NA} on S_S (h^{-1})	0.40	0.35-0.70 (Henze et al., 2000; Ni & Yu, 2008; Nogaj et al., 2015; Torretta et al., 2014)
$K_{S,\,NA}$	Half-saturation constant for X_{NA} on S_S (g-COD_S. m^{-3})	9.8	2-11.38 (Lemos et al., 2008; Ni et al., 2010; Ni & Yu, 2007)
$Y_{NA,S}$	Yield coefficient for X_{NA} on S_S (g-COD_X.g-COD_S^{-1})	0.65	0.47-0.90 (Gujer et al., 1999; Henze et al., 2000; Jiang, Marang, et al., 2011a)
b_{NA}	Decay rate coefficient for X_{NA} (h^{-1})	0.017	0.0083-0.052 (Henze et al., 2000; Ni & Yu, 2007, 2008)
$K_{N,\,NA}$	N affinity constant for X_{NA} (g-N.m^{-3})	0.50	0.01-0.50 (Marang et al., 2018; Ni & Yu, 2008)
$K_{P,\,NA}$	P affinity constant for X_{NA} (g-P.m^{-3})	0.01	0.01 (Fang et al., 2019; Henze et al., 2000; Ni et al., 2009; Ni & Yu, 2007)
$K_{O,\,NA}$	Oxygen affinity constant for X_{NA} (g-O_2.m^{-3})	0.20	0.20 (Ni et al., 2010; Ni & Yu, 2007, 2008)
$m_{S,\,NA}$	Maintenance coefficient for X_{NA} on S_S (h^{-1})	0.0066	0.0066-0.01 (Chen et al., 2019; Chinwetkitvanich et al., 2004; Jiang, Marang, et al., 2011a; Johnson, van Geest, et al., 2010; X. Wang et al., 2017)
Stoichiometric constants			
f_I	Fraction of X_I in biomass lysis (g-COD. g-COD^{-1})	0.20	0.1-0.20 (Fang et al., 2019; Henze et al., 2000; Ni & Yu, 2008)
i_{NBM}	Nitrogen content of biomass (g-N. g-COD^{-1})	0.08	0.07 (Henze et al., 2000)
i_{NXI}	Nitrogen content in X_I (g-N. g-COD^{-1})	0.02	0.02 (Henze et al., 2000)
i_{PBM}	Phosphorus content in biomass (g-P. g-COD^{-1})	0.02	0.02 (Henze et al., 2000; Ni & Yu, 2008)
i_{PXI}	Phosphorus content in X_I (g-P. g-COD^{-1})	0.01	0.01 (Henze et al., 2000; Ni & Yu, 2008)
K_H	Maximum hydrolysis rate (h^{-1})	0.125	0.125 (Henze et al., 2000)
K_X	Hydrolysis affinity constant (g-COD. g-COD^{-1})	1.00	1.00 (Henze et al., 2000)

* Unless otherwise mentioned below the figures, the estimated kinetic constants were applied in all simulations to produce all figures.

5.3. Results and Discussion

5.3.1. Model calibration using previous lab-scale studies

The model was successfully calibrated by simulating previously reported lab-scale experiment data for enriching *P. acidivorans* in mixed microbial cultures (Figs. 5.1 and A4.1 to A4.6) (Jiang et al., 2011; Jiang, Marang, et al., 2011b, 2011a; Johnson et al., 2009; Johnson, Kleerebezem, et al., 2010a; Korkakaki et al., 2017; Marang et al., 2013, 2016, 2018). For instance, PHA accumulators (X_{PA}) were enriched over fourteen 12-hr batch cycles as X_{PA} fraction (f_{PA}) increased to 86.6% (Fig. 5.1A) (Jiang, Marang, et al., 2011a). The model was also verified for the changes in the 3 model components (X_{PA}, X_{PHA}, and S_S) during a single feast-famine cycle (Fig. 5.1B) (Jiang, Marang, et al., 2011b). In this experiment, S_S was rapidly consumed from 1600 to < 0.10 g-COD$_S$/L in the 40-min feast stage. During this feast stage, X_{PHA} was accumulated up to 1080 g-COD$_{PHA}$/L (~60% (w/w)) after 40 min. After complete acetate depletion, X_{PHA} was gradually utilized by X_{PA} for cell synthesis (the famine stage). The model was also examined with additional feast-famine cultivations under various experimental conditions, as illustrated in Figs. A4.1A, A4.3, A4.4A, A4.5, A4.6A, and A4.6C.

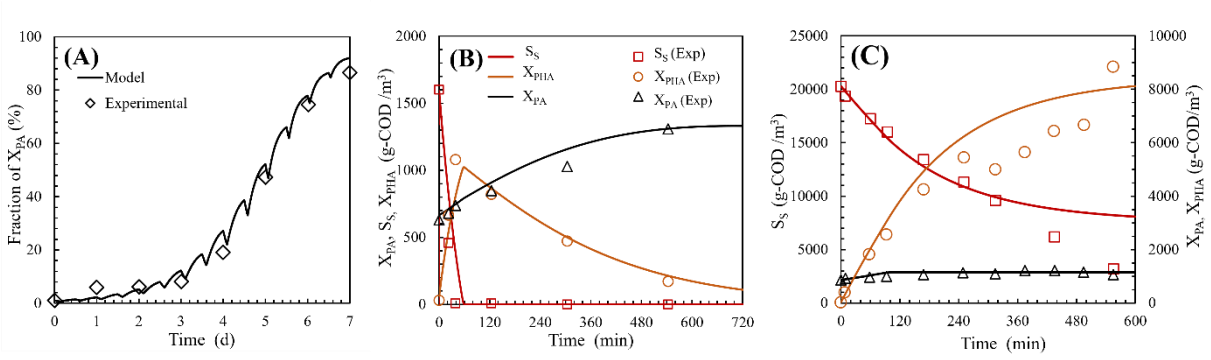

Fig. 5.1. Model calibration simulations for X_{PA} under various cultivation conditions. (**A)** The competition between X_{PA} and X_{NA} ($Y_{PHA,S}$=0.80) (Jiang, Marang, et al., 2011a). (**B)** A repeated feast-famine cycle for a culture dominated by *P. acidivorans* ($Y_{PHA,S}$ = 0.80) (Jiang, Marang, et al., 2011b). (**C)** PHA-accumulation experiment by X_{PA} with excess substrate ($f_{(PHA)}^{max}$ = 7.33) (Jiang, Marang, et al., 2011b). Acetate was the sole organic substrate in both studies. All applied kinetic constants and initial conditions are summarized in Tables 5.2 and 5.3.

In addition to the feast-famine strategy for X_{PA} enrichment, the model was further validated for PHA-accumulation scenarios (Figs. 5.1C, A4.1B, A4.2, A4.4B, A4.6B, A4.6D). For instance, the model successfully described high PHA accumulation (8830 g-COD_{PHA}/L ~ 89% (w/w)) from 20,000 g-$COD_{Substrate}$/L in the absence of NH_4^+ (Fig. 5.1C) (Jiang, Marang, et al., 2011b).

The calibrated model parameters using previous lab-experiments results (Fig. 5.1, Figs. A4.1 to A4.6) were consistent with the previous modeling studies (Table 5.2). For instance, the estimated $\mu_{PA,S}$ (0.20 h^{-1}) and $\mu_{PA,PHA}$ (0.40 h^{-1}) values are within the reported ranges for PHA accumulators on the external substrate and PHA, respectively (Fang et al., 2019; Jiang, Marang, et al., 2011b; Johnson, Kleerebezem, et al., 2010a; Korkakaki et al., 2017; Marang et al., 2016; Mozumder et al., 2020). The found $\mu_{NA,S}$ value (0.40 h^{-1}) also agrees well with the values reported for non-PHA-accumulating microorganisms (Henze et al., 2000; Ni & Yu, 2008; Nogaj et al., 2015; Torretta et al., 2014). The yield coefficients ($Y_{PA,S}$, $Y_{PHA,S}$, and $Y_{NA,S}$) were also consistent with the previous studies while $Y_{PA,PHA}$ was slightly higher at 0.90 g-COD_X / g-COD_{PHA} than the reported range for the PHA accumulators (0.67-0.85 g-COD_X / g-COD_{PHA}) (Table 5.2) (Mozumder et al., 2020; Ni et al., 2010; Ni & Yu, 2007).

5.3.2. Sensitivity analysis

The sensitivity analysis results indicated that $f_{PHA}^{(max)}$, $\mu_{PA,S}$, k_{sto}, $\mu_{PA,PHA}$, $Y_{PA,PHA}$, b_{PA} (Fig. 5.2A) and $\mu_{NA,S}$, $Y_{NA,S}$, b_{NA} (Fig. 5.2B) significantly impacted the X_{PA} enrichment simulations. Among the model constants, $\mu_{NA,S}$ (δ = -2.08) and $f_{PHA}^{(max)}$ (δ=1.85) had the highest sensitivity to the competitive growth between X_{NA} and X_{PA}. In addition, the δ value in the sensitivity simulations with varying half-saturation affinity constants (K_N, K_P, K_S, and $K_{PHA,PA}$), maintenance coefficients ($m_{PA,S}$, $m_{NA,S}$, $m_{PA,PHA}$), and hydrolysis coefficients (K_X, K_H) was

always small (< 0.08) (Fig. 5.2), indicating that these model parameters have minimal impacts on the model output.

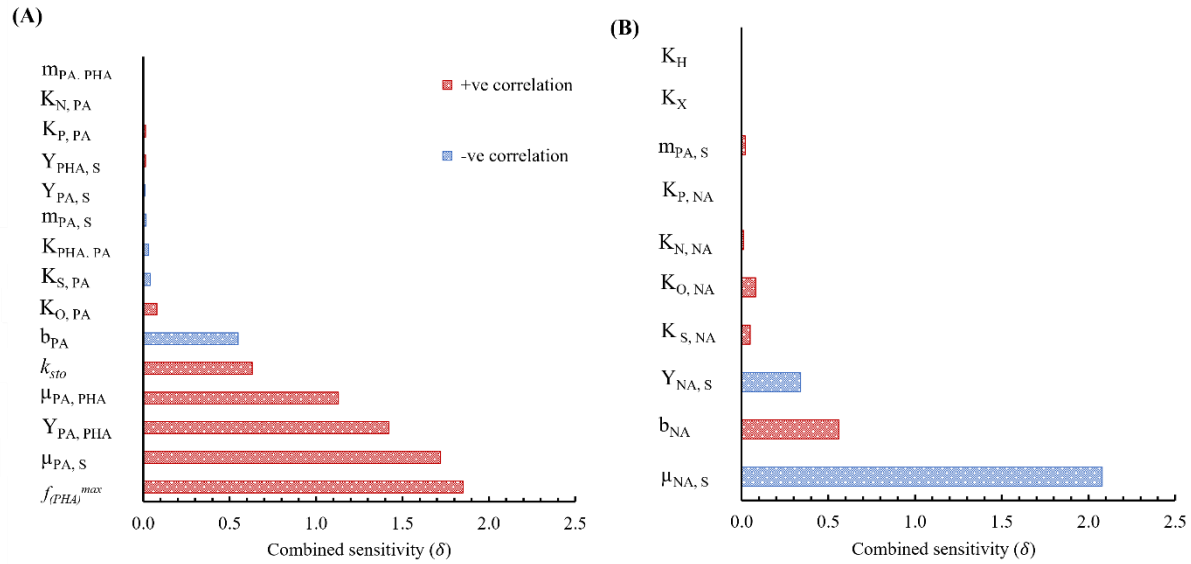

Fig. 5.2. Results of the combined sensitivity analysis for model parameters for a feast-famine enrichment simulation for: **(A)** X_{PA} and **(B)** X_{NA} after 5 days. δ values were calculated for X_{PA} fraction (f_{PA}) after changing the parameter values (Table 5.2) by ±1%. Initial conditions are summarized in Table 5.2.

In a different set of simulations, PHA accumulation was highly sensitive to only $f_{PHA}^{(max)}$ and k_{sto} (Table A4.2), signifying the importance of both parameters in modeling PHA accumulation (Reaction 2 in Table 5.1). It should be noted that $f_{PHA}^{(max)}$ (2.0–7.33) and k_{sto} (0.35–2.50 h^{-1}) varied widely according to the experimental conditions in the previous studies (Figs. 5.1 and A4.1 to A4.6, Table 5.3).

5.3.3. Three-X model simulations to study the microbial diversity impact on the X_{PA} enrichment

The three-X model showed different results compared to the single-X model when $\mu_{PA,S}$, $f_{PHA,max}$, or $\mu_{NA,S}$ varied for the 3 species for the X_{PA} enrichment in mixed cultures (Fig. 5.3). It should be noted that the average value of the varied parameters in the three-X model

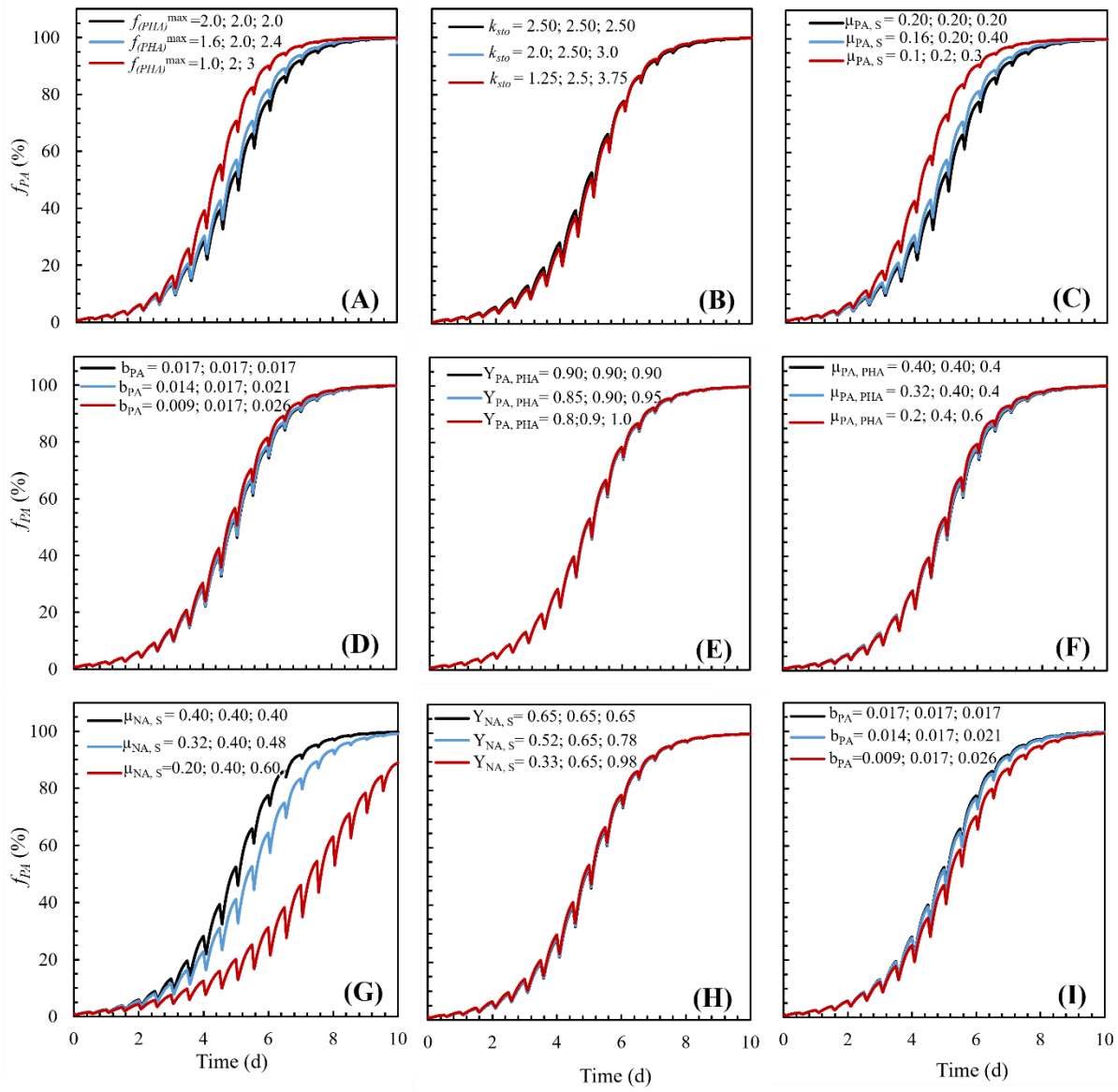

Fig. 5.3. Simulations of three-X_{PA} model (A to F) and three-X_{NA} model (G to I) components. The average values for parameters and initial conditions are shown in Tables 5.2 and 5.3, respectively. For every figure, only one parameter was changed. For figures A to F, Initial X_{PA1}=X_{PA2}=X_{PA3}=10/3 g-COD/m^3 and initial X_{NA}=990 g-COD/m^3. For figures G to I, initial X_{NA1}=X_{NA2}=X_{NA3}=990/3 g-COD/m^3 and initial X_{PA}=10 g-COD/m^3. Other initial conditions are the same as in Table 5.2.

(e.g., $\mu_{PA,S1\text{-}3}$= 0.10, 0.20, 0.30 h^{-1}) was the same as that in the single-X model (e.g., $\mu_{PA,S}$= 0.20 h^{-1}) (Table A4.1). In the three-X model simulations, X_{PA} species with ±50% variation in $\mu_{PA,S}$ or $f_{PHA,max}$ dominated the mixed culture slightly faster than one X_{PA} species with an average $\mu_{PA,S}$ or $f_{PHA,max}$ value (Fig. 5.3A, C and Fig. A4.7B, C). In contrast, when $\mu_{NA,S}$ varied for three X_{NA} species (0.20−0.60 h^{-1}), f_{PA} dropped to 89% compared to 99.9% for X_{NA} species with

the same $\mu_{NA,S}$ (0.40 h^{-1}) after 10 days (Fig. 5.3G and Fig. A4.7D). For other model parameters such as yield and decay coefficients and PHA storage rate (k_{sto}), there was no variance between the results of the three-X and single-X models. According to our simulations, the three-X model is recommended to be applied when individual species with various specific growth rates or different PHA-accumulating capacities exist in mixed cultures.

5.3.4. Influence of cycle length on X_{PA} enrichment

The model simulations revealed that short cycle lengths (1−12 hrs) were necessary for successful X_{PA} enrichment and to maintain lower feast-to-famine (F/F) ratios (Fig. 5.4A, B).

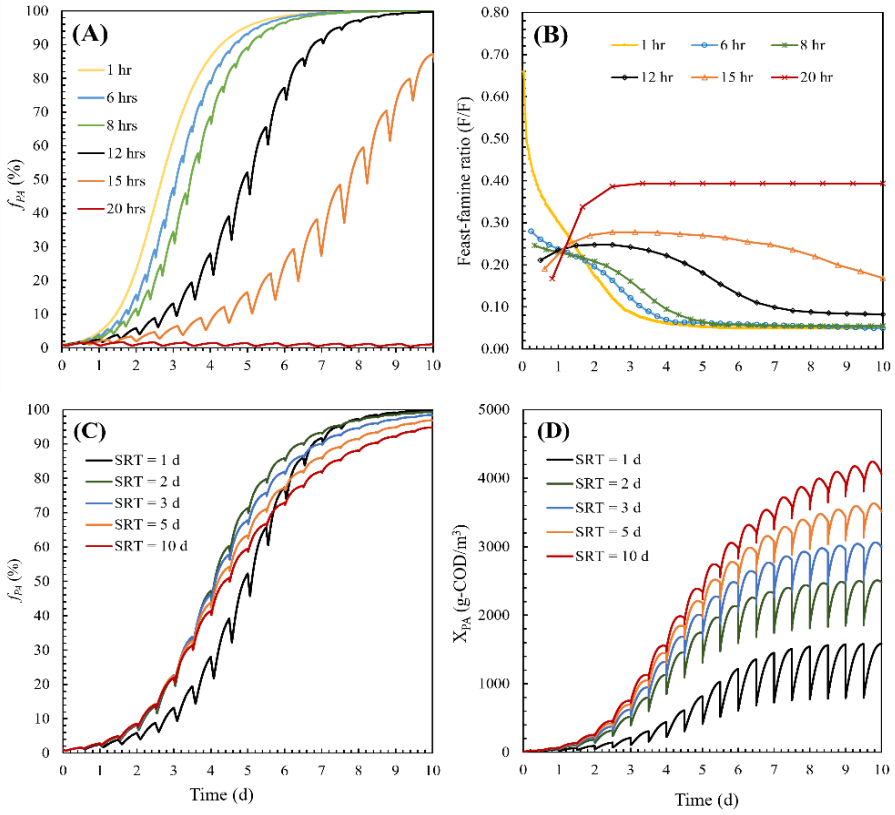

Fig. 5.4. The effect of cycle length (**A** and **B**) and SRT (**C** and **D**) on X_{PA} enrichment. **(A)**. f_{PA} at 1 to 20-hr cycles; **(B)**. The feast-to-famine ratios at 1 to 20-hr cycles; **(C)**. f_{PA} at 1 to 10 SRTs; and **(D)**. X_{PA} concentration at 1 to 10 SRTs. All initial conditions are shown in Table 3.2. SRT is the ratio between the mass of biological solids in the reactor and the biomass wasting rate: $(SRT\ (d) = \frac{VX}{fraction\ of\ \text{wasted}\ biomass\ .\ VX.\ \frac{24\ (hr/d)}{cycle\ length\ (hr)}} = \frac{cycle\ length\ (hr)}{fraction\ of\ \text{wasted}\ biomass\ x\ 24\ (hr/d)})$.

At 1 to 12-h cycles, X_{PA} accumulated high PHA amounts in the feast stage and grew at higher rates in the famine phase (Reaction 2 in Table 5.3), and thus f_{PA} was > 99.7% after 10 days (Fig. 5.4A). *P. acidivorans* was previously shown to dominate the mixed cultures (>80%) at 12-hr cycles within six days (Jiang, Marang, et al., 2011a), which agrees well with our model results (f_{PA}=78.8% at day 6). In addition, the rapid substrate consumption for simultaneous microbial growth and PHA storage resulted in short feast periods with F/F ratios < 0.10 (Fig. 5.4B). F/F ratios less than 0.20 were previously suggested for successful X_{PA} enrichment in the feast-famine strategy (Beun et al., 2002). In contrast, the lower X_{PHA} amounts stored in the feast stage were rapidly consumed in the famine phase at longer cycle lengths (15 to 20 hr) (Fig. 5.4A). As a result, the X_{PA} enrichment was slower (15-hr cycles) or was not successful at 20-hr cycles with F/F ratios ~ 0.39 (Fig. 5.4B).

5.3.5. Impact of SRTs and C/N ratios on X_{PA} enrichment

The simulation results indicated that X_{PA} successfully dominated the microbial cultures (f_{PA} = 95 − 99%) at 1−10 d SRTs after 10 days (Fig. 5.4C). *P. acidovorans* was previously enriched in sequential batch reactors (SBRs) operated at 1 and 4 d SRT (Jiang et al., 2011; Jiang, Marang, et al., 2011a; Johnson et al., 2009; Tamis et al., 2014; X. Wang et al., 2018). The lower f_{PA} at 1 d SRT during the first 8 days could be attributed to the higher biomass wasting ratio (50% v/v) at the end of each cycle compared to at longer SRTs. As a result, X_{PA} concentration at longer SRTs (e.g., X_{PA}= 4133 g-COD.m^{-3} at 10 d SRT) was greater than at 1 d SRT (1583 g-COD.m^{-3}) (Fig. 5.4D), suggesting that SRTs > 1 d could be applied to achieve higher X_{PA} concentrations in the enrichment phase.

In additional simulations to investigate the C/N ratio impact, sufficient nitrogen concentrations were required for successful X_{PA} enrichment in mixed cultures. At 1 d SRT, X_{PA} dominated the mixed cultures (> 99%) after 10 days at C/N ratio ≤ 12 Cmol/Nmol (Fig. 5.5A), which agrees well with the previous experimental results (Johnson, Kleerebezem, et al.,

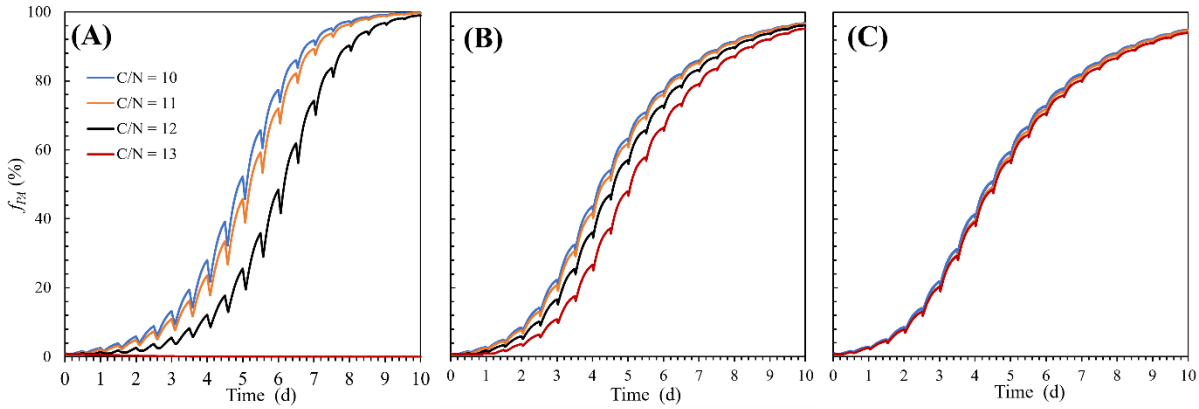

Fig. 5.5. The effect of C/N ratio (Cmol/Nmol) on X_{PA} enrichment at: (**A**) 1 d SRT, (**B**) 5 d SRT, and (**C**) 10 d SRT. In all simulations, the same substrate (S_S=3500 g-COD/m^3/d) was fed at the beginning of each cycle and S_N was changed accordingly (mole-to-mole ratio). Other initial conditions were set constant as in Table 3.3.

2010b). When nitrogen was limited (C/N ≥ 13 Cmol/Nmol, SRT = 1 d), S_N was quickly consumed resulting in the absence of the feast-famine regime and consequently X_{PA} enrichment failure (Fig. 5.5A). In additional simulations at longer SRTs (5 and 10 d), X_{PA} enrichment was less sensitive to higher C/N ratios compared to at 1 d SRT (Figs. 5B, C), indicating that waste streams with limited nitrogen concentrations could still be utilized to enrich X_{PA} and produce PHA at longer SRTs.

5.4. Conclusions

A numerical model was developed to simulate the enrichment of *P. acidovorans* in mixed microbial cultures. The model successfully simulated previous lab-scale experimental data for the enrichment of *P. acidovorans* in the feast-famine strategy. The sensitivity analysis for the model parameters indicated that the kinetics of $f_{PHA}^{(max)}$, $\mu_{PA,S}$, k_{sto}, $\mu_{PA,PHA}$, $Y_{PA,PHA}$, and b_{PA} had a significant impact on the X_{PA} enrichment. In PHA-accumulation scenarios, only $f_{PHA}^{(max)}$ and k_{sto} impacted the accumulated PHA quantity. Furthermore, the three-X model simulations were different from the single-X model results for the same parameters, signifying the importance to involve individual microbial capabilities in the enrichment models. The

calibrated model was then applied to study the impact of operational conditions on X_{PA} enrichment in mixed cultures. For instance, the application of short cycle lengths (1−12 hr) resulted in rapid X_{PA} enrichment (f_{PA} exceeded 97% after 6 days) compared to longer cycle lengths. Although 1−10 d SRTs can be applied to obtain enriched cultures dominated by X_{PA} (f_{PA} > 95%), SRTs longer than 1 d can produce higher X_{PA} biomass concentrations which are more appropriate for commercial PHA production. In addition, sufficient nitrogen concentrations (C/N ≤ 12 Cmol/Nmol at 1d SRT) were required to sustain the X_{PA} growth in the feast and famine stages. The calibrated model provides significant insights into *P. acidovorans* enrichment using the aerobic dynamic feeding strategy and can be applied in commercial PHA production by *P. acidovorans*.

References

Amini, M., Yousefi-Massumabad, H., Younesi, H., Abyar, H., & Bahramifar, N. (2020). Production of the polyhydroxyalkanoate biopolymer by *Cupriavidus necator* using beer brewery wastewater containing maltose as a primary carbon source. *Journal of Environmental Chemical Engineering*, *8*(1), 103588. https://doi.org/10.1016/j.jece.2019.103588

Argiz, L., Fra-Vázquez, A., del Río, Á. V., & Mosquera-Corral, A. (2020). Optimization of an enriched mixed culture to increase PHA accumulation using industrial saline complex wastewater as a substrate. *Chemosphere*, *247*, 125873. https://doi.org/10.1016/j.chemosphere.2020.125873

Beun, J. J., Dircks, K., Van Loosdrecht, M. C. M., & Heijnen, J. J. (2002). Poly-β-hydroxybutyrate metabolism in dynamically fed mixed microbial cultures. *Water Research*, *36*(5), 1167–1180. https://doi.org/10.1016/S0043-1354(01)00317-7

Chen, Z., Guo, Z., Wen, Q., Huang, L., Bakke, R., & Du, M. (2016). Modeling polyhydroxyalkanoate (PHA) production in a newly developed aerobic dynamic discharge (ADD) culture enrichment process. *Chemical Engineering Journal*, *298*, 36–43. https://doi.org/10.1016/j.cej.2016.03.133

Chen, Z., Zhao, L., Ji, Y., Wen, Q., & Huang, L. (2019). Reconsideration on the effect of nitrogen on mixed culture polyhydroxyalkanoate production toward high organic loading enrichment history. *Frontiers of Environmental Science and Engineering*, *13*(4), 54. https://doi.org/10.1007/s11783-019-1135-2

Chinwetkitvanich, S., Randall, C. W., & Panswad, T. (2004). Effects of phosphorus limitation and temperature on PHA production in activated sludge. *Water Science and Technology*, *50*(8), 135–143. https://doi.org/10.2166/wst.2004.0507

Dias, J. M. L., Serafim, L. S., Lemos, P. C., Reis, M. A. M., & Oliveira, R. (2005). Mathematical modelling of a mixed culture cultivation process for the production of polyhydroxybutyrate. *Biotechnology and Bioengineering*, *92*(2), 209–222. https://doi.org/10.1002/bit.20598

Fang, F., Xu, R. Z., Huang, Y. Q., Wang, S. N., Zhang, L. L., Dong, J. Y., Xie, W. M., Chen, X., & Cao, J. S. (2019). Production of polyhydroxyalkanoates and enrichment of associated microbes in bioreactors fed with rice winery wastewater at various organic loading rates. *Bioresource Technology*, *292*, 121978. https://doi.org/10.1016/j.biortech.2019.121978

Gujer, W., Henze, M., Mino, T., & Van Loosdrecht, M. (1999). Activated sludge model no. 3. *Water Science and Technology*, *39*(1), 183–193.

Henze, M., Gujer, W., Mino, T., & Van Loosedrecht, M. (2000). Activated Sludge Models ASM1, ASM2, ASM2d and ASM3. In *Water Intelligence Online* (Vol. 5, Issue 0). IWA publishing. https://doi.org/10.2166/9781780402369

Jiang, Y., Dimitry, Y., Kleerebezem, R., Muyzer, G., & Van Loosdrecht, M. (2011). *Plasticicumulans acidivorans* gen. nov., sp. nov., a polyhydroxyalkanoate-accumulating gammaproteobacterium from a sequencing-batch bioreactor. *International Journal of Systematic and Evolutionary Microbiology*, *61*(9), 2314–2319. https://doi.org/10.1099/ijs.0.021410-0

Jiang, Y., Hebly, M., Kleerebezem, R., Muyzer, G., & Van Loosdrecht, M. C. M. (2011). Metabolic modeling of mixed substrate uptake for polyhydroxyalkanoate (PHA) production. *Water Research*, *45*(3), 1309–1321. https://doi.org/10.1016/j.watres.2010.10.009

Jiang, Y., Marang, L., Kleerebezem, R., Muyzer, G., & Van Loosdrecht, M. C. M. (2011a). Effect of temperature and cycle length on microbial competition in PHB-producing sequencing batch reactor. *ISME Journal*, *5*(5), 896–907. https://doi.org/10.1038/ismej.2010.174

Jiang, Y., Marang, L., Kleerebezem, R., Muyzer, G., & Van Loosdrecht, M. C. M. (2011b). Polyhydroxybutyrate production from lactate using a mixed microbial culture. *Biotechnology and Bioengineering*, *108*(9), 2022–2035. https://doi.org/10.1002/bit.23148

Johnson, K., Jiang, Y., Kleerebezem, R., Muyzer, G., & Van Loosdrecht, M. C. M. (2009). Enrichment of a mixed bacterial culture with a high polyhydroxyalkanoate storage capacity. *Biomacromolecules*, *10*(4), 670–676. https://doi.org/10.1021/bm8013796

Johnson, K., Kleerebezem, R., & Van Loosdrecht, M. C. M. (2009). Model-based data evaluation of polyhydroxybutyrate producing mixed microbial cultures in aerobic sequencing batch and fed-batch reactors. *Biotechnology and Bioengineering*, *104*(1), 50–67. https://doi.org/10.1002/bit.22380

Johnson, K., Kleerebezem, R., & Van Loosdrecht, M. C. M. (2010a). Influence of ammonium on the accumulation of polyhydroxybutyrate (PHB) in aerobic open mixed cultures. *Journal of Biotechnology*, *147*(2), 73–79. https://doi.org/10.1016/j.jbiotec.2010.02.003

Johnson, K., Kleerebezem, R., & Van Loosdrecht, M. C. M. (2010b). Influence of the C/N ratio on the performance of polyhydroxybutyrate (PHB) producing sequencing batch reactors at short SRTs. *Water Research*, *44*(7), 2141–2152. https://doi.org/10.1016/j.watres.2009.12.031

Johnson, K., van Geest, J., Kleerebezem, R., & Van Loosdrecht, M. C. M. (2010). Short- and long-term temperature effects on aerobic polyhydroxybutyrate producing mixed cultures. *Water Research*, *44*(6), 1689–1700. https://doi.org/10.1016/j.watres.2009.11.022

Korkakaki, E., Van Loosdrecht, M. C. M., & Kleerebezem, R. (2016). Survival of the fastest: Selective removal of the side population for enhanced PHA production in a mixed substrate enrichment. *Bioresource Technology*, *216*, 1022–1029. https://doi.org/10.1016/j.biortech.2016.05.125

Korkakaki, E., Van Loosdrecht, M. C. M., & Kleerebezem, R. (2017). Impact of phosphate limitation on PHA production in a feast-famine process. *Water Research*, *126*, 472–480. https://doi.org/10.1016/j.watres.2017.09.031

Kumar, M., Rathour, R., Singh, R., Sun, Y., Pandey, A., Gnansounou, E., Lin, K.-Y. A., Tsang, D. C. W., & Thakur, I. S. (2020). Bacterial polyhydroxyalkanoates: Opportunities, challenges, and prospects. *Journal of Cleaner Production*, 121500.

Lemos, P. C., Levantesi, C., Serafim, L. S., Rossetti, S., Reis, M. A. M., & Tandoi, V. (2008). Microbial characterisation of polyhydroxyalkanoates storing populations selected under different operating conditions using a cell-sorting RT-PCR approach. *Applied Microbiology and Biotechnology*, *78*(2), 351–360. https://doi.org/10.1007/s00253-007-1301-5

Marang, L., Jiang, Y., Van Loosdrecht, M. C. M., & Kleerebezem, R. (2013). Butyrate as preferred substrate for polyhydroxybutyrate production. *Bioresource Technology*, *142*, 232–239. https://doi.org/10.1016/j.biortech.2013.05.031

Marang, L., Van Loosdrecht, M. C. M., & Kleerebezem, R. (2015). Modeling the competition between PHA-producing and non-PHA-producing bacteria in feast-famine SBR and staged CSTR systems. *Biotechnology and Bioengineering*, *112*(12), 2475–2484. https://doi.org/10.1002/bit.25674

Marang, L., Van Loosdrecht, M. C. M., & Kleerebezem, R. (2016). Combining the enrichment and accumulation step in non-axenic PHA production: Cultivation of *Plasticicumulans acidivorans* at high volume exchange ratios. *Journal of Biotechnology*, *231*, 260–267. https://doi.org/10.1016/j.jbiotec.2016.06.016

Marang, L., Van Loosdrecht, M. C. M., & Kleerebezem, R. (2018). Enrichment of PHA-producing bacteria under continuous substrate supply. *New Biotechnology*, *41*, 55–61. https://doi.org/10.1016/j.nbt.2017.12.001

Mozumder, M. S. I., Amin, M. S. A., & Shishir, M. F. R. (2020). Unified model to predict and enhance the mixed culture polyhydroxyalkanoates (PHA) production. *Bioresource Technology Reports*, *11*, 100537. https://doi.org/10.1016/j.biteb.2020.100537

Mozumder, M. S. I., Goormachtigh, L., Garcia-Gonzalez, L., de Wever, H., & Volcke, E. I. P. (2014). Modeling pure culture heterotrophic production of polyhydroxybutyrate (PHB). *Bioresource Technology*, *155*, 272–280. https://doi.org/10.1016/j.biortech.2013.12.103

Ni, B. J., Fang, F., Rittmann, B. E., & Yu, H. Q. (2009). Modeling microbial products in activated sludge under feast-famine conditions. *Environmental Science and Technology*, *43*(7), 2489–2497. https://doi.org/10.1021/es8026693

Ni, B. J., Rittmann, B. E., Fang, F., Xu, J., & Yu, H. Q. (2010). Long-term formation of microbial products in a sequencing batch reactor. *Water Research*, *44*(13), 3787–3796. https://doi.org/10.1016/j.watres.2010.04.035

Ni, B. J., & Yu, H. Q. (2007). A new kinetic approach to microbial storage process. *Applied Microbiology and Biotechnology*, *76*(6), 1431–1438. https://doi.org/10.1007/s00253-007-1104-8

Ni, B. J., & Yu, H. Q. (2008). Simulation of heterotrophic storage and growth processes in activated sludge under aerobic conditions. *Chemical Engineering Journal*, *140*(1–3), 101–109. https://doi.org/10.1016/j.cej.2007.09.017

Nogaj, T., Randall, A., Jimenez, J., Takacs, I., Bott, C., Miller, M., Murthy, S., & Wett, B. (2015). Modeling of organic substrate transformation in the high-rate activated sludge process. *Water Science and Technology*, *71*(7), 971–979. https://doi.org/10.2166/wst.2015.051

Oliveira, C. S. S., Silva, C. E., Carvalho, G., & Reis, M. A. (2017). Strategies for efficiently selecting PHA producing mixed microbial cultures using complex feedstocks: Feast and famine regime and uncoupled carbon and nitrogen availabilities. *New Biotechnology*, *37*, 69–79. https://doi.org/10.1016/j.nbt.2016.10.008

Oshiki, M., Satoh, H., & Mino, T. (2011). Rapid quantification of polyhydroxyalkanoates (PHA) concentration in activated sludge with the fluorescent dye Nile blue A. *Water Science and Technology*, *64*(3), 747–753. https://doi.org/10.2166/wst.2011.707

Porras, M. A., Villar, M. A., & Cubitto, M. A. (2018). Improved intracellular PHA determinations with novel spectrophotometric quantification methodologies based on Sudan black dye. *Journal of Microbiological Methods*, *148*, 1–11. https://doi.org/10.1016/j.mimet.2018.03.008

Ramirez, I., Volcke, E. I. P., Rajinikanth, R., & Steyer, J.-P. (2009). Modeling microbial diversity in anaerobic digestion through an extended ADM1 model. *Water Research*, *43*(11), 2787–2800. https://doi.org/https://doi.org/10.1016/j.watres.2009.03.034

Sin, G., Guisasola, A., de Pauw, D. J. W., Baeza, J. A., Carrera, J., & Vanrolleghem, P. A. (2005). A new approach for modelling simultaneous storage and growth processes for activated sludge systems under aerobic conditions. *Biotechnology and Bioengineering*, *92*(5), 600–613. https://doi.org/10.1002/bit.20741

Tamang, P., Banerjee, R., Köster, S., & Nogueira, R. (2019). Comparative study of polyhydroxyalkanoates production from acidified and anaerobically treated brewery wastewater using enriched mixed microbial culture. *Journal of Environmental Sciences (China)*, *78*, 137–146. https://doi.org/10.1016/j.jes.2018.09.001

Tamis, J., Lužkov, K., Jiang, Y., Loosdrecht, M. C. M. van, & Kleerebezem, R. (2014). Enrichment of Plasticicumulans acidivorans at pilot-scale for PHA production on industrial wastewater. *Journal of Biotechnology*, *192*(Part A), 161–169. https://doi.org/10.1016/j.jbiotec.2014.10.022

Torretta, V., Ragazzi, M., Trulli, E., de Feo, G., Urbini, G., Raboni, M., & Rada, E. C. (2014). Assessment of biological kinetics in a conventional municipal WWTP by means of the oxygen uptake rate method. *Sustainability (Switzerland)*, *6*(4), 1833–1847. https://doi.org/10.3390/su6041833

Vjayan, T., & Vadivelu, V. M. (2017). Effect of famine-phase reduced aeration on polyhydroxyalkanoate accumulation in aerobic granules. *Bioresource Technology*, *245*, 970–976. https://doi.org/10.1016/j.biortech.2017.09.038

Wang, X., Bengtsson, S., Oehmen, A., Carvalho, G., Werker, A., & Reis, M. A. M. (2019). Application of dissolved oxygen (DO) level control for polyhydroxyalkanoate (PHA) accumulation with concurrent nitrification in surplus municipal activated sludge. *New Biotechnology*, *50*, 37–43. https://doi.org/10.1016/j.nbt.2019.01.003

Wang, X., Carvalho, G., Reis, M. A. M., & Oehmen, A. (2018). Metabolic modeling of the substrate competition among multiple VFAs for PHA production by mixed microbial cultures. *Journal of Biotechnology*, *280*, 62–69. https://doi.org/10.1016/j.jbiotec.2018.06.342

Wang, X., Oehmen, A., Freitas, E. B., Carvalho, G., & Reis, M. A. M. (2017). The link of feast-phase dissolved oxygen (DO) with substrate competition and microbial selection in PHA production. *Water Research*, *112*, 269–278. https://doi.org/10.1016/j.watres.2017.01.064

6. Rapid enrichment of *Cupriavidus necator* in microbial communities using its autotrophic and alternating growth characteristics

The employment of microbial communities to produce polyhydroxyalkanoate (PHA) has been intensively studied to reduce the high PHA production costs. The feast-famine feeding strategy is commonly applied to obtain enriched cultures that can produce significant amounts of PHA. Nevertheless, this heterotrophic enrichment strategy requires long periods to obtain enriched cultures with high PHA-accumulating capacities. *Cupriavidus necator* is well-known for its ability to grow and accumulate high fractions of PHA under various growth conditions. Therefore, we proposed two new methods to enrich *Cupriavidus necator* in mixed cultures by applying autotrophic-only and alternating autotrophic-heterotrophic enrichment cycles. The proposed methods were compared to the conventional heterotrophic enrichment strategy. The findings of the current work will contribute to the employment of *C. necator* in large-scale PHA production without sterilization and reduce the high prices of biodegradable plastics.

The following manuscript was prepared for future journal publication.

- Amer, A., and Kim, Y. Rapid enrichment of *Cupriavidus necator* in microbial communities using its autotrophic and alternating growth characteristics.

The co-author's contributions include:

- Funding acquisition.
- Supervision and technical support.
- Manuscript revision.

Abstract

Polyhydroxyalkanoate (PHA) is a biodegradable polymer that can replace petroleum-based plastics. Potential uses of microbial mixed cultures can significantly reduce the high costs of PHA production using pure cultures. The feast-famine strategy has been widely investigated to enrich PHA accumulators in mixed mixtures; however, the feast-famine method requires multiple repeated cycles to attain sufficiently high population of PHA-accumulating bacteria. In this work, we developed an innovative enrichment method to rapidly select and enrich *Cupriavidus necator* that can accumulate PHA up to 90% of the cell weight. The developed approach utilizes the various metabolic characteristics of *C. necator* to establish three enrichment methods: autotrophic-only; alternating autotrophic-heterotrophic; and heterotrophic-only cycles. Each enrichment method was examined with two wastewater sources (return activated sludge and primary sedimentation tank effluent). In the autotrophic-only cycles, the fractions of *C. necator* exceeded 92.1% of the total microbial population after the fifth cycle (60 h) while the alternating enrichment method showed > 81.3% enrichment of *C. necator* after 60 h. However, the heterotrophic-only method resulted in practically no enrichment of *C. necator*. Moreover, the enriched cultures under the autotrophic and alternating conditions accumulated significant amounts of PHA, confirming the selectivity and rapid domination of *C. necator* over other microorganisms. The mixed cultures dominated by *C. necator* are recommended for commercial large-scale PHA facilities, which will substantially reduce the high PHA prices.

Keywords: Autotrophic growth; Heterotrophic growth; Feast-famine; PHA accumulation; *Ralstonia eutropha;* PHA-accumulating bacteria

6.1. Introduction

Polyhydroxyalkanoates (PHAs) are biodegradable polyesters with a potential to substitute conventional petrochemical plastics. Current industrial PHA production employs pure cultures that require rigorous cultivation conditions and expensive pure organic substrates (Argiz et al., 2020; Korkakaki et al., 2016). PHA production using microbial mixed mixtures could lower the PHA production costs because of the possibility to use cheap feedstocks and eliminate the requirements for sterilization (Fang et al., 2019; Kumar et al., 2020; Oliveira et al., 2017). Therefore, it is essential to enrich PHA-accumulating microorganisms before PHA production, especially when organic wastes are used as the carbon source for PHA production. PHA accumulators were historically enriched under heterotrophic conditions (i.e., using organic substrates) by applying a dynamic feeding strategy known as the feast-famine enrichment (Chen et al., 2016; Fang et al., 2019). However, the feast-famine regime may extend for several months to obtain cultures with sufficient PHA-accumulation capacities (Jiang, Marang, et al., 2011b; Johnson, Kleerebezem, et al., 2010a, 2010b; Marang et al., 2014). Thus, this study aimed to develop a rapid enrichment strategy for PHA accumulators in mixed mixtures, which may replace the slow feast-famine enrichment strategy.

*Cupriavidus necator***,** also known as *Ralstonia eutropha*, is a well-studied PHA accumulator that can accumulate up to 90% (w/w) of cell dry weight as PHA (Jawed et al., 2022; López-Cuellar et al., 2011; Passanha et al., 2013). Thus, *C. necator* has been widely employed in large-scale PHA production facilities as a pure culture. In addition to pure organic substrates, *C. necator* has been extensively investigated for PHA accumulation using sterilized organic wastes (Passanha et al., 2013; Salakkam & Webb, 2018). For instance, PHA accumulation by *C. necator* on fermented food-waste liquid was investigated after filtering the medium using 0.45-μm membrane filters (Hafuka et al., 2011). Also, citric molasses (sterilized by direct steam) was investigated for PHA accumulation by *C. necator* (Pavan et al., 2019).

The sterilization requirement substantially increases the PHA production costs from organic wastes, making it difficult to achieve economical large-scale PHA production using organic wastes.

While most PHA accumulators can grow heterotrophically only, *C. necator* can efficiently switch between autotrophic and heterotrophic growth conditions. Under autotrophic conditions, *C. necator* can utilize CO_2 as the carbon source, H_2 as the electron donor, and O_2 as the terminal electron acceptor (Ishizaki et al., 2001; Khosravi-Darani et al., 2013). In addition, *C. necator* can grow heterotrophically on organic substrates as the energy and carbon sources (Belfares et al., 1995; Repaske & Repaske, 1976; Roy, 1962). *C. necator* can also grow under simultaneous autotrophic and heterotrophic conditions, which is known as mixotrophic growth (Rittenberg et al., 1969; Jawed et al., 2022; Kärst and Friedrich, 1984). Thus, in this study, we employed these unique metabolic characteristics for rapid and selective enrichment of *C. necator* in mixed cultures. It should be emphasized that *C. necator* can accumulate up to 90% PHA (w/w) regardless of the growth conditions (Sohn et al., 2021). Therefore, the selective enrichment of *C. necator* in microbial mixtures will allow utilizing organic wastes without media sterilization. The specific objectives of this work were to: (1) examine two new methods to cultivate and enrich *C. necator* in mixed mixtures by applying autotrophic and alternating autotrophic-heterotrophic enrichment cycles; (2) compare the proposed methods to the heterotrophic feast-famine enrichment strategy; (3) study PHA accumulation by the enriched cultures.

6.2. Materials and Methods

6.2.1. Growth solutions

The autotrophic growth solution was composed of $Na_2HPO_4.2H_2O$ (2.9 g/L); KH_2PO_4 (2.30 g/L); $NaHCO_3$ (1.0 g/L); NH_4Cl (0.30 g/L); and a trace amount of minerals and vitamins (Amer & Kim, 2022b). In all autotrophic experiments (both the seed cultivation and enrichment cycles), the headspace gas was replaced with a gas mixture of 70% H_2, 20% O_2, and 10% CO_2 (by volume) at 20°C (Garcia-Gonzalez et al., 2015; Morinaga et al., 1978; Volova et al., 2013). For the heterotrophic experiments (both the seed cultivation and enrichment cycles), the headspace was filled with the atmospheric gas only. The growth solution in the heterotrophic experiments was identical to the autotrophic growth solution with 1.0 g-acetate/L ($CH_3COONa.3H_2O$). The initial pH of the autotrophic and heterotrophic solutions was always ~ 7.40 and 6.80, respectively (SevenMulti, Mettler-Toledo International Inc., OH). Microbial growth was monitored by measuring the optical density at 600 nm (Hach, DR3000, US). In all seed cultivation and enrichment experiments, the used vials were placed horizontally in a mechanical shaker rotating at 150 rpm at 30°C to increase gas transfer kinetics.

6.2.2. Seed preparation

Primary sedimentation tank (PST) effluent and return activated sludge (RAS) samples were collected from the Dundas wastewater treatment plant (Dundas, ON, Canada). *C. necator* Makkar and Casida 17697 (Cedarlane Cor., Canada) was cultivated autotrophically using the abovementioned autotrophic growth solution and gas mixture composition. The seed samples (PST-0 and RAS-0) were prepared by adding *C. necator* into PST and RAS sludge samples with a ratio of ~1% based on the optical density measurements (Fig. 6.1). Samples from the original wastewater samples and from inoculated seed mixtures were collected and stored at -20°C for qPCR and Illumina sequencing analyses.

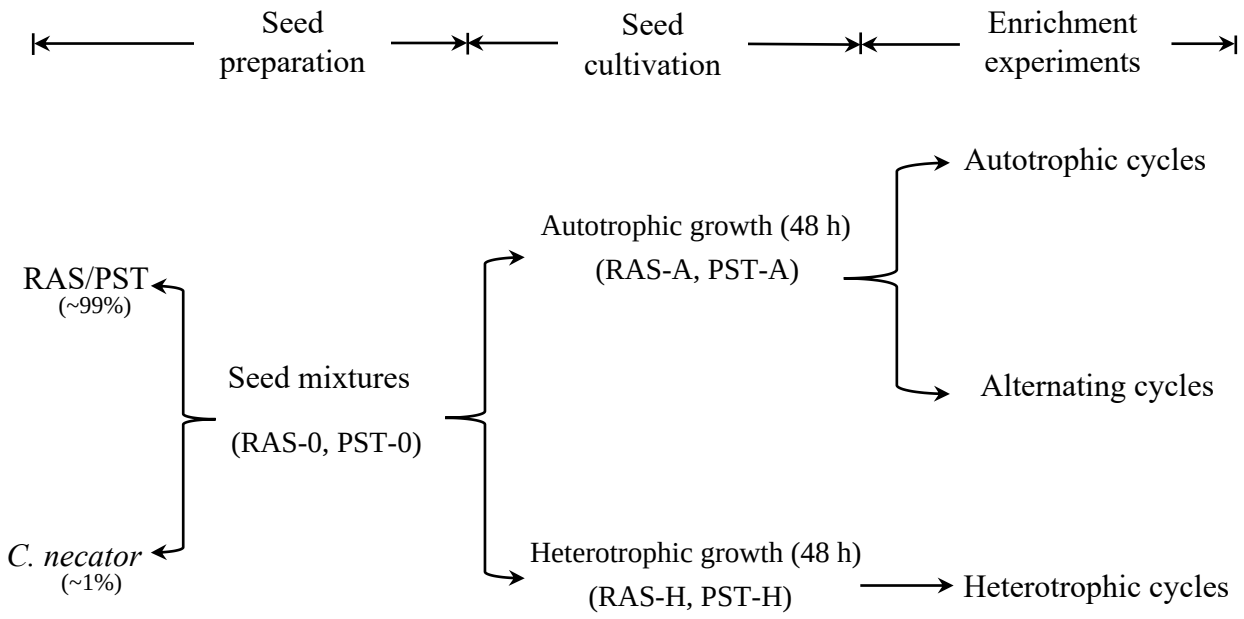

Fig. 6.1. A schematic summary for the enrichment strategies applied in this study. The seed mixtures (RAS-0, PST-0) were prepared by adding ~1% of *C. necator* to PST and RAS samples based on the OD_{600} measurements. Then, the mixed seeds were inoculated into fresh solutions (~3%) and grown under autotrophic (RAS-A, PST-A) and heterotrophic (RAS-H, PST-H) conditions. The cultivated seed mixtures were then used to inoculate new solutions (~ 3%)in the three enrichment strategies.

6.2.3. Seed cultivation

The seed mixtures were first cultivated before the enrichment cycles to avoid the hysteresis impact in the following enrichment experiments (Fig. 6.1) (Amer & Kim, 2022b). To illustrate, if the seed was prepared under heterotrophic conditions, the microbial cultures may take a longer time for the exponential growth in the autotrophic enrichment experiments. For the seed cultivation under autotrophic conditions, 100 µL from the seed mixture sample (PST-0 and RAS-0) was transferred into 17-mL vials with 2.9-mL working solutions under autotrophic conditions. After 48 h, the cultivated mixtures cultures (PST-A and RAS-A) were used to inoculate new vials for the autotrophic and alternating enrichment cycles. Similarly, for the heterotrophic seed cultivation, 100 µL from PST-0 and RAS-0 was transferred into new 17-mL vials with 2.9-mL working solutions with 1.0 g-acetate/L (Fig. 6.1). The cultivated heterotrophic (PST-H and RAS-H) were used (after 48 h) as the inoculation seed for the

heterotrophic enrichment cycles. Samples after the autotrophic and heterotrophic cultivation were collected and stored at -20 °C for qPCR analysis.

6.2.4. Autotrophic enrichment cycles

100 µL from the autotrophic cultivated seed mixtures (PST-A and RAS-A) was mixed with 2.90 mL of the fresh autotrophic growth solution in 10-mL glass vials (i.e., the headspace volume was 7.0 mL) under autotrophic conditions. 50% of the solutions were replaced (without settling) every 12 h with the fresh autotrophic growth solution, and the headspace gas was replaced with 7.0 mL of the autotrophic gas mixture (70% H_2, 20% O_2, and 10% CO_2). The solution replacement and gas injections were repeated over 5 cycles (total 60 h). All enrichment experiments were conducted in duplicate. Samples from the homogenous solution were collected after the 2nd, 4th, and 5th cycles and stored at -20 °C for qPCR analysis. The microbial communities in the samples after the 5th cycle were also analyzed in Illumina sequencing.

6.2.5. Heterotrophic enrichment cycles

100 µL from the heterotrophic seed mixtures (RAS-H and PST-H) was used to inoculate 10-mL glass vials with 2.9-mL working solutions for the heterotrophic enrichment cycles. In this strategy, 50% of the solutions were replaced with fresh medium with a final 1.0 g-acetate/L. The heterotrophic enrichment experiments were conducted in duplicate per the same conditions. Samples were collected after the 2nd, 4th, and 5th cycles and stored at -20 °C for qPCR analysis. Samples after the 5th cycle were also analyzed in Illumina sequencing.

6.2.6. Alternating autotrophic-heterotrophic enrichments

100 µL from the autotrophic cultivated seed mixtures (PST-A and RAS-A) was mixed with 2.90 mL of the fresh autotrophic growth solution in 10-mL glass vials. The heterotrophic (1.0 g-acetate/L) and autotrophic (70% H_2, 20% O_2, and 10% CO_2) conditions were altered every 12 h after replacing 50% of the homogenous solutions with fresh growth solutions. The

alternating enrichment experiments were conducted in duplicate per the same conditions. Samples were collected after the 2nd, 4th, and 5th cycles and stored at -20 °C for qPCR analysis. Samples after the 5th cycle were also analyzed in Illumina sequencing.

6.2.7. PHA-accumulation experiments

Samples after the 5th enrichment cycle (at 60 h) in addition to the inoculated mixtures (RAS-0 and PST-0) were examined for PHA accumulation. In these tests, 1.0 mL from each sample was mixed with 3.0 mL of the heterotrophic growth solution (without NH_4Cl) with 1.0 g-acetate/L and incubated at 30 °C for 12 h. After 12-h incubation, 5.0 g-acetate/L were further added to induce PHA accumulation. It should be noted that the enriched microbes experienced nitrogen limitation conditions since NH_4Cl was not added.

After further incubation for 24 h, the final samples were pretreated using Nile Blue A dye, as described by (Oshiki et al., 2011b; Ostle & Holt, 1982). In brief, the bacterial smears were heat-fixed to microscopic glass slides before staining in 1% (w/v) Nile Blue A solution at 55 °C for 30 min. The slides were then washed with 8% acetic acid solution and kept in the air for 1 – 2 min. After that, the slides were washed with deionized water followed by air drying to remove the remaining water. The stained cells were scanned using Olympus BX53 fluorescence microscope (Biointerfaces Institute, McMaster University). The microscope was provided with the PI(TritC) filter with an excitation range of 532 – 552 nm and an emission range of 594 – 646 nm.

6.2.8. Monitoring *C. necator* fractions using qPCR analysis

The fractions of *C. necator* in mixed cultures were regularly monitored by conducting qPCR analyses (Jiang, Marang, et al., 2011a). The stored samples (from both seed cultivation and enrichment experiments) and *C. necator* pure cultures were diluted so that the optical

density ranged between 0.14 – 0.20. The cell biomass density was assumed to correlate linearly with OD_{600} measurement: 1.0 OD = 1 x 10^8 cells/mL (Nicolaisen et al., 2008).

DNA was extracted using Instagene™ Matrix according to the manufacturer's instructions (Bio-Rad, Canada). The DNA templates of *C. necator* were serially diluted (in 10-fold dilutions) to prepare the standard curves, as previously described (Arya et al., 2005). Specific 16S rDNA primers for *C. necator* (Nec222 F: CGCAACCCTTGTCTCATGTT; and Nec222 R: GCGATTCCAGCTTCACGTAG) were designed as previously described (Lorenz, 2012). The general primer set BAC 338F (ACTCCTACGGGAGGCAG) and BAC 805R (GACTACCAGGGTATCTAATCC) were used to target the total bacteria 16S rDNA gene (Call et al., 2009; Morgan-Sagastume et al., 2015). Both primer sets were synthesized by ThermoFisher scientific (Canada). The qPCR reaction matrix contained: 10 µL of iTaq™ Universal SYBR® Green Supermix; 6 µL dH_2O; and 1 µL of 10 µM of both forward and reverse primers; and 2 µL of DNA template per plate well. The qPCR program consisted of 40 cycles (94°C for 5 sec and 60°C for 30 sec) followed by the melt curve analysis (65-95°C with 0.5°C increments at 5 sec/step). Samples were run in triplicate on a 96-well plate with Bio-Rad CFX 96 Real-time detection system (Bio-Rad, Canada). The standard curves were constructed for the general bacterial primer and specific *C. necator* primer sets. The number of *C. necator* and total bacteria cells were estimated by using the qPCR threshold number (C_q) and the standard curve equation for each primer set (Fig. A5.1). The fraction of *C. necator* in each sample was approximately estimated as,

$$f_{C.\ necator}(\%) = \frac{Cells_{C.necator}\ (cells/mL)}{Cells_{\ Bacteria}\ (cells/mL)}\ x\ 100 \qquad (5.1)$$

6.2.9. Microbial community analysis by Illumina sequencing

Samples after the 5th enrichment cycles along with the initial mixed mixtures (PST-0 and RAS-0) were analyzed for microbial community analysis by conducting Illumina PCR sequencing (Millar et al., 2022). Genomic DNA was extracted and amplified as described by (Stearns et al., 2015). Purified DNA was used to amplify the variable region V4 of the 16S rRNA gene by PCR using Illumina adapted primers (Bartram et al., 2011). The primers were modified to amplify 515f (GTGYCAGCMGCCGCGGTAA) and 806r (GGACTACNVGGGTWTCTAAT). PCR was performed using 50 ng of DNA templates with 5 µL of 10x PCR buffer, 2 µL of 0.4 mg/mL bovine serum albumin, 1.50 µL of 50 mM $MgCl_2$, 1.0 µL of 10 mM dNTPs, 5 µL of 1 µM of each primer, 0.25 µL of Taq polymerase, and dH_2O up to 50 µL. The reaction was carried out at 94℃ for 5 min, 35 cycles of 94℃ for 30 sec, 50℃ for 30 sec, and 72℃ for 30 sec, with a final extension of 72℃ for 10 min. PCR products were sequenced with the Illumina MiSeq platform (paired-end reads, 2 ×300 base pairs (bp)) at the Farncombe Institute (McMaster University, Hamilton, ON, Canada).

The Illumina raw reads were filtered and trimmed using Cutadapt version 1.18 with a minimum quality score of 30 and a minimum read length of 100 bp (Martin, 2011). DADA2 was used to resolve the amplicon sequence variants (ASVs) from the trimmed raw reads (Callahan et al., 2016). Microbial taxonomy was assigned using the SILVA database (version 1.3.8).

6.3. Results and discussions

6.3.1. Autotrophic and heterotrophic seed cultivation

The seed cultivation experiment showed a rapid increase in the optical densities in 48 h for both RAS and PST cultivations (Fig. 6.2A). The autotrophic cultivation resulted in higher optical densities for both RAS (0.80) and PST (0.70) than the heterotrophic samples (0.37 and 0.25, respectively) at 48 h. In addition, the fractions of *C. necator* increased significantly from 6.2 and 4.7% in the initial mixtures to 35.6 and 53.7% in the RAS and PST cultivations (as shown by qPCR analysis) under autotrophic conditions (Fig. 6.2B), suggesting that the autotrophic conditions significantly endorsed *C. necator* growth over other microbes. However, the fractions of *C. necator* did not change for RAS (5.9%) and substantially decreased for PST (0.4%) mixtures cultivated under heterotrophic conditions (Fig. 6.2B), indicating the hard competition between *C. necator* and other heterotrophic microbes.

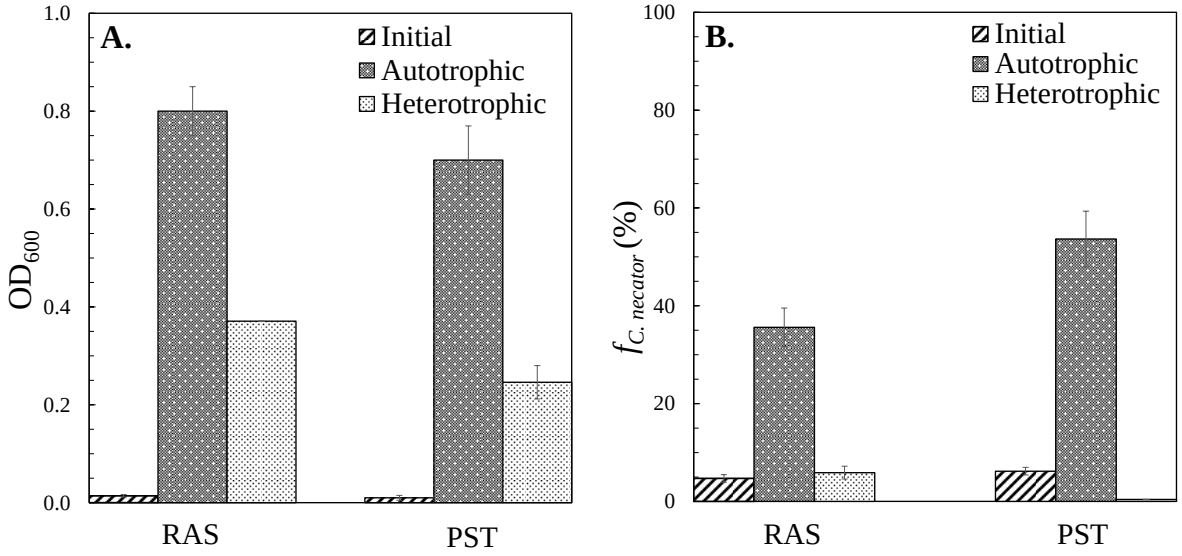

Fig. 6.2. A. The optical densities for the initial seed mixtures (at 0 h) and the cultivated autotrophic and heterotrophic samples after 48 h (n = 2). **B**. The average fractions of *C. necator* in the initial seed mixtures and cultivated autotrophic and heterotrophic samples after 48 h (n = 2). Total *C. necator* and bacteria cell numbers were calculated using the standard curves shown in Fig. 4A.1. PST: primary sedimentation tank effluent. RAS: return activated sludge.

6.3.2. Microbial growth during enrichment cycles

In the enrichment experiments, all enriched cultures attained high optical densities (0.90 – 1.02) in 2 – 3 cycles (Fig. 6.3). In the autotrophic enrichment cycles, the average optical densities were relatively low after the first cycle (0.16 for RAS and 0.09 for PST) (Fig. 6.3A), indicating a longer lag time for the autotrophic growth compared to the heterotrophic growth. For the alternating enrichment, the optical density results indicated rapid transition between the heterotrophic and autotrophic growth modes in less than 12 h (Fig. 6.3B), signifying the ability of the enriched cultures to grow either autotrophically or heterotrophically. For the heterotrophic enrichment, the microbial growth was also fast as the highest OD values (~0.97) were achieved within 48 h (Fig. 6.3C).

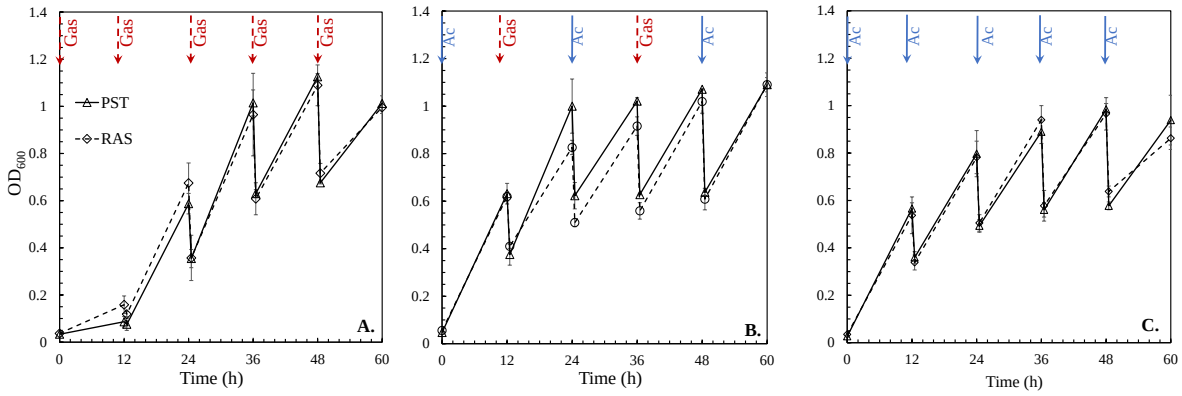

Fig. 6.3. A. Autotrophic cycles: 50% of the solution was replaced every 12 h with new autotrophic medium and the standard gas mixture (red dash arrows). **B.** Alternating enrichment cycles: the cultivation conditions were switched between heterotrophic (blue solid arrows) and autotrophic (red dash arrows) conditions when replacing 50% of the solution every 12 h; and **C.** Heterotrophic: 50% of the solution was replaced every 12 h with new medium containing 1.0 g-acetate/L (blue solid arrows). PST and RAS samples were inoculated from the highest autotrophic culture (Fig. 6.2) in **A** and **B**, and from the highest heterotrophic culture in **C**. All cultures were conducted in duplicate (n = 2).

6.3.3. *C. necator* domination over mixed mixtures

C. necator rapidly dominated the microbial cultures in the autotrophic and alternating enrichments (Fig. 6.4). For the RAS cultures, the autotrophic and alternating enrichment achieved > 91.5% of *C. necator* after 5 cycles (i.e., 60 h) (Fig. 6.4A). The alternating and autotrophic cycles were also found to be effective for the PST samples (Fig. 6.4B). However, the heterotrophic enrichment resulted in decreased fractions of *C. necator* in both RAS and PST cultures (~0.10 and 0.0%, respectively) (Fig. 6.4A, B). It should be noted that the cell growth was active during the heterotrophic enrichment as the optical density was 0.86 (RAS) and 0.94 (PST) after the 5th cycle (Fig. 6.3C). The negligible gene fractions indicated that other heterotrophs competed with *C. necator*. This finding explains why the conventional enrichment methods with organic substrates (e.g., the feast-famine strategy) requires at least 10 or even more cycles to achieve significant fractions of PHA accumulators (Chen et al., 2015; Dias et al., 2008; Tamang et al., 2019).

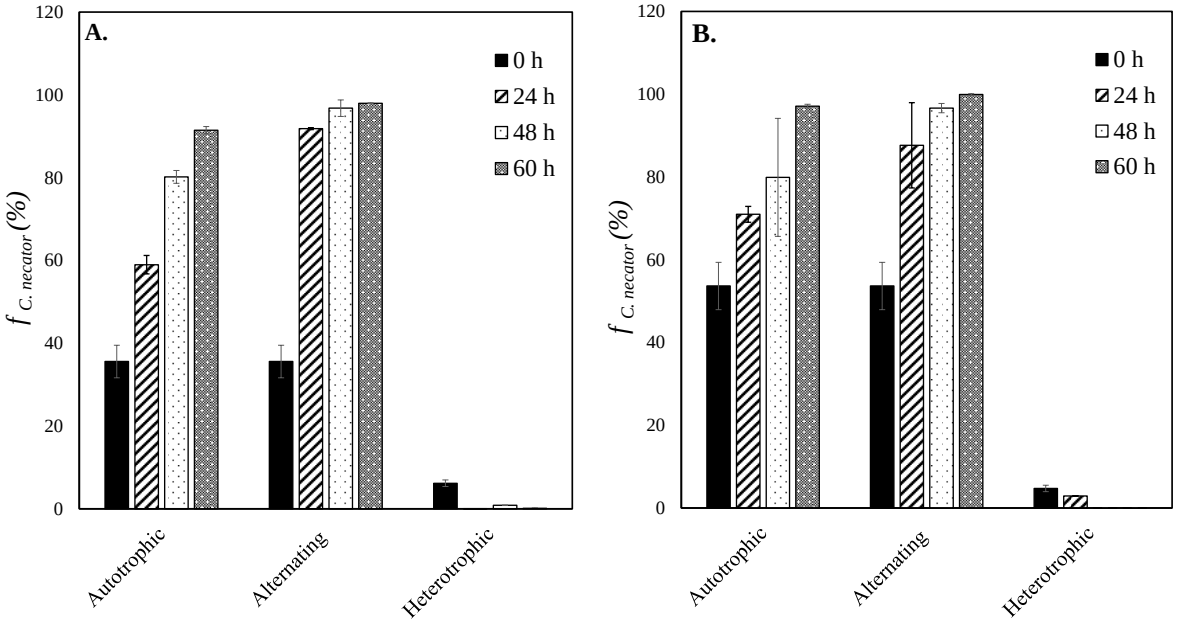

Fig. 6.4. The fractions of *C. necator* ($f_{C.\ necator}$) in RAS (**A**) and PST (**B**) cultures at 0, 24, 48, and 60 h. For each condition, two sample were tested (n = 2). qPCR analysis was performed in triplicate for each sample (Fig. A5.1B, C).

6.3.4. Microbial community analysis

The rapid *C. necator* domination was confirmed in the Illumina sequencing results for the autotrophic-only and alternating methods (Fig. 6.5). For the RAS samples, the fractions of *C. necator* increased from 0.9% in the original sample (RAS-0) to 92.1 and 81.3% in the autotrophic (RAS-AA) and alternating (RAS-AH) enrichments after 60 h, respectively (Fig. 6.5A). The *C. necator* fraction in the microbial community was less than 0.3% after the heterotrophic-only (RAS-HH) cycles, confirming that the heterotrophic-only enrichment was not successful in enriching *C. necator* in mixed cultures. Among the 3 enrichment methods, the autotrophic-only cycles achieved the highest fractions of *C. necator* (93.8%) in the PST samples after 60 h (Fig. 6.5B), similar to the RAS samples. These results suggested that the autotrophic metabolic characteristics can be utilized for highly selective enrichment of *C. necator* over other microbial species.

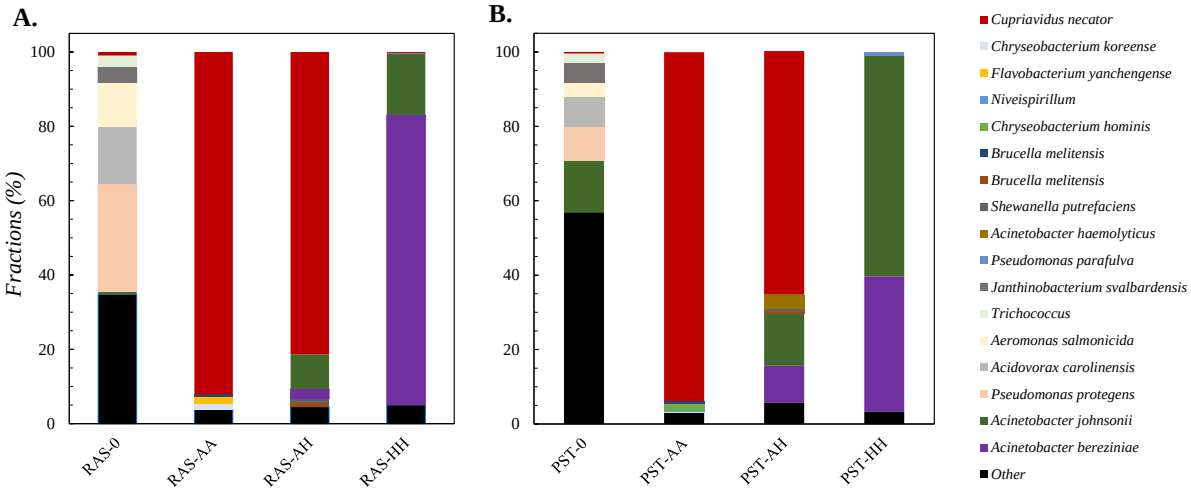

Fig. 6.5. Illumina sequencing results for the microbial community analysis for original wastewater samples (RAS-0 and PST-0) and enriched cultures under autotrophic (RAS-AA, PST-AA), alternating (RAS-AH, PST-AH), and heterotrophic (RAS-HH, PST-HH) cycles for RAS (**A**) and PST (**B**) sludge sources.

6.3.5. PHA accumulation by the enriched cultures

The RAS and PST cultures enriched by the autotrophic or alternating cycles accumulated significant PHA amounts under nitrogen limited conditions (Figs. 6.6 – 7, A5.2 – 4). For the RAS cultures, the bright field (black and white) images show the presence of microbial cells fixed to the slides (Figs. 6.6A and 6.6C) while the orange dots in the fluorescent microscopy images indicate stained PHA granules (Figs. 6.6B and 6.6D) (Oshiki et al., 2011b; Ostle & Holt, 1982). Unlike the autotrophic and alternating enrichments, the samples from the heterotrophic enrichment did not accumulate any substantial PHA amounts (Figs. 6.6E and 6.6F), suggesting that the fractions of *C. necator* (or other PHA accumulators) were insignificant in the enriched heterotrophic cultures. These results are consistent with the absence of *C. necator* 16S rDNA genes in the qPCR and Illumina sequencing results for the

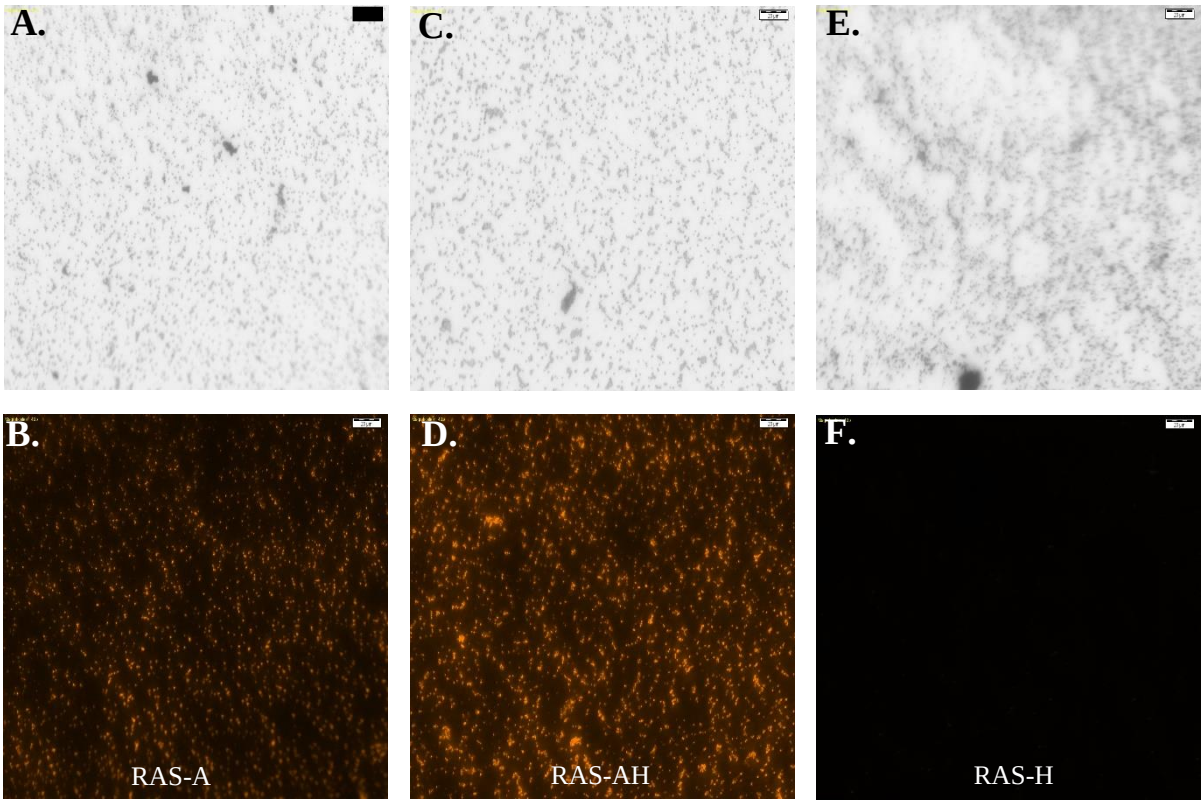

Fig. 6.6. Bright field (top) and fluorescent (bottom) microscopy images for PHA accumulation by the enriched RAS cultures under autotrophic (A, B), alternating (C, D), and heterotrophic (E, F) conditions (40 x magnification). Scale bar (▬) is 20 µm.

heterotrophic enriched cultures (Figs. 6.4 and 6.5). Consistent results were also found for the enriched PST cultures: significant PHA accumulation for the autotrophic-only (Fig. 6.7B) and alternating (Fig. 6.7D) enrichments; and no PHA accumulation for the heterotrophically enriched cultures (Fig. 6.7F). It should be noted that the initial PST and RAS mixtures did not show any significant PHA accumulation, indicating negligible PHA accumulators before the enrichment experiments. These results confirmed that the *C. necator* growth was highly selective in the autotrophic-only and alternating enrichment cycles.

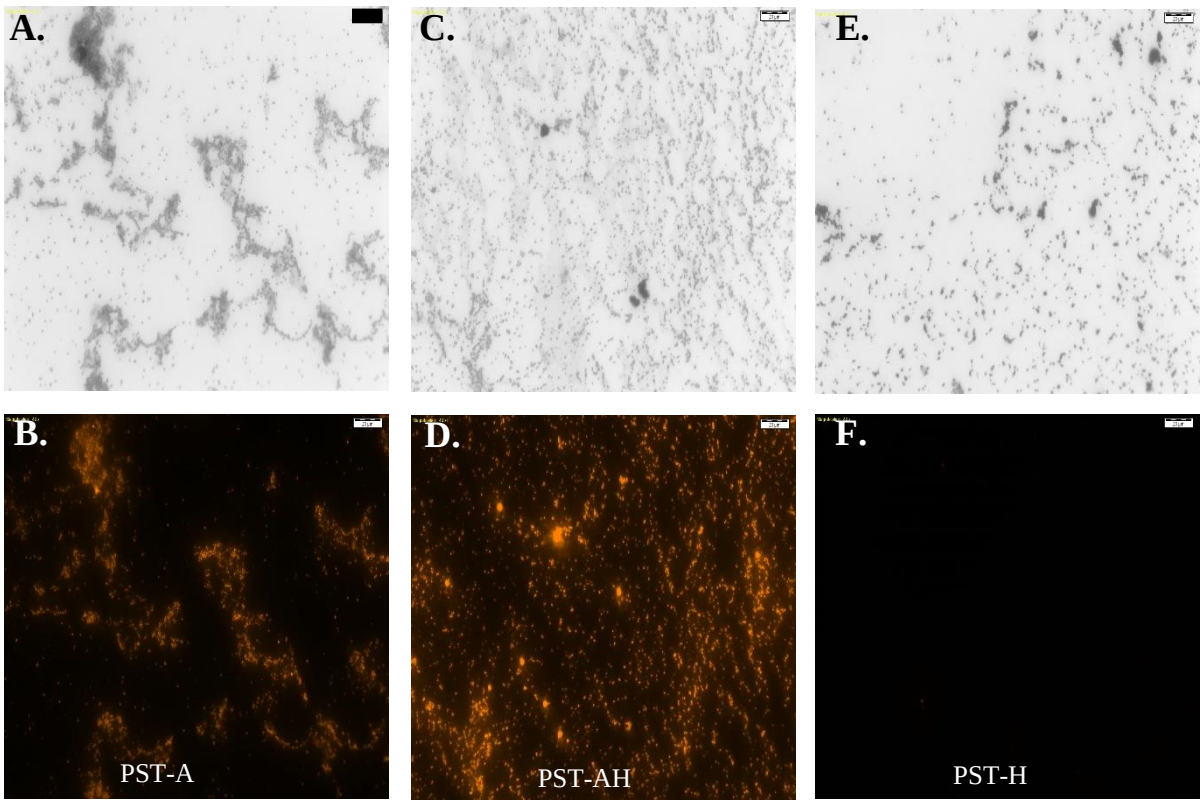

Fig. 6.7. Bright field (top) and fluorescent (bottom) microscopy images for PHA accumulation in enriched PST cultures under autotrophic (A, B), alternating (C, D), and heterotrophic (E, F) conditions (40 x magnification). Scale bar (▬) is 20 µm.

6.3.6. Autotrophic-based vs. feast-famine enrichment strategies

To our knowledge, the rapid enrichment of *C. necator* over other microbial species (up to 94% in 60 h) achieved in the current work is among the fastest enrichments of PHA accumulators (Jiang, Marang, et al., 2011b; Johnson, Kleerebezem, et al., 2010a, 2010b; Marang et al., 2014). The heterotrophic feast-famine enrichments could extend for several months or even years to obtain an enriched culture with sufficient PHA-accumulating capacities (Chen et al., 2015; Dias et al., 2008; Tamang et al., 2019). For instance, an acetate-fed sequential batch reactor (SBR) operated for 4 years obtained a microbial culture that accumulated up to 89% PHA (w/w) (Johnson et al., 2009). In another study, applying additional physical selective pressure to the conventional feast-famine strategy enriched a high PHA-accumulating culture (up to 74% (w/w)) in 30 days (Chen et al., 2015). Therefore, employing the autotrophic or alternating enrichment strategies could potentially replace the feast-famine regime to obtain mixed cultures dominated by *C. necator*. It should be emphasized that *C. necator* can accumulate up to 90% (w/w) of the cell dry weight as PHA under heterotrophic, autotrophic, or mixotrophic conditions (Jawed et al., 2022; López-Cuellar et al., 2011; Passanha et al., 2013), which suggests *C. necator* as a promising candidate for commercial PHA production using enriched mixed cultures.

6.4. Conclusions

C. necator can rapidly grow and accumulate PHA under heterotrophic and autotrophic growth conditions. In this work, we employed this ecological advantage to enrich *C. necator* in primary clarifier effluent and return activated sludge mixed mixtures. By applying autotrophic enrichment cycles, *C. necator* was enriched to more than 92.1% in the enriched cultures within 60 h. The alternating cycles resulted in lower *C. necator* fractions in the RAS (81.3%) and PST (65.5%) than the autotrophic-only enrichment. The enrichment method using the heterotrophic-only cycles was not successful as the fractions of *C. necator* in the mixed

cultures was less than 0.3% in the Illumina sequencing results. In addition, the enriched cultures under autotrophic and alternating conditions accumulated significant PHA amounts, as demonstrated in the fluorescent microscopy images. The rapid autotrophic and alternating enrichment of *C. necator* in mixed mixtures is among the fastest enrichments of PHA accumulators reported in the literature. Based on this study findings, *C. necator* could be employed to produce PHA in large-scale facilities using waste feedstocks, which is expected to substantially reduce the current high PHA production costs.

Acknowledgement

This study was supported by Natural Sciences and Engineering Research Council of Canada (Discovery Grants, RGPIN-2019-06747 and Discovery Accelerator Supplement, RGPAS-2019-00102), and Ontario Ministry of Research and Innovation (Early Researcher Awards, ER16-12-126 and Ontario Research Fund-Research Excellence, RE09-077).

References

Amer, A., & Kim, Y. (2022). Minimizing the lag phase of *Cupriavidus necator* growth under autotrophic, heterotrophic, and mixotrophic conditions. *Unpublished Results*.

Argiz, L., Fra-Vázquez, A., del Río, Á. V., & Mosquera-Corral, A. (2020). Optimization of an enriched mixed culture to increase PHA accumulation using industrial saline complex wastewater as a substrate. *Chemosphere*, *247*, 125873. https://doi.org/10.1016/j.chemosphere.2020.125873.

Arya, M., Shergill, I. S., Williamson, M., Gommersall, L., Arya, N., & Patel, H. R. H. (2005). Basic principles of real-time quantitative PCR. *Expert Review of Molecular Diagnostics*, *5*(2), 209–219. https://doi.org/10.1586/14737159.5.2.209.

Bartram, A. K., Lynch, M. D. J., Stearns, J. C., Moreno-Hagelsieb, G., & Neufeld, J. D. (2011). Generation of multimillion-sequence 16S rRNA gene libraries from complex microbial communities by assembling paired-end Illumina reads. *Applied and Environmental Microbiology*, *77*(11), 3846–3852. https://doi.org/10.1128/AEM.02772-10.

Belfares, L., Perrier, M., Ramsay, B. A., Ramsay, J. A., Jolicoeur, M., & Chavarie, C. (1995). Multi-inhibition kinetic model for the growth of *Alcaligenes eutrophus*. *Canadian Journal of Microbiology*, *41*(13), 249–256.

Rittenberg, S. C., & Goodman, N. S. (1969). Mixotrophic Growth of *Hydrogenomonas eutropha*. *Journal of Bacteriology*, *98*(2), 617–622. https://doi.org/10.1128/jb.98.2.617-622.1969.

Call, D. F., Wagner, R. C., & Logan, B. E. (2009). Hydrogen production by *Geobacter* species and a mixed consortium in a microbial electrolysis cell. *Applied and Environmental Microbiology*, *75*(24), 7579–7587. https://doi.org/10.1128/AEM.01760-09.

Callahan, B. J., McMurdie, P. J., Rosen, M. J., Han, A. W., Johnson, A. J. A., & Holmes, S. P. (2016). DADA2: High-resolution sample inference from Illumina amplicon data. *Nature Methods*, *13*(7), 581–583.

Chen, Z., Guo, Z., Wen, Q., Huang, L., Bakke, R., & Du, M. (2015). A new method for polyhydroxyalkanoate (PHA) accumulating bacteria selection under physical selective pressure. *International Journal of Biological Macromolecules*, *72*, 1329–1334. https://doi.org/10.1016/j.ijbiomac.2014.10.027.

Chen, Z., Guo, Z., Wen, Q., Huang, L., Bakke, R., & Du, M. (2016). Modeling polyhydroxyalkanoate (PHA) production in a newly developed aerobic dynamic discharge (ADD) culture enrichment process. *Chemical Engineering Journal*, *298*, 36–43. https://doi.org/10.1016/j.cej.2016.03.133.

Dias, J. M. L., Oehmen, A., Serafim, L. S., Lemos, P. C., Reis, M. A. M., & Oliveira, R. (2008). Metabolic modelling of polyhydroxyalkanoate copolymers production by mixed microbial cultures. *BMC Systems Biology*, *2*(1), 59. https://doi.org/10.1186/1752-0509-2-59.

Fang, F., Xu, R. Z., Huang, Y. Q., Wang, S. N., Zhang, L. L., Dong, J. Y., Xie, W. M., Chen, X., & Cao, J. S. (2019). Production of polyhydroxyalkanoates and enrichment of associated microbes in bioreactors fed with rice winery wastewater at various organic loading rates. *Bioresource Technology*, *292*, 121978. https://doi.org/10.1016/j.biortech.2019.121978.

Garcia-Gonzalez, L., Mozumder, M. S. I., Dubreuil, M., Volcke, E. I. P., & de Wever, H. (2015). Sustainable autotrophic production of polyhydroxybutyrate (PHB) from CO_2 using a two-stage cultivation system. *Catalysis Today*, *257*(Part 2), 237–245. https://doi.org/10.1016/J.CATTOD.2014.05.025.

Hafuka, A., Sakaida, K., Satoh, H., Takahashi, M., Watanabe, Y., & Okabe, S. (2011). Effect of feeding regimens on polyhydroxybutyrate production from food wastes by *Cupriavidus necator*. *Bioresource Technology*, *102*(3), 3551–3553. https://doi.org/https://doi.org/10.1016/j.biortech.2010.09.018.

Ishizaki, A., Tanaka, K., & Taga, N. (2001). Microbial production of poly-D-3-hydroxybutyrate from CO_2. *Applied Microbiology and Biotechnology*, *57*(1–2), 6–12.

Jawed, K., Irorere, V. U., Bommareddy, R. R., Minton, N. P., & Kovács, K. (2022). Establishing Mixotrophic Growth of *Cupriavidus necator* H16 on CO_2 and Volatile Fatty Acids. In *Fermentation* (Vol. 8, Issue 3). https://doi.org/10.3390/fermentation8030125.

Jiang, Y., Marang, L., Kleerebezem, R., Muyzer, G., & Van Loosdrecht, M. C. M. (2011a). Effect of temperature and cycle length on microbial competition in PHB-producing

sequencing batch reactor. *ISME Journal*, *5*(5), 896–907. https://doi.org/10.1038/ismej.2010.174.

Jiang, Y., Marang, L., Kleerebezem, R., Muyzer, G., & Van Loosdrecht, M. C. M. (2011b). Polyhydroxybutyrate production from lactate using a mixed microbial culture. *Biotechnology and Bioengineering*, *108*(9), 2022–2035. https://doi.org/10.1002/bit.23148.

Johnson, K., Jiang, Y., Kleerebezem, R., Muyzer, G., & Van Loosdrecht, M. C. M. (2009). Enrichment of a mixed bacterial culture with a high polyhydroxyalkanoate storage capacity. *Biomacromolecules*, *10*(4), 670–676. https://doi.org/10.1021/bm8013796.

Johnson, K., Kleerebezem, R., & Van Loosdrecht, M. C. M. (2010a). Influence of ammonium on the accumulation of polyhydroxybutyrate (PHB) in aerobic open mixed cultures. *Journal of Biotechnology*, *147*(2), 73–79. https://doi.org/10.1016/j.jbiotec.2010.02.003.

Johnson, K., Kleerebezem, R., & Van Loosdrecht, M. C. M. (2010b). Influence of the C/N ratio on the performance of polyhydroxybutyrate (PHB) producing sequencing batch reactors at short SRTs. *Water Research*, *44*(7), 2141–2152. https://doi.org/10.1016/j.watres.2009.12.031.

Kärst, U. W. E., & Friedrich, C. G. (1984). Mixotrophic capabilities of *Alcaligenes eutrophus*. *Microbiology*, *130*(8), 1987–1994. https://doi.org/10.1099/00221287-130-8-1987.

Khosravi-Darani, K., Mokhtari, Z. B., Amai, T., & Tanaka, K. (2013). Microbial production of poly(hydroxybutyrate) from C1 carbon sources. *Applied Microbiology and Biotechnology*, *97*(4), 1407–1424. https://doi.org/10.1007/s00253-012-4649-0.

Korkakaki, E., Van Loosdrecht, M. C. M., & Kleerebezem, R. (2016). Survival of the fastest: Selective removal of the side population for enhanced PHA production in a mixed substrate enrichment. *Bioresource Technology*, *216*, 1022–1029. https://doi.org/10.1016/j.biortech.2016.05.125.

Kumar, M., Rathour, R., Singh, R., Sun, Y., Pandey, A., Gnansounou, E., Lin, K.-Y. A., Tsang, D. C. W., & Thakur, I. S. (2020). Bacterial polyhydroxyalkanoates: Opportunities, challenges, and prospects. *Journal of Cleaner Production*, 121500.

López-Cuellar, M. R., Alba-Flores, J., Rodríguez, J. N. G., & Pérez-Guevara, F. (2011). Production of polyhydroxyalkanoates (PHAs) with canola oil as carbon source. *International Journal of Biological Macromolecules*, *48*(1), 74–80. https://doi.org/https://doi.org/10.1016/j.ijbiomac.2010.09.016

Lorenz, T. C. (2012). Polymerase chain reaction: Basic protocol plus troubleshooting and optimization strategies. *Journal of Visualized Experiments*, *63*, e3998. https://doi.org/10.3791/3998.

Marang, L., Jiang, Y., Van Loosdrecht, M. C. M., & Kleerebezem, R. (2014). Impact of non-storing biomass on PHA production: An enrichment culture on acetate and methanol. *International Journal of Biological Macromolecules*, *71*, 74–80. https://doi.org/10.1016/j.ijbiomac.2014.04.051.

Martin, M. (2011). Cutadapt removes adapter sequences from high-throughput sequencing reads. *EMBnet. Journal*, *17*(1), 10–12.

Millar, E. N., Kidd, K. A., Surette, M. G., Bennett, C. J., Salerno, J., & Gillis, P. L. (2022). Effects of municipal wastewater effluents on the digestive gland microbiome of wild freshwater mussels (Lasmigona costata). *Ecotoxicology and Environmental Safety*, *241*, 113774. https://doi.org/https://doi.org/10.1016/j.ecoenv.2022.113774.

Morgan-Sagastume, F., Hjort, M., Cirne, D., Gérardin, F., Lacroix, S., Gaval, G., Karabegovic, L., Alexandersson, T., Johansson, P., Karlsson, A., Bengtsson, S., Arcos-Hernández, M. v, Magnusson, P., & Werker, A. (2015). Integrated production of polyhydroxyalkanoates (PHAs) with municipal wastewater and sludge treatment at pilot scale. *Bioresource Technology*, *181*, 78–89. https://doi.org/https://doi.org/10.1016/j.biortech.2015.01.046.

Morinaga, Y., Yamanaka, S., Ishizaki, A., & Hirose, Y. (1978). Growth Characteristics and Cell Composition of *Alcaligenes Eutrophus* in Chemostat Culture. *Agricultural and Biological Chemistry*, *42*(2), 439–444. https://doi.org/10.1271/bbb1961.42.439.

Nicolaisen, M. H., Bælum, J., Jacobsen, C. S., & Sørensen, J. (2008). Transcription dynamics of the functional tfdA gene during MCPA herbicide degradation by *Cupriavidus necator* AEO106 (pRO101) in agricultural soil. *Environmental Microbiology*, *10*(3), 571–579. https://doi.org/https://doi.org/10.1111/j.1462-2920.2007.01476.

Oliveira, C. S. S., Silva, C. E., Carvalho, G., & Reis, M. A. (2017). Strategies for efficiently selecting PHA producing mixed microbial cultures using complex feedstocks: Feast and famine regime and uncoupled carbon and nitrogen availabilities. *New Biotechnology*, *37*, 69–79. https://doi.org/10.1016/j.nbt.2016.10.008.

Oshiki, M., Satoh, H., & Mino, T. (2011). Rapid quantification of polyhydroxyalkanoates (PHA) concentration in activated sludge with the fluorescent dye Nile blue A. *Water Science and Technology*, *64*(3), 747–753. https://doi.org/10.2166/wst.2011.707.

Ostle, A. G., & Holt, J. G. (1982). Nile blue A as a fluorescent stain for poly-beta-hydroxybutyrate. *Applied and Environmental Microbiology*, *44*(1), 238–241. https://doi.org/10.1128/aem.44.1.238-241.1982.

Passanha, P., Esteves, S. R., Kedia, G., Dinsdale, R. M., & Guwy, A. J. (2013). Increasing polyhydroxyalkanoate (PHA) yields from *Cupriavidus necator* by using filtered digestate liquors. *Bioresource Technology*, *147*, 345–352. https://doi.org/https://doi.org/10.1016/j.biortech.2013.08.050.

Pavan, F. A., Junqueira, T. L., Watanabe, M. D. B., Bonomi, A., Quines, L. K., Schmidell, W., & de Aragao, G. M. F. (2019). Economic analysis of polyhydroxybutyrate production by *Cupriavidus necator* using different routes for product recovery. *Biochemical Engineering Journal*, *146*, 97–104. https://doi.org/https://doi.org/10.1016/j.bej.2019.03.009.

Repaske, R., & Repaske, A. C. (1976). Quantitative requirements for exponential growth of *Alcaligenes eutrophus*. *Applied and Environmental Microbiology*, *32*(4), 585–591. https://doi.org/10.1128/aem.32.4.585-591.1976.

Roy, R. (1962). Nutritional requirements of requirements for *Hydrogenomonas eutropha*. *Journal of Bacteriology*, *83*(2), 418–422. https://doi.org/10.1128/jb.83.2.418-422.1962

Salakkam, A., & Webb, C. (2018). Production of poly(3-hydroxybutyrate) from a complete feedstock derived from biodiesel by-products (crude glycerol and rapeseed meal). *Biochemical Engineering Journal*, *137*, 358–364. https://doi.org/https://doi.org/10.1016/j.bej.2018.06.018

Sohn, Y. J., Son, J., Jo, S. Y., Park, S. Y., Yoo, J. I., Baritugo, K.-A., Na, J. G., Choi, J., Kim, H. T., Joo, J. C., & Park, S. J. (2021). Chemoautotroph *Cupriavidus necator* as a potential game-changer for global warming and plastic waste problem: A review. *Bioresource Technology*, *340*, 125693. https://doi.org/https://doi.org/10.1016/j.biortech.2021.125693

Stearns, J. C., Davidson, C. J., McKeon, S., Whelan, F. J., Fontes, M. E., Schryvers, A. B., Bowdish, D. M. E., Kellner, J. D., & Surette, M. G. (2015). Culture and molecular-based profiles show shifts in bacterial communities of the upper respiratory tract that occur with age. *The ISME Journal*, *9*(5), 1246–1259.

Tamang, P., Banerjee, R., Köster, S., & Nogueira, R. (2019). Comparative study of polyhydroxyalkanoates production from acidified and anaerobically treated brewery wastewater using enriched mixed microbial culture. *Journal of Environmental Sciences (China)*, *78*, 137–146. https://doi.org/10.1016/j.jes.2018.09.001

Volova, T. G., Kiselev, E. G., Shishatskaya, E. I., Zhila, N. O., Boyandin, A. N., Syrvacheva, D. A., Vinogradova, O. N., Kalacheva, G. S., Vasiliev, A. D., & Peterson, I. v. (2013). Cell growth and accumulation of polyhydroxyalkanoates from CO_2 and H_2 of a hydrogen-oxidizing bacterium, Cupriavidus eutrophus B-10646. *Bioresource Technology*, *146*, 215–222. https://doi.org/https://doi.org/10.1016/j.biortech.2013.07.070

7. Conclusions and future work

This thesis presented novel biotechnological solutions to the environmental challenges associated with Pb(II) contamination in water streams, petroleum-based plastics, and climate change as a result of elevated CO_2 levels in the atmosphere. We employed microorganisms to reduce Pb(II) to metallic Pb to lower its toxicity in aquatic environments. In addition, we also investigated the microbial growth of *Cupriavidus necator* to enhance the biological CO_2 fixation. Also, the enrichment of PHA accumulators in mixed microbial cultures was investigated and mathematically modeled in order to enhance and optimize the enrichment process and reduce the current high PHA production prices.

Chapter 2: Isolation of Pb(II)-reducing bacteria and demonstration of biological Pb(II) reduction to metallic Pb

The current work aimed to isolate several bacterial species that can obtain energy required for microbial growth by oxidizing acetate as the carbon and energy source and reducing Pb(II) to metallic Pb^0. Samples from a lab-scale MEC fed with acetate and Pb(II) were used as the inoculum source in the isolation experiments. Two isolation methods were applied to isolate the Pb(II)-reducing bacteria: dilution-to-extinction and streak-plate methods. As a result, *D. acidovorans* and *A. caeni* were isolated by the streak-plate method, while *A. caeni* and *C. testosteroni* were obtained by the dilution-to-extinction method. The isolated species were furthered investigated for their ability to reduce Pb(II) to metallic Pb. Among the isolated species, *D. acidovorans* strain Pb11 and *A. caeni* strain Pb2 were shown to couple acetate oxidation with Pb(II) reduction to Pb^0. XPS combined with SEM-EDS analyses were necessary to differentiate between biologically reduced lead and lead-phosphate precipitation. *D. acidovorans* strain Pb11 and *A. caeni* strain Pb2 are suggested for biological Pb(II) remediation.

In this study, we examined lower Pb(II) concentrations (≤ 10.0 mg/L). The ability of the isolated bacteria to reduce high Pb(II) concentrations should be further investigated. Future work should also examine the capability of the isolated bacteria to remove Pb(II) in natural environments such as Pb(II)-contaminated sediments and wastewater. The capability of the isolated bacteria to reduce other metals as potential TEAs should be also examined in a separate study.

Chapter 3: Theoretical estimation of yield coefficients for polyhydroxyalkanoate production and biomass

The estimation of theoretical PHA yields from organic and inorganic carbon substrates is essential to evaluate the efficiency of PHA production in large-scale facilities. The Thermodynamic Electron Equivalents Model (TEEM1) was applied to calculate theoretical PHA and cell yields under autotrophic and heterotrophic conditions. First, the free energy of formation and half-reactions for several PHA monomers such as PHB and PHV were estimated. Then, the TEEM1 was applied to construct stochiometric balanced equations for PHA accumulation and substrate utilization. As a result, the theoretical PHB yields on organic substrates (e.g., 0.76 $Cmol_{PHB}/\,Cmol_{acetate}$) and under autotrophic conditions (3.18 $g_{PHB}/\,mol_{H_2}$) were estimated at the standard conditions. The ambient cultivation conditions and the number of monomeric units in PHA polymers were found not to influence the true PHB yield values. Furthermore, the model results indicated that the ratio of H_2: O_2: CO_2 = 7: 2: 1 can achieve the highest autotrophic PHB yields. Along with theoretical PHB yield estimation, the heterotrophic and autotrophic cell yields for *C. necator* were determined to be 0.34 ($g_{PHB}/\,g_{acetate}$) and 4.11 ($g_{cells}/\,mol_{H_2}$), respectively.

The TEEM1 was applied to calculate PHB yields under nutrient-limited conditions (i.e., without simultaneous growth). In future work, the simultaneous PHA accumulation and cell growth may be further investigated. In addition, The TEEM1 can be used to estimate theoretical

cell and PHA yields under uncommon environmental conditions (e.g., electron donors, terminal electron acceptors) in future work.

Chapter 4: Transition between autotrophic, heterotrophic, and mixotrophic metabolisms of *Cupriavidus necator*

Cupriavidus necator is commonly applied in commercial PHA production because of the high PHA accumulation capacity (up to 90% w/w). The impact of autotrophic, heterotrophic, and mixotrophic growth conditions on the metabolic responses of *C. necator* was investigated in lab-scale experiments. Under autotrophic conditions, the lag phases were short (< 12 h) when 1.0 atm of the gas mixture with a ratio of H_2: O_2: CO_2 = 7: 2: 1 was supplied. Increasing the supplied gas volumes resulted in increased biomass yields. We also studied the impact of the partial pressure increase of individual gaseous substrates. The autotrophic growth was inhibited when P_{CO_2} exceeded 0.70 atm. Increasing P_{CO_2} higher than 0.6 atm resulted in longer lag phases (> 16 h) and severely impacted the optical densities. The autotrophic lag phase was not impacted by elevated hydrogen (up to 2.7 atm) or nitrogen (up to 2.0 atm) partial pressures. In addition, acetate concentrations ≥ 5.0 g/L had an inhibition impact on *C. necator* and resulted in longer lag periods (> 24 h). When *C. necator* was fed with 1.0 – 10.0 g/L of glucose, glycerol, or mixed substrates, the lag phase lengths (< 12 h) were not impacted. The organic substrates should be kept in the lower range (≤ 5.0 g/L) as the optical densities did not improve at higher substrate concentrations. When *C. necator* was cultivated under mixotrophic conditions, the optical densities were always better than the optical densities on individual substrates. In two-stage cultivation systems, *C. necator* could completely switch between the three metabolic pathways in less than 12 h. The highest optical densities (1.17 – 1.24) were achieved in two-stage systems with initial heterotrophic conditions followed by

mixotrophic or autotrophic conditions. The current results can improve the application of *C. necator* in large-scale industrial systems for biological CO_2 fixation and PHA production.

The impact of the autotrophic, heterotrophic, and mixotrophic conditions on PHA accumulation by *C. necator* may be investigated in future work. The application of two-stage systems to attain higher biomass densities along with producing significant PHA amounts needs to be further studied.

Chapter 5: Modeling the growth of diverse microorganisms during feast-famine enrichment

The dynamic feast-famine feeding regime is the most accepted approach to enriching PHA accumulators in mixed microbial cultures. In this thesis, a mathematical model was developed to comprehensively describe the feast-famine enrichment by including the kinetics of two microbial groups: PHA accumulators (X_{PA}) and non-PHA accumulators (X_{NA}). The model was successfully calibrated and validated using published lab-scale experimental data for *Plasticicumulans acidivorans*, a PHA accumulator that can store PHA up to 90%. As a result, the microbial kinetics for X_{PA} and X_{NA} were estimated and compared to the previously reported values. The sensitivity analysis for the model parameters indicated that the kinetics of $f_{PHA}^{(max)}$, $\mu_{PA,S}$, k_{sto}, $\mu_{PA,PHA}$, $Y_{PA,\,PHA}$, and b_{PA} had a substantial effect on X_{PA} enrichment. In PHA-accumulation scenarios, only $f_{PHA}^{(max)}$ and k_{sto} played a key role in determining the accumulated PHA quantity. In addition, the impact of microbial diversity of microbial communities on the enrichment process was studied. As a result, the three-X model simulations were different from the single-X model results for the same parameters, suggesting the importance to involve individual microbial capabilities in enrichment modeling studies. Additionally, the calibrated model was applied to optimize the enrichment operational

conditions. The application of short cycle lengths (1−12 hr) resulted in rapid X_{PA} enrichments (f_{PA} exceeded 97% after 6 d) compared to longer cycle lengths. Although 1−10 d SRTs can be applied to enrich cultures dominated by X_{PA} (f_{PA} > 95%), SRTs longer than 1 d resulted in higher X_{PA} biomass concentrations which are more appropriate for commercial PHA production. In addition, sufficient nitrogen concentrations (C/N ≤ 12 Cmol/Nmol at 1d SRT) were required to maintain sufficient X_{PA} growth in the feast and famine stages. The calibrated model provides significant insights into *P. acidovorans* enrichment using the feast-famine strategy and could be applied to scale up PHA production using mixed cultures.

The numerical model proposed in this work focused on the enrichment of heterotrophic PHA accumulators. Autotrophic PHA accumulators could also be enriched in a strategy similar to the feast-famine enrichment with applying autotrophic feast-famine cycles. The mathematical modeling of the enrichment of autotrophic PHA accumulators may be investigated in future work.

Chapter 6: Rapid enrichment of *Cupriavidus necator* in microbial communities using the autotrophic and alternating growth characteristics

C. necator is commonly employed in industrial PHA production by pure cultures as it can accumulate high amounts of PHA inside their cells. The bacterium can rapidly grow and accumulate PHA under heterotrophic or autotrophic cultivation conditions. In this work, we employed this ecological advantage to enrich *C. necator* in mixed cultures. By applying autotrophic or autotrophic-heterotrophic enrichment cycles, *C. necator* was enriched to more than 92% of the total microbial communities in 2.50 d. The conventional heterotrophic cycles resulted in lower fractions of *C. necator* (< 0.10%) in the mixed cultures. The enriched cultures under autotrophic or alternating conditions accumulated high PHA fractions, as proven by the

Nile Blue A staining and demonstrated in the fluorescence microscopy images. The rapid autotrophic or alternating enrichment of *C. necator* in mixed cultures is among the fastest enrichments reported in the literature. Based on this study findings, *C. necator* could be employed to produce PHA in large-scale production facilities without sterilization, usually required for pure cultures. As a result, waste feedstock could be directly used as the carbon and energy sources for PHA production. Removing the strict sterilization step is expected to substantially reduce the current high PHA production costs.

In future work, the ability of the enriched cultures dominated by *C. necator* need to be investigated for the capability to grow and accumulate PHA using organic wastes without sterilization. A continuous two-stage system with autotrophic followed by heterotrophic conditions (or vice versa) can be tested. In addition, the mathematical modeling of the enrichment of *C. necator* using autotrophic and alternating autotrophic-heterotrophic cycles can provide more useful insights into the enrichment process.

Appendices

Appendix A1: Supplementary information for Chapter 2.

Part A: Supplementary Figures

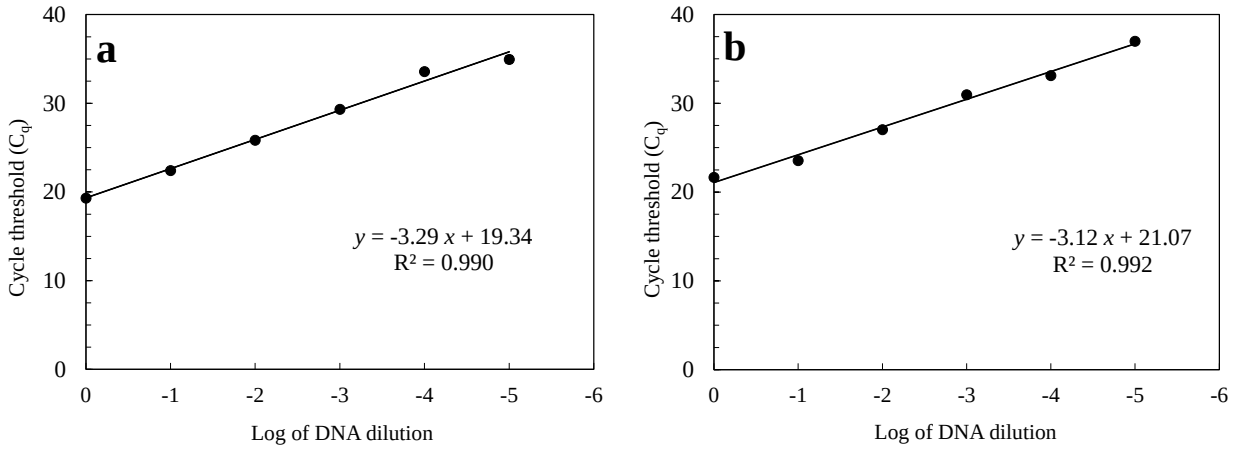

Fig. A1.1. Standard curves for diluted DNA samples in qPCR for: a. *D. acidovorans* strain Pb11 and b. *A. Caeni* strain Pb2. Results are for triplicate samples, and the standard error symbols are smaller than the data symbols. The amplification efficiency was 101% for *D. acidovorans* strain Pb11 and 109% for *A. Caeni* strain Pb2.

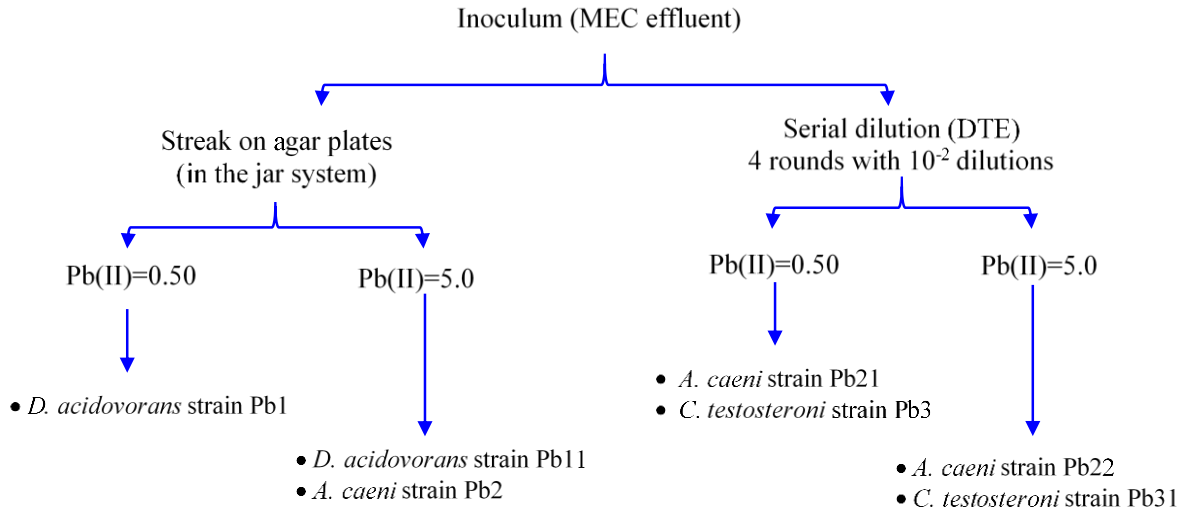

Fig. A1.2. Summary of the isolation procedure applied in our study.

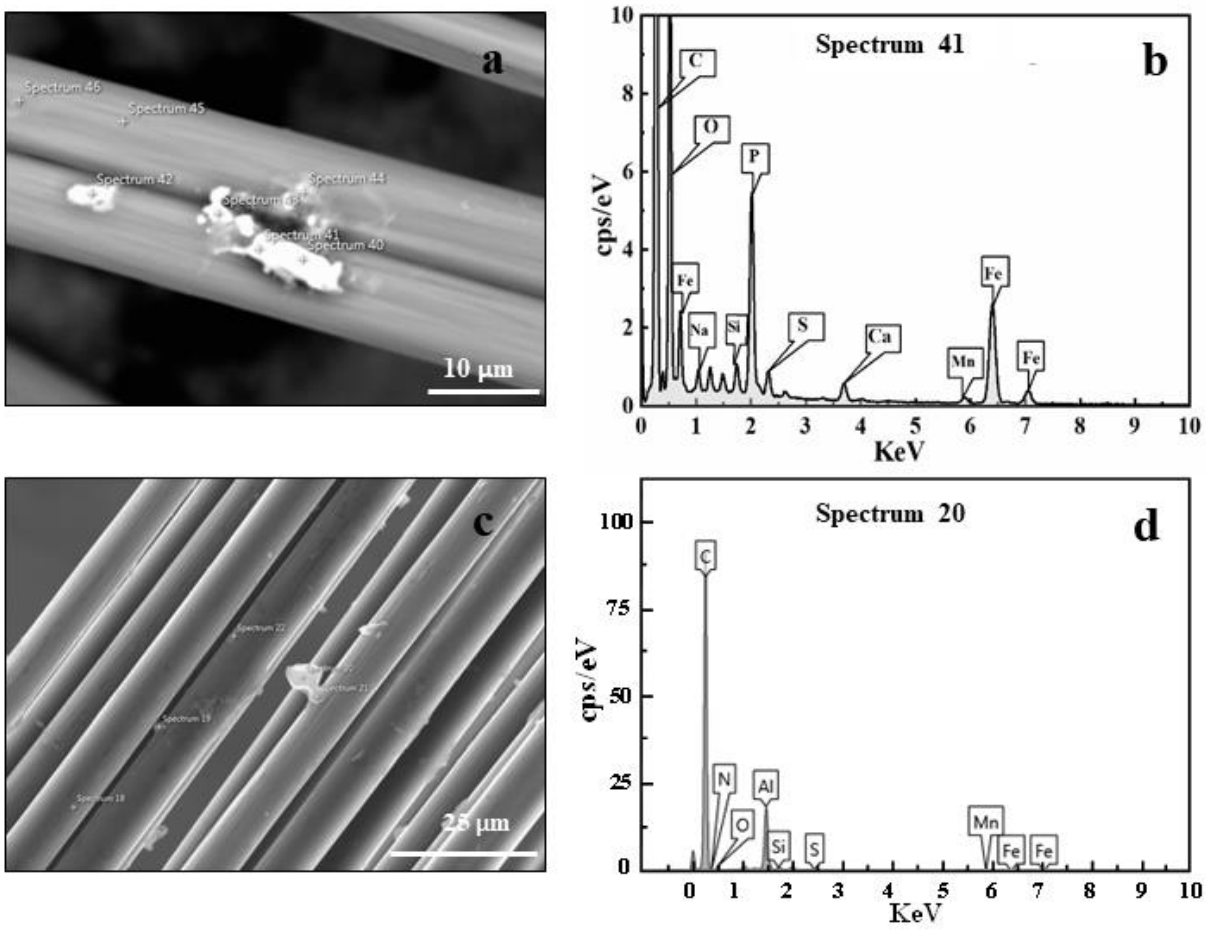

Fig. A1.3. SEM (a, c) and EDS analysis (b, d) results for *C. testosteroni* strain Pb31 at different locations. All fibers were cleaned with ethanol to remove biofilms prior to the analysis.

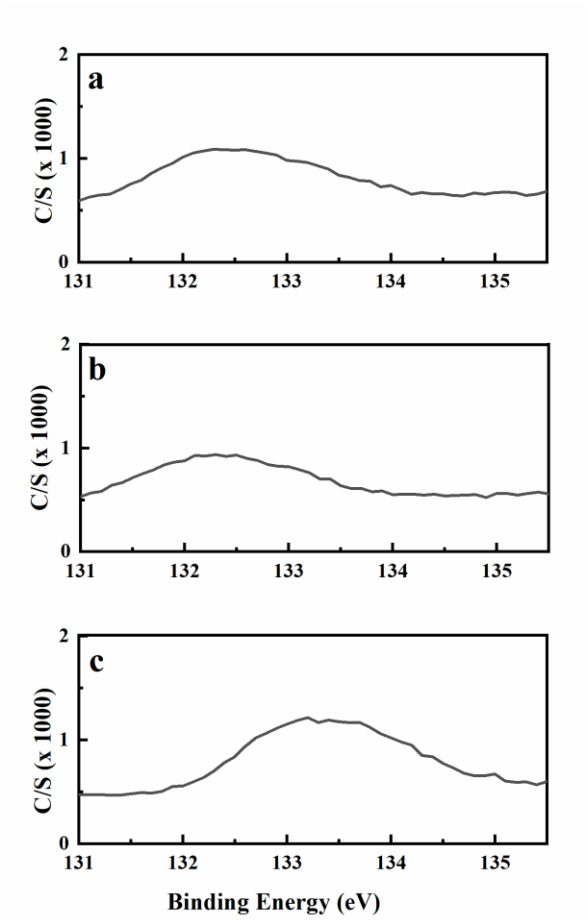

Fig. A1.4. XPS spectrums for P 2p peaks for: a. *D. acidovorans* strain Pb11; b. *A. caeni* strain Pb2; and c. control samples. All peaks were referenced to the adventitious C1s peak at 284.8 eV.

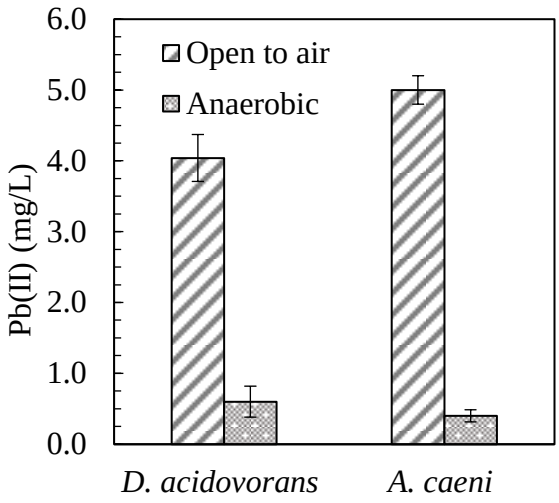

Fig. A1.5. Effect of oxygen on Pb(II) removal by *D. acidovorans* strain Pb11 and *A. caeni* strain Pb2. The initial Pb(II) concentration was 5.0 mg-Pb(II)/L.

Part B: Thermodynamic calculations of actual free energy

In the main manuscript, the following equations were mentioned:

$$CH_3COO^- + 4Pb^{2+} + 4\,H_2O \rightarrow 4Pb^0 + 2HCO_3^- + 9H^+ \quad (2.1)$$

$$Pb^{2+} + H_2O \rightarrow PbO + 2\,H^+ \quad (2.4)$$

$$Pb^{(0)} + H_2O \rightarrow PbO + H_2 \quad (2.5)$$

The following table summarizes the ΔG_f^o values (Arnold & Brezonik, 2009) and experimental concentration used in our study for the above-mentioned chemical species.

Species	ΔG_f^o (KJ/mol)	Concentration [M]
CH_3COO^-	-369.41	1.23 x 10^{-2} (1 g /L)
H_2O	-237.17	1
HCO_3^-	-586.58	1.21 x 10^{-4}
H^+	0	1.0 x 10^{-7}
H_2	0	5.3 x 10^{-7}
Pb^{2+}	-24.4	2.41 x 10^{-5} (5 mg/L)
Pb^0	0	1 (pure solids)
PbO	-187.9	1 (pure solids)

The following table summarizes ΔG^o, quotient (Q), and ΔG values for equations 1, 4, and 5 (Faraday's constant=9.649 x 10^4 C/mol; Gas constant (R) =8.314 J mol/K; and T=303.15°K)

Equation	ΔG^o (KJ/mol)	Q	ΔG (KJ/mol)
1	242.53	3.49 x 10^{-51}	-50.3
4	73.67	4.14 x 10^{-10}	19.21
5	49.27	5.30 x 10^{-7}	12.85

I. Theoretical calculations of cell Yield on Pb(II) (Bruce & McCarty, 2020; McCarty, 2007):

1. *Half reactions for electron donor oxidation, electron acceptor reduction, and cell synthesis (at experimental conditions):*
   - Electron donor (acetate) ½ reaction (Rd)

     $\frac{1}{8}CO_2 + \frac{1}{8}HCO_3^{-1} + H^+ + e^- \rightarrow \frac{1}{8}\,CH_3COO^- + \frac{3}{8}H_2O \qquad \Delta G_d^{o'} = 75.26\ KJ/e\ eq$
   - Electron acceptor (Ra)

     $\frac{1}{2}Pb^{2+} + e^- \rightarrow \frac{1}{2}Pb^0 \qquad \Delta G_a^{o'} = 25.59\ \ KJ/e\ eq$
   - Cell synthesis ½ reaction (R_c)

     $\frac{1}{5}CO_2 + \frac{1}{20}NH_4^+ + \frac{1}{20}HCO_3 + \ H^+ + e^- \ \rightarrow \frac{1}{20}C_5H_7O_2N + \frac{9}{20}H_2O$

2. *Fractions of electrons used for cell synthesis and energy*

$$A = -\frac{\frac{\Delta G_{AcCoA}^{0'} - \Delta G_{e\,donor}^{0'}}{\varepsilon^n} + \frac{\Delta G_{cells}^{o'} - \Delta G_{Acetyl-CoA}^{0'}}{\varepsilon^n}}{\varepsilon\left(\Delta G_a^{o'} - \Delta G_{e\,donor}^{o'}\right)} = -\frac{\frac{30.9 - 75.26}{0.65} + \frac{18.8}{0.65}}{0.65\,(25.59 - 75.26)} = 0.90$$

$$f_s^0 = \frac{1}{1+A} = 0.528 \quad \& \quad f_e^0 = \frac{A}{1+A} = 0.472$$

3. *Balanced stochiometric equation* $(f_s^0 R_C + f_e^0 R_a - R_d)$:

$$0.106\ CO_2 + 0.027\ NH_4^+ + 0.027\ HCO_3^{-1} + 0.53\ H^+ + 0.53e^- \rightarrow 0.027\ C_5H_7O_2N + 0.239\ H_2O$$

$$+\ \ 0.235\ Pb^{2+} + 0.47\ e^- \rightarrow 0.235\ Pb^0$$

$$+\ \ \frac{1}{8}\,CH_3COO^- + \frac{3}{8}H_2O \rightarrow \frac{1}{8}CO_2 + \frac{1}{8}HCO_3^{-1} + H^+ + e^-$$

$$0.125\ CH_3COO^- + \ 0.235\ Pb^{2+}\ + 0.027\ NH_4^+ + 0.137\ H_2O \rightarrow \ 0.235\ Pb^0 + \ 0.027\ C_5H_7O_2N + 0.019\ CO_2 + 0.099\ HCO_3^{-1} + 0.47\ H^+$$

$$Y = 12.62\ \frac{g_{cells}}{mol\ Pb^{2+}}$$

II. Observed Yield from qPCR results (Using absolute quantification method):

1. In separate experiments, the relation between cell numbers and optical density at 600 nm (OD600) was estimated to be 2.38 x 10^9 and 10^9 CFU/mL per 1.0 optical density unit (OD_{600}) for *D. acidovorans* and *A. caeni*, respectively. The OD_{600} values for the samples used to prepare the qPCR standard curves were 0.207 and 0.139 for *D. acidovorans* and *A. caeni*, respectively.

2. Using the standard curve equations, the following cell numbers could be estimated:

Pb(II) (mg/L)	*Average D. acidovorans* cells (CFU/mL)			*Average A. caeni* cells (CFU/mL)		
	Initial	Final	Cell increase	Initial	Final	Cell increase
0	2.78 x 10^6	1.20 x 10^7	9.17 x 10^6	4.62 x 10^6	1.70 x 10^7	1.24 x 10^7
5.0	3.96 x 10^6	2.74 x 10^7	2.34 x 10^7	3.69 x 10^6	2.91 x 10^7	2.54 x 10^7
10.0	4.20 x 10^6	4.35 x 10^7	3.93 x 10^7	2.51 x 10^6	2.92 x 10^7	2.67 x 10^7

3. The net microbial yield on Pb(II) is assumed to be the difference between microbial yield in samples with 5 or 10 mg-Pb(II)/L and control samples after correcting the control biomass to be equal to the initial biomass at 5.0 or 10.0 mg-Pb(II)/L. The microbial cell weight is assumed to be 2 x 10^{-14} g per cell (M. et al., 1998).

Pb(II) (mg/L)	*D. acidovorans*		*A. caeni*	
	Net yield (CFU/mL)	Yield (g cells/mol Pb(II))	Net yield (CFU/mL)	Yield (g cells/mol Pb(II))
5.0	1.20 x 10^6	0.99	1.55 x 10^7	12.8
10.0	1.63 x 10^7	6.75	1.99 x 10^7	8.2
Average yield	8.74 x 10^6	3.87	1.77 x 10^7	10.5

References:

Arnold, W., & Brezonik, P. (2009). Water Chemistry An Introduction to the Chemistry of Natural and Engineered Aquatic Systems. In *Introduction to Environmental Management*. Oxford University Press.

Bruce, E. R., & McCarty, P. L. (2020). *Environmental biotechnology: principles and applications* (2nd edition). McGraw-Hill Education.

M., L.-K., J., K., & R., P. (1998). Determination of Bacterial Cell Dry Mass by Transmission Electron Microscopy and Densitometric Image Analysis. *Applied and Environmental Microbiology*, *64*(2), 688–694. https://doi.org/10.1128/AEM.64.2.688-694.1998

McCarty, P. L. (2007). Thermodynamic electron equivalents model for bacterial yield prediction: modifications and comparative evaluations. *Biotechnology and Bioengineering*, *97*(2), 377–388.

Appendix A2: Supplementary information for Chapter 3.

Part A. supplementary tables

Table A2.1. Thermodynamic properties of the compounds studied in this work

Substance	$\Delta G^0_{f,298}$ (kJ/mol)	Reference
Acetate (CH_3COOH)	-369.41	(McCarty, 2007)
Glucose	-917.22	
Glycerol	-488.52	
PHB ($C_4H_8O_3$)	-506.30	This study
PHV ($C_5H_{10}O_3$)	-492.25	
PHB-PHV ($C_9H_{16}O_5$)	-554.25	
HCO_3^-	-586.85	(McCarty, 2007)
CO_2	-394.36	
H^+ (pH 7)	-39.87	
H_2O	-237.18	
O_2	0	
H_2	0	
– CH_3	-43.96	(Joback & Reid, 1987)
– CH	58.36	
– CH_2–	8.42	
– OH	-208.04	
– COOH	-426.72	

Table A2.2. Half-reactions of several components used in this study

Reduced Compound	Half-reaction	$\Delta G^{0\prime}$ (kJ/mol)	Reference
PHB	$\frac{4}{18}CO_2 + H^+ + e^- \rightarrow \frac{1}{18}C_4H_8O_3 + \frac{5}{18}H_2O$	33.84	This study
PHB-PHV	$\frac{5}{24}\mathrm{CO_2} + \mathrm{H^+} + \mathrm{e^-} \rightarrow \frac{1}{24}\mathrm{C_5H_{10}O_3} + \frac{7}{24}\mathrm{H_2O}$	32.40	
Acetate	$\frac{1}{4}CO_2 + H^+ + e^- \rightarrow \frac{1}{8}CH_3COOH + \frac{1}{4}H_2O$	32.99	(Bruce & McCarty, 2020)
Glucose	$\frac{1}{4}CO_2 + H^+ + e^- \rightarrow \frac{1}{24}C_6H_{12}O_6 + \frac{1}{4}H_2O$	40.95	
Glycerol	$\frac{3}{14}CO_2 + H^+ + e^- \rightarrow \frac{1}{14}C_3H_8O_3 + \frac{3}{14}H_2O$	38.66	
O_2	$\frac{1}{4}O_2 + H^+ + e^- \rightarrow \frac{1}{2}H_2O$	– 78.72	
H_2	$H^+ + e^- \rightarrow \frac{1}{2}H_2$	39.87	

Table A2.3. PHB and biomass stochiometric balanced reactions on glucose and glycerol

PHB synthesis reaction	
Glucose	$0.042\ C_6H_{12}O_6 + \ 0.020\ O_2 \rightarrow 0.051\ C_4H_8O_3\ + \ 0.045\ H_2O + \ 0.045\ CO_2$
Glycerol	$0.071\ C_3H_8O_3 + \ 0.024\ O_2 \rightarrow 0.050\ C_4H_8O_3\ + \ 0.085\ H_2O + \ 0.014\ CO_2$
Biomass synthesis reaction	
Glucose	$0.042\ C_6H_{12}O_6 + 0.022\ NH_4^+ + \ 0.125\ O_2 + 0.022\ HCO_3\ \rightarrow$ $0.029\ C_{4.09}H_{7.13}O_{1.89}N_{0.76} + \ 0.202\ H_2O\ + \ 0.154\ CO_2$
Glycerol	$0.071\ C_3H_8O_3 + 0.022\ NH_4^+ + \ 0.127\ O_2 + 0.022\ HCO_3\ \rightarrow$ $0.028\ C_{4.09}H_{7.13}O_{1.89}N_{0.76} + \ 0.239\ H_2O\ + \ 0.121\ CO_2$

Part B. Example calculation of PHB yield at a specific gas composition

1. The autotrophic PHB yield balanced equation was estimated as,

$$4\ CO_2 + 11.8\ O_2\ + 32.7\ H_2 \rightarrow\ C_4H_8O_3 + 28.7\ H_2O \tag{6.16}$$

2. The theoretical PHB yields can be estimated as,

$$Y_{PHB-H_2} = \ 3.19 \quad g - PHB.mole - {H_2}^{-1}$$

$$Y_{PHB-O_2} = \ 0.085\ \ g - PHB.mole - {O_2}^{-1}$$

$$Y_{PHB-CO_2} = \ 2.15\ \ g - PHB.mole - {CO_2}^{-1}$$

3. Assume the solution and gas volumes are 0.20 mL and 2 L, respectively (Fig. 3.3).

4. For a gas mixture of H_2: O_2: CO_2 = 7: 2: 1, the number of individual gas moles at the assumed system (step 3) can be calculated using the universal gas law ($PV = nRT$):

$$n_{H_2} = \frac{PV}{RT} = \frac{0.70\ x\ 2}{.00813\ x\ 298.15} = 0.58\ H_2 - moles \rightarrow Y_{PHB-H_2} = \frac{3.19\ \left(\frac{g-PHB}{mole\ H_2}\right) x\ 0.58\ (mole\ H_2)}{0.20\ (L)} = 9.25\ g - PHB/L$$

$$n_{O_2} = \frac{PV}{RT} = \frac{0.20\ x\ 2}{.00813\ x\ 298.15} = 0.165\ O_2 - moles \rightarrow Y_{PHB-O_2} = \frac{0.085\left(\frac{g-PHB}{mole\ O_2}\right) x\ 0.165\ (mole\ O_2)}{0.20\ (L)} = 7.26\ g - PHB/L$$

$$n_{CO_2} = \frac{PV}{RT} = \frac{0.10\ x\ 2}{.00813\ x\ 298.15} = 0.083\ O_2 - moles \rightarrow Y_{PHB-CO_2} = \frac{2.15\left(\frac{g-PHB}{mole\ CO_2}\right) x\ 0.083\ \ (mole\ CO_2)}{0.20\ (L)} = 10.73\ g - PHB/L$$

Thus, the maximum PHB yield is 7.26 g-PHB/L (Figure 3.4B red line)

Appendix A3: Supplementary information for Chapter 4.

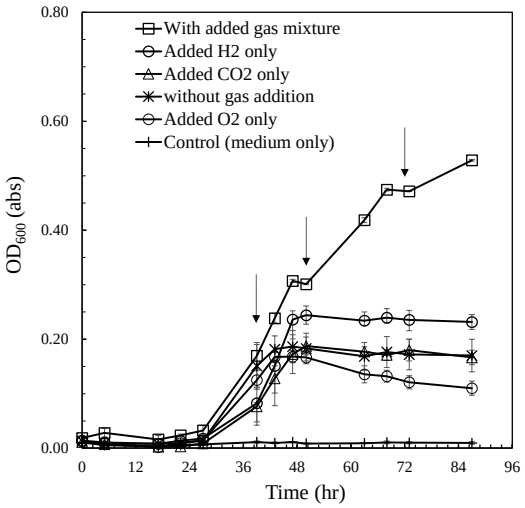

Fig. A3.1. Impact of adding gas mixture (H_2 : O_2 : CO_2 = 7 : 2 : 1) or separate gases (H_2, O_2, or CO_2) on the autotrophic biomass yield conditions (n = 2) using 10-mL vials with 5-mL starting volume.

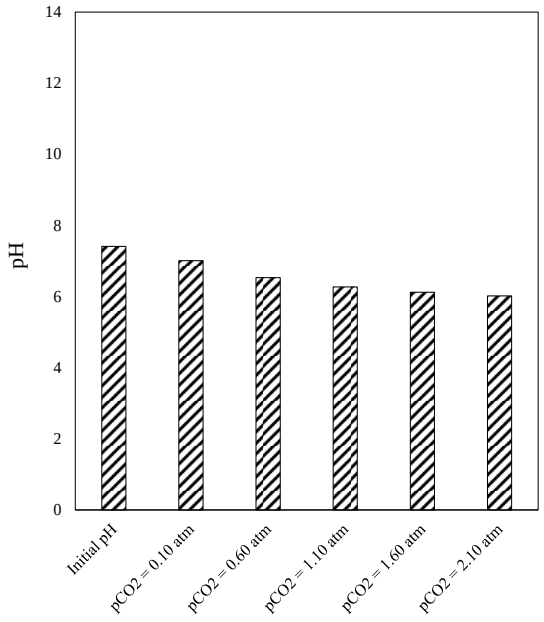

Fig. A3.2: pH change with increased CO_2 partial pressure.

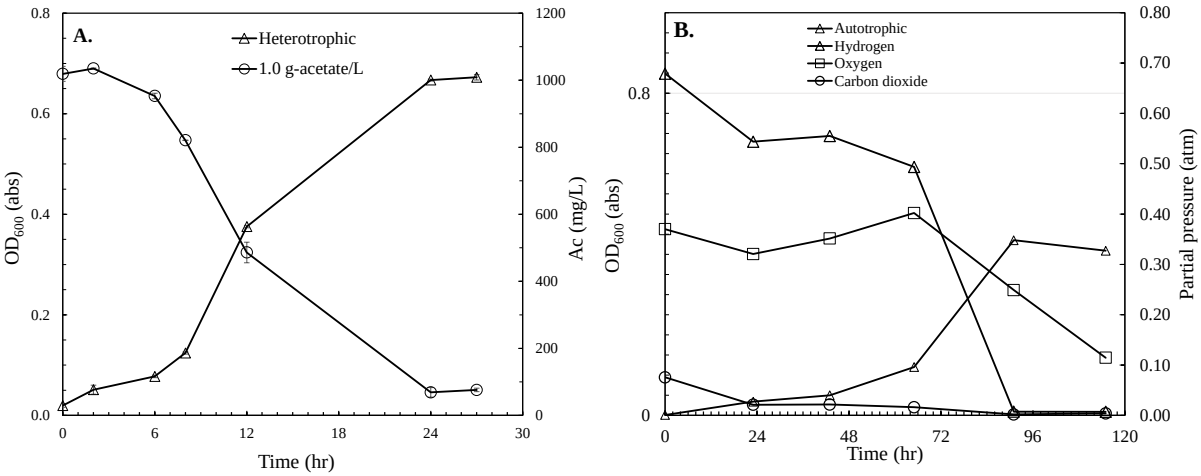

Fig. A3.3. Detailed growth of *C. necator* under: **A.** heterotrophic conditions with 1.0 g-acetate/L (n = 2) and **B**. autotrophic conditions with a gas mixture of H_2 : O_2 : H_2 = 7 : 2 : 1 (n = 1). The experiments were conducted using 100-mL bottles with 50-mL starting volume. All gas measurements were adjusted for sampling volumes.

Appendix A4: Supplementary information for Chapter 5.

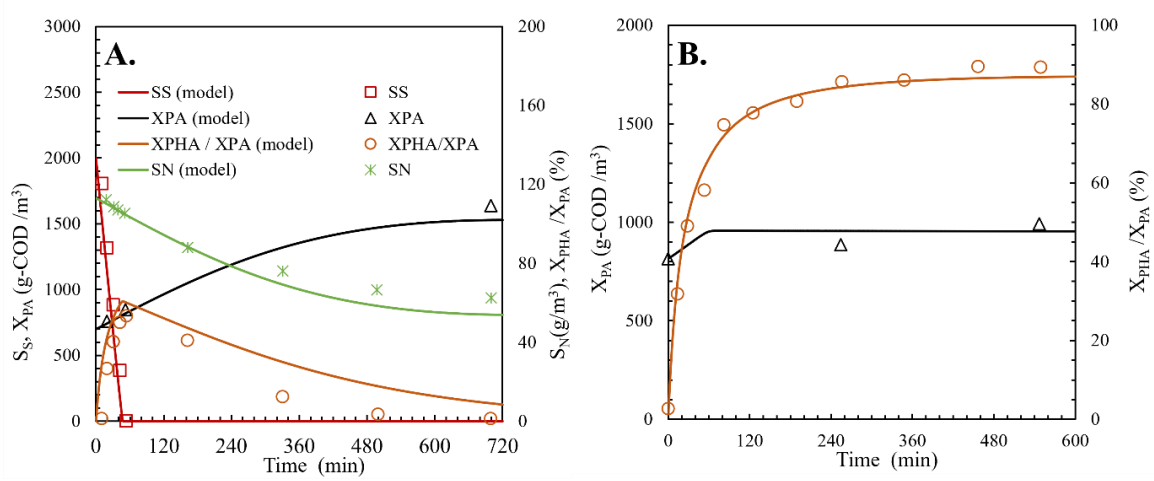

Fig. A4.1. Validation of *P. acidivorans* kinetic constants by simulating results for a repeated cycle (A) and an accumulation experiment (B) on acetate (Johnson et al., 2009). Initial conditions and kinetic constants are listed in tables 5.2 and 5.3.

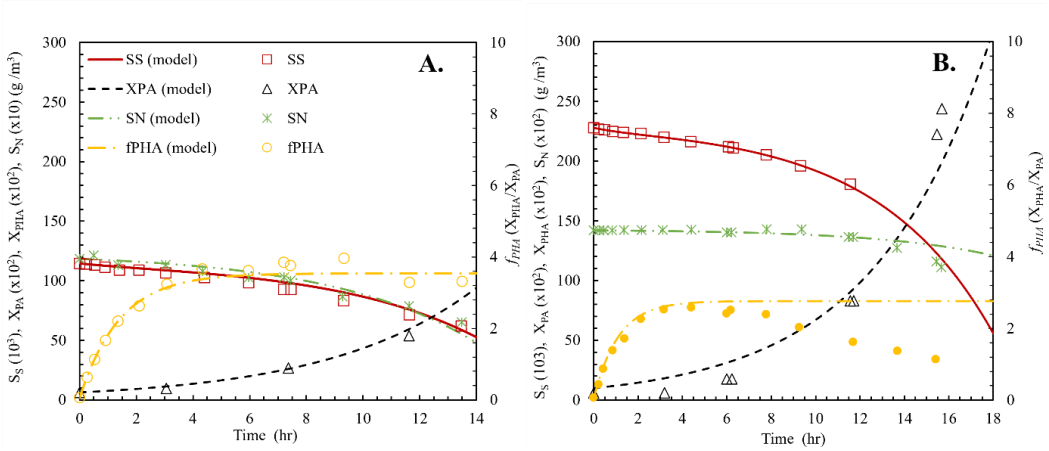

Fig. A4.2. Model validation by simulating the effect of ammonium on PHA accumulation by X_{PA} on acetate. To left: A. C/N = 40 ($f_{(PHA)}^{max}$ = 4.88); B. for C/N = 8 ($f_{(PHA)}^{max}$ = 3.50) (Johnson, Kleerebezem, et al., 2010a). Initial conditions and kinetic constants are listed in tables 5.2 and 5.3.

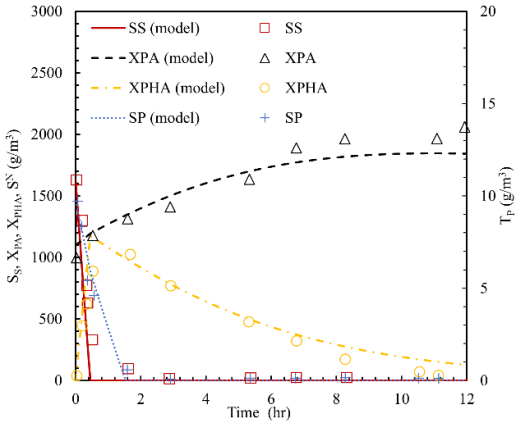

Fig. A4.3. Model validation by simulating the effect of phosphorus on PHA accumulation by an enriched culture on acetate ($Y_{PHA,S}$=0.80; i_{PBM} = 0.04; $f_{(PHA)}^{max}$=7.33)(Korkakaki et al., 2017). Initial conditions and kinetic constants are listed in tables 5.2 and 5.3.

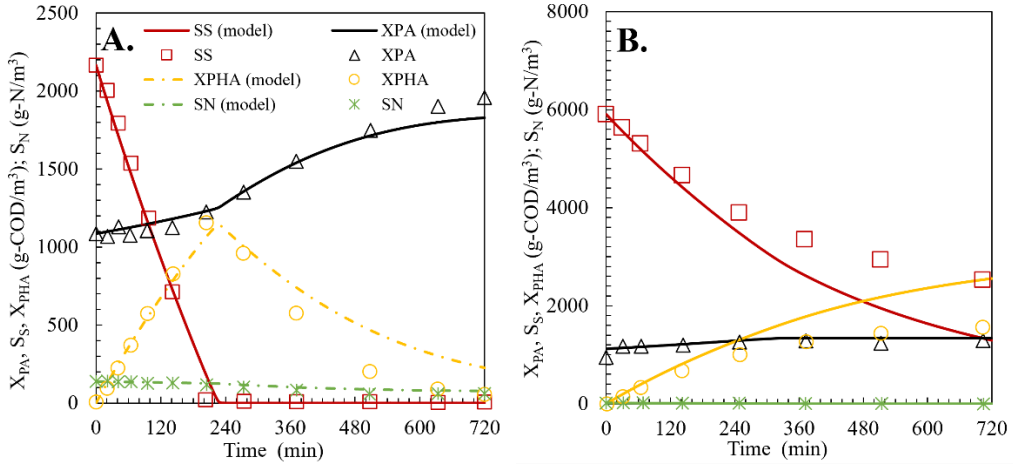

Fig. A4.4. Model simulations for *P. acidovorans* enrichment under different feeding strategy ($\mu_{PA,S}$=0.05; $Y_{PA,S}$=0.60; $Y_{PA,PHA}$=0.80; $Y_{PHA,S}$=0.65; *ksto*=0.35; $f_{(PHA)}^{max}$=2.33) (Marang et al., 2018). Initial conditions and kinetic constants are listed in tables 5.2 and 5.3.

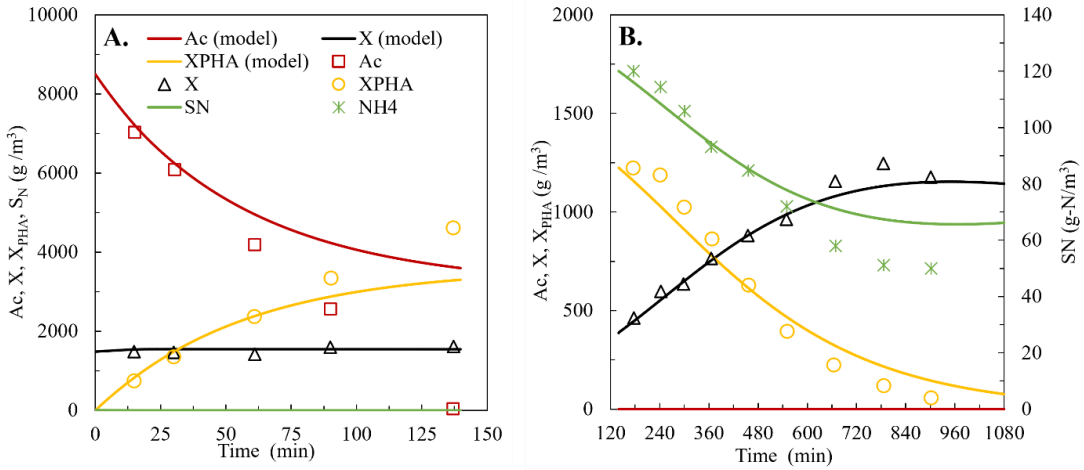

Fig. A4.5. Model simulations for *P. acidovorans* enrichment under high-volume exchange ratio ($Y_{PA,\,PHA}$=0.90; $f_{(PHA)}^{max}$=2.33) (Marang et al., 2016). A. A repeated cycle after achieving steady-state conditions. B. PHA-accumulation experiment. Initial conditions and kinetic constants are listed in tables 5.2 and 5.3.

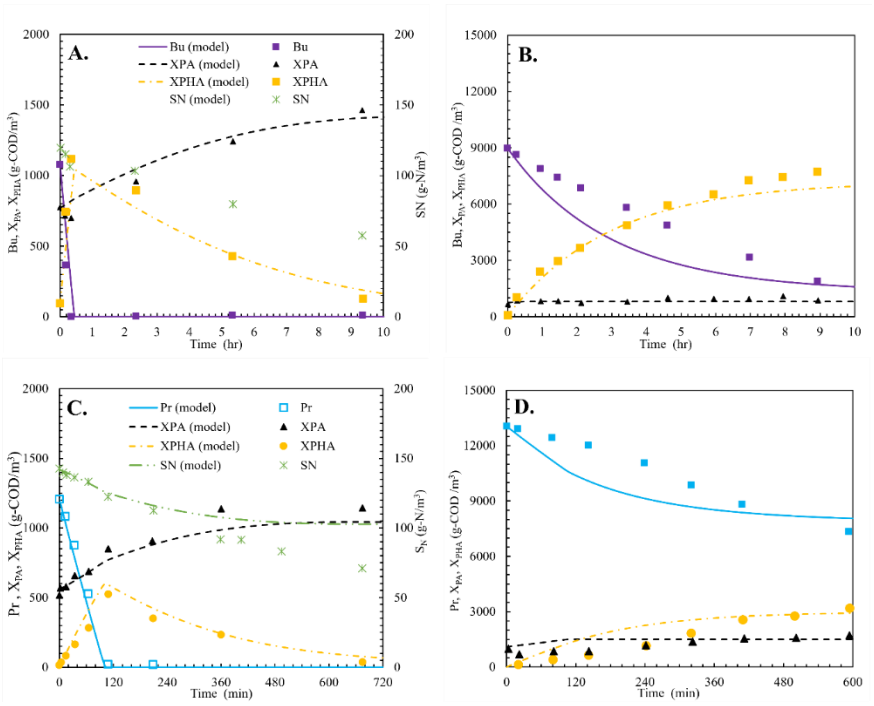

Fig. A4.6. Enrichment of *P. acidovorans* and PHA-accumulation experiments on butyrate (A, B) (($Y_{PA,\,PHA}$=0.90; $f_{(PHA)}^{max}$=4.88) (Marang et al., 2013) and propionate (E, F) ($Y_{PA,\,PHA}$=0.75; *Ksto*=0.75; $f_{(PHA)}^{max}$=2.0) (Jiang et al., 2011). Initial conditions and kinetic constants are listed in tables 5.2 and 5.3.

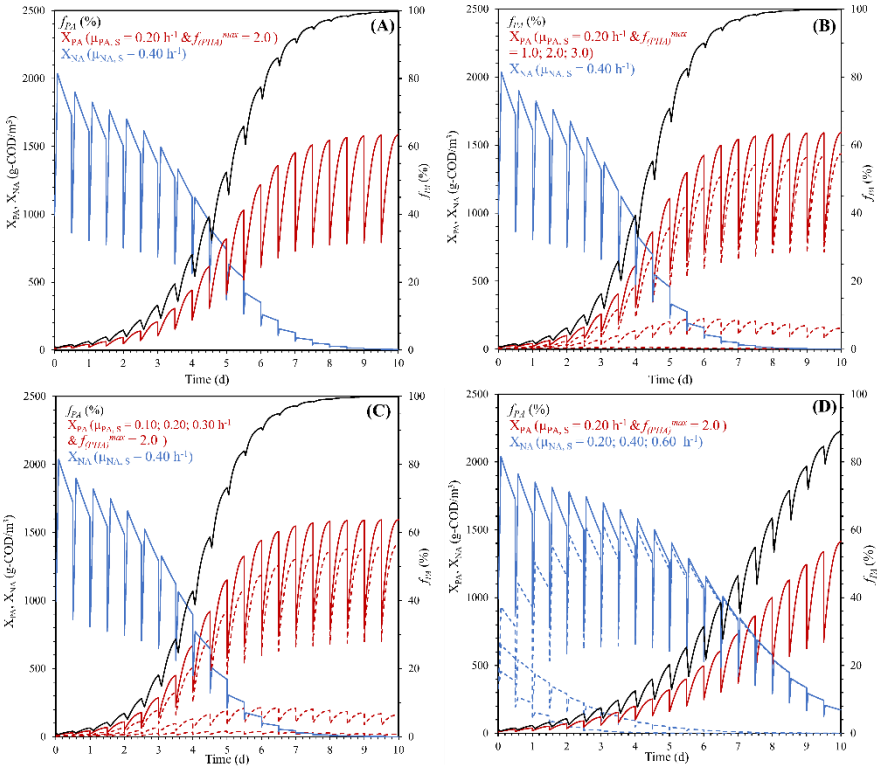

Fig. A4.7. Biomass concentrations for: (**A**). Single-X model; (**B**). Three-X_{PA} model with $f_{(PHA)}^{max}$= 1.0; 2.0; 3.0; (**C**). Three-X_{PA} model with $\mu_{PA,S}$ = 0.10; 0.20; 0.30 (h^{-1}); and (**D**). Three-X_{NA} model with $\mu_{NA,S}$ = 0.20; 0.40; 0.40 (h^{-1}) simulations. The average values for parameters and initial conditions are shown in Table 5.2 and 5.3, respectively. For every figure, only one parameter was changed.

Table A4.1: Comparison between the parameters applied in the single-X and three-X models.

Parameter (unit)	Single-X model	Three-X model			Figure
		X_{PA_1}	X_{PA_2}	X_{PA_3}	
$X_{PA,0}$ *(g.COD.m^{-3})*	10	10/3	10/3	10/3	5.3A-5.3F
$f_{(PHA)}^{max}$	2.0	1.60 1.0	2.0 2.0	2.40 3.0	5.3A
Ksto (h^{-1})	2.50	2.0 1.25	2.50 2.50	3.0 3.75	5.3B
$\mu_{PA,S}$ (h^{-1})	0.20	0.16 0.10	0.20 0.20	0.24 0.30	5.3C
b_{PA} (h^{-1})	0.017	0.014 0.009	0.017 0.017	0.021 0.026	5.3D
$Y_{PA,PHA}$	0.90	0.85 0.80	0.90 0.90	0.95 1.00	5.3E
$\mu_{PA,PHA}$ (h^{-1})	0.40	0.32 0.20	0.40 0.40	0.48 0.60	5.3F
		X_{NA_1}	X_{NA_2}	X_{NA_3}	
$X_{NA,0}$ *(g.COD.m^{-3})*	990	330	330	330	5.3G-5.3I
$\mu_{NA,S}$ (h^{-1})	0.40	0.32 0.20	0.40 0.40	0.48 0.60	5.3G
$Y_{NA,S}$	0.65	0.52 0.33	0.65 0.65	0.78 0.98	5.3H
b_{NA} (h^{-1})	0.017	0.014 0.009	0.017 0.017	0.021 0.026	5.3I

Table A4.2. Combined sensitivity analysis for PHA-accumulation simulation.

Parameter	Combined sensitivity analysis (δ) after 12 hr
$f^{(PHA)}_{max}$	0.8383
Ksto	0.1624
$K_{PHA, PA}$	-0.0007
$\mu_{PA, S}$	0.0004
$K_{N, PA}$	-0.0003
$K_{s, PA}$	0.0001
$Y_{PHA, S}$	0.0000
$\mu_{PA, PHA}$	0.0000
$m_{PA, PHA}$	0.0000
$Y_{PA, PHA}$	0.0000
b_{PA}	0.0000
$K_{O, PA}$	0.0000
$K_{P, PA}$	0.0000
$m_{PA, S}$	0.0000
$Y_{PA, S}$	0.0000

References:

Jiang, Y., Hebly, M., Kleerebezem, R., Muyzer, G., & Van Loosdrecht, M. C. M. (2011). Metabolic modeling of mixed substrate uptake for polyhydroxyalkanoate (PHA) production. *Water Research*, *45*(3), 1309–1321. https://doi.org/10.1016/j.watres.2010.10.009

Johnson, K., Jiang, Y., Kleerebezem, R., Muyzer, G., & Van Loosdrecht, M. C. M. (2009). Enrichment of a mixed bacterial culture with a high polyhydroxyalkanoate storage capacity. *Biomacromolecules*, *10*(4), 670–676. https://doi.org/10.1021/bm8013796

Johnson, K., Kleerebezem, R., & Van Loosdrecht, M. C. M. (2010). Influence of ammonium on the accumulation of polyhydroxybutyrate (PHB) in aerobic open mixed cultures. *Journal of Biotechnology*, *147*(2), 73–79. https://doi.org/10.1016/j.jbiotec.2010.02.003

Korkakaki, E., Van Loosdrecht, M. C. M., & Kleerebezem, R. (2017). Impact of phosphate limitation on PHA production in a feast-famine process. *Water Research*, *126*, 472–480. https://doi.org/10.1016/j.watres.2017.09.031

Marang, L., Jiang, Y., Van Loosdrecht, M. C. M., & Kleerebezem, R. (2013). Butyrate as preferred substrate for polyhydroxybutyrate production. *Bioresource Technology*, *142*, 232–239. https://doi.org/10.1016/j.biortech.2013.05.031

Marang, L., Van Loosdrecht, M. C. M., & Kleerebezem, R. (2016). Combining the enrichment and accumulation step in non-axenic PHA production: Cultivation of Plasticicumulans acidivorans at high volume exchange ratios. *Journal of Biotechnology*, *231*, 260–267. https://doi.org/10.1016/j.jbiotec.2016.06.016

Marang, L., Van Loosdrecht, M. C. M., & Kleerebezem, R. (2018). Enrichment of PHA-producing bacteria under continuous substrate supply. *New Biotechnology*, *41*, 55–61. https://doi.org/10.1016/j.nbt.2017.12.001

Appendix A5: Supplementary information for Chapter 6.

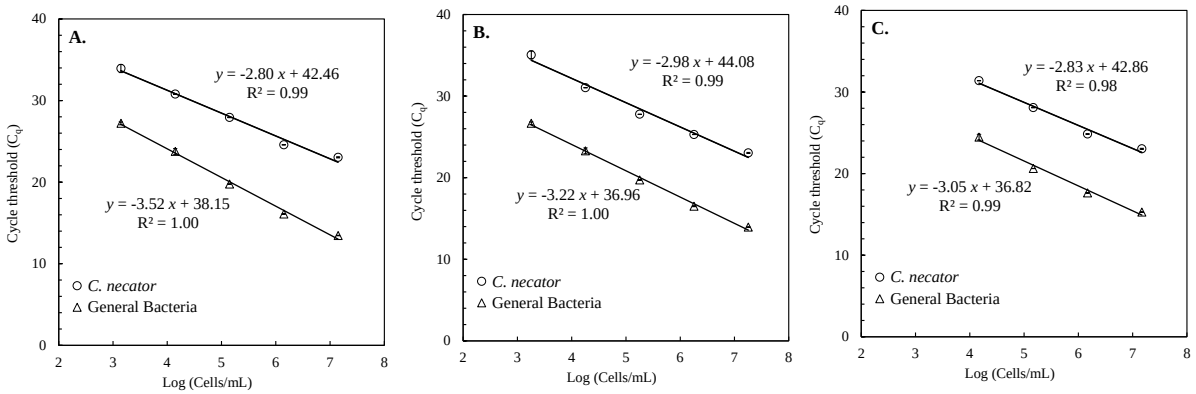

Fig. A5.1. Examples of the standard curves used to calculate the microbial cell concentrations in this work. A. a standard curve for the specific primer set (Nec222) for *C. necator*. B. A standard curve for the general primer set (Bac 338F and BAC 805R). Samples were run in triplicate. Error bars are included in the graph.

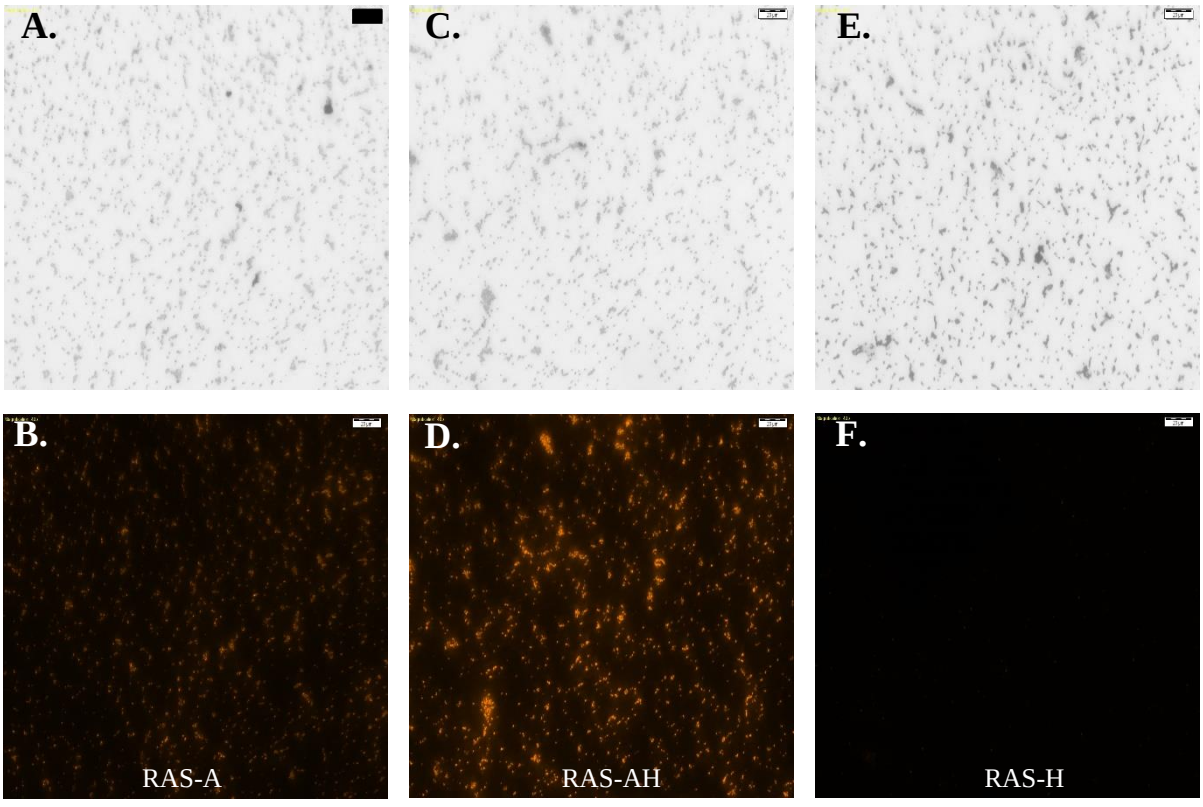

Fig. A5.2. Additional bright field (top) and fluorescent (bottom) microscopy images of enriched RAS mixtures under autotrophic (A, B), alternating (C, D), and heterotrophic (E, F) cultures (40 x magnification). Scale bar (▬) is 20 µm.

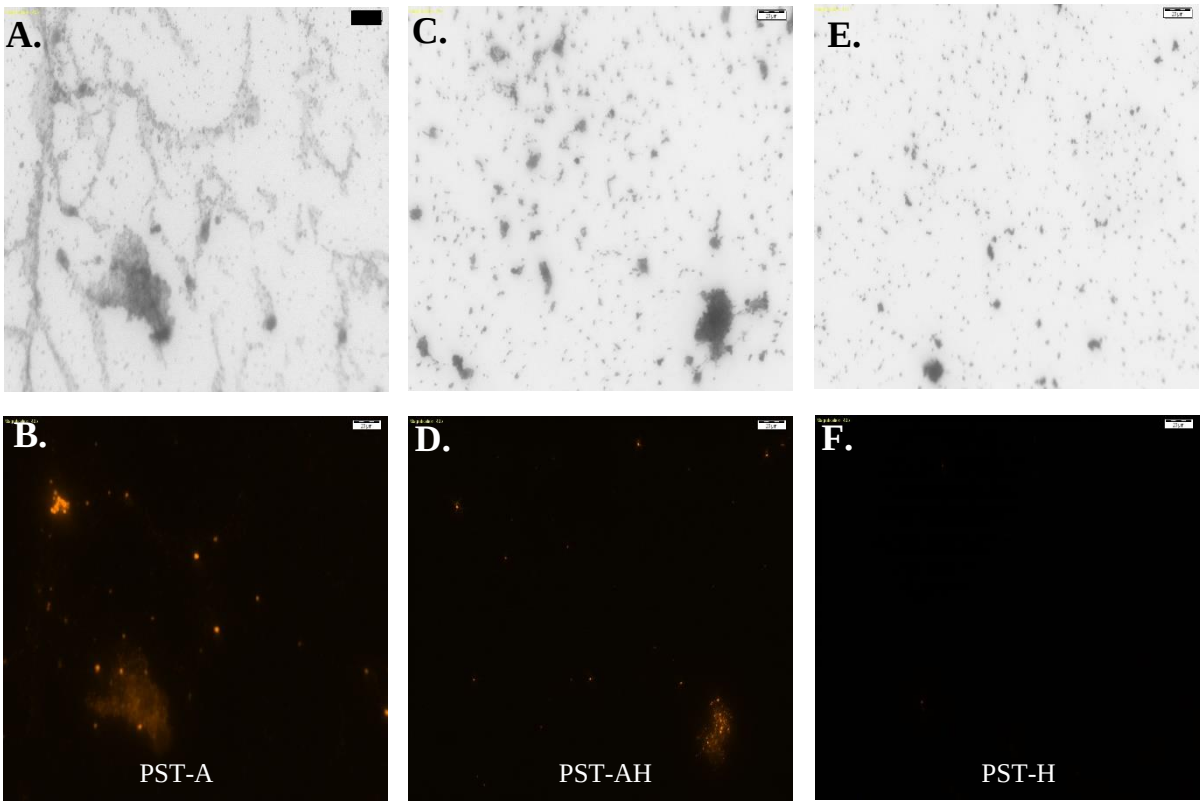

Fig. A5.3. Additional bright field (top) and fluorescent (bottom) microscopy images of enriched PST mixtures under heterotrophic (A, B), autotrophic (C, D), and alternating (E, F) cultures (40 x magnification). Scale bar (▬) is 20 µm.

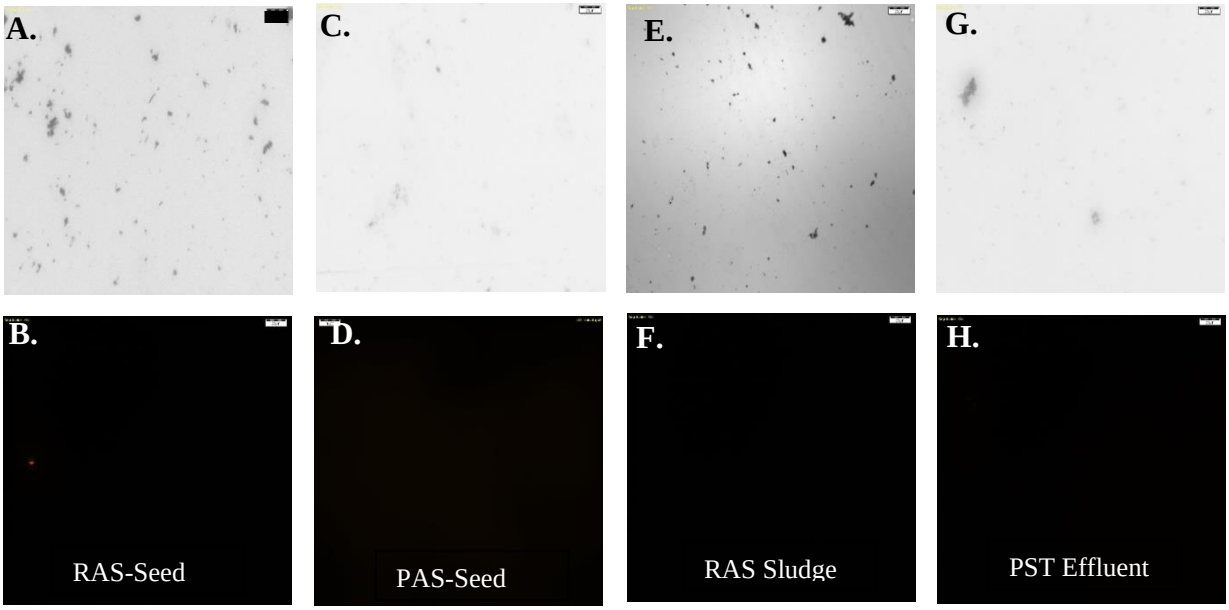

Fig. A5.4. Bright field (top) and fluorescent (bottom) microscopy images of RAS seed mixture (A, B), PST seed mixture (C, D), RAS sludge (E, F), PST effluent (G, H) cultures inoculated with 1% **C. necator** (40 x magnification). Scale bar (▬) is 20 µm.